

THE DIETARY PHYTOCHEMICAL MYRICETIN INDUCES ROS-DEPENDENT
BREAST CANCER CELL DEATH

by

Allison F. Knickle

Submitted in partial fulfilment of the requirements
for the degree of Master of Science

at

Dalhousie University
Halifax, Nova Scotia
December 2014

© Copyright by Allison F. Knickle, 2014

Table of Contents

| | |
|---|-----------|
| List of Figures | iv |
| List of Tables | vi |
| Abstract..... | vii |
| List of Abbreviations and Symbols Used | viii |
| Acknowledgements | xiii |
| CHAPTER 1 INTRODUCTION | 1 |
| 1.1. Cancer | 1 |
| 1.2 Breast Cancer | 1 |
| 1.2.1 Triple-negative breast cancer | 3 |
| 1.3 Cell death | 4 |
| 1.3.1 Apoptosis..... | 4 |
| 1.3.2 Necrosis/Necroptosis..... | 6 |
| 1.3.3 Caspase-independent cell death involving the mitochondria | 8 |
| 1.4 ROS | 9 |
| 1.4.1 The role of ROS in cell signaling..... | 10 |
| 1.4.2 ROS and cancer..... | 12 |
| 1.5 Phytochemicals | 14 |
| 1.6 Phytochemicals and Cancer | 17 |
| 1.7 Myricetin and cancer | 20 |
| 1.8 Rationale and Objectives | 22 |
| CHAPTER 2 MATERIALS AND METHODS..... | 33 |
| 2.1. Cell lines and primary cells | 33 |
| 2.2. Reagents | 33 |
| 2.3. Antibodies | 34 |
| 2.4. Culture medium and conditions | 35 |
| 2.5. Cell seeding | 35 |
| 2.5.1. Human breast carcinoma cells | 36 |
| 2.5.2. Mouse mammary carcinoma cells..... | 36 |
| 2.5.3. Human dermal fibroblasts | 36 |

| | |
|---|------------|
| 2.5.4. Human mammary epithelial cells (HMEpiC) | 37 |
| 2.6. Acid Phosphatase Assay | 37 |
| 2.7. Amplex® Red Assay | 38 |
| 2.8. Flow Cytometry | 38 |
| 2.8.1. Annexin-V-FLUOS/PI staining | 39 |
| 2.8.2. DiOC ₆ staining | 40 |
| 2.8.3. DCFDA assay..... | 41 |
| 2.8.4. Intracellular antibody staining for γ -H2AX | 41 |
| 2.9. Protein isolation | 42 |
| 2.10. Protein quantification | 43 |
| 2.11. Western blotting | 43 |
| 2.12. Statistical analysis..... | 45 |
| CHAPTER 3 RESULTS | 46 |
| 3.1. Myricetin reduces mammary carcinoma cell phosphatase activity..... | 46 |
| 3.2. Myricetin is cytotoxic to mammary carcinoma cells..... | 47 |
| 3.3. Myricetin causes a loss of mammary carcinoma cell mitochondrial membrane integrity. | 48 |
| 3.4. Myricetin induces accumulation of intracellular reactive oxygen species (ROS), which promotes mammary carcinoma cell death..... | 50 |
| 3.5. Myricetin causes ROS-dependent DNA damage in mammary carcinoma cells. | 51 |
| 3.6. Myricetin forms extracellular ROS in cell culture medium..... | 52 |
| 3.7. Myricetin causes p38 MAPK activation in mammary carcinoma cells..... | 53 |
| CHAPTER 4 DISCUSSION | 103 |
| 4.1. Myricetin is cytotoxic for breast cancer cells..... | 103 |
| 4.2 Myricetin-induced mammary carcinoma cell death is ROS-dependent. | 107 |
| 4.3 Myricetin forms ROS in the extracellular environment..... | 108 |
| 4.4 Summary of the effects of myricetin on mammary carcinoma cells..... | 111 |
| 4.5. Limitations of this study | 112 |
| 4.6 Future Directions..... | 113 |
| 4.7 Concluding remarks..... | 115 |
| APPENDIX..... | 120 |
| REFERENCES | 128 |

LIST OF FIGURES

| | |
|--|----|
| Figure 1.1 The apoptotic and necroptotic cell death pathways | 24 |
| Figure 1.2 The effects of ROS on cancer | 26 |
| Figure 1.3 Classification of phytochemicals | 28 |
| Figure 1.4 The chemical structure of myricetin..... | 30 |
| Figure 3.1 Myricetin reduces mammary carcinoma cell phosphatase activity..... | 55 |
| Figure 3.2 Myricetin reduces human mammary epithelial cell, but not human dermal fibroblast cell phosphatase activity | 57 |
| Figure 3.3 The effect of myricetin on mammary carcinoma cell phosphatase activity is similar to the effects on phosphatase activity seen with EGCG, and greater than the effect of resveratrol | 59 |
| Figure 3.4 The dose-dependent inhibitory effect of myricetin on mammary carcinoma cell phosphatase activity is similar to the effects of conventional chemotherapeutic drugs | 61 |
| Figure 3.5 Myricetin reduces mammary carcinoma cell number and size..... | 63 |
| Figure 3.6 Myricetin induces human mammary carcinoma cell death..... | 65 |
| Figure 3.7 Myricetin induces mouse mammary carcinoma cell death..... | 68 |
| Figure 3.8 The stability of the mitochondrial membrane in human mammary carcinoma cells is decreased by myricetin | 70 |
| Figure 3.9 The stability of the mitochondrial membrane in mouse mammary carcinoma cells is decreased by myricetin | 73 |
| Figure 3.10 Myricetin-induced mammary carcinoma cell death is caspase-independent and RIPK1-independent | 75 |
| Figure 3.11 Intracellular ROS levels are increased in mammary carcinoma cells treated with myricetin..... | 77 |
| Figure 3.12 NAC prevents myricetin-induced human mammary carcinoma cell death..... | 80 |
| Figure 3.13 NAC prevents myricetin-induced mouse mammary carcinoma cell death..... | 83 |
| FIGURE 3.14 Changes in mitochondrial membrane stability caused by myricetin are inhibited by NAC..... | 85 |
| Figure 3.15 . Sodium pyruvate added to cell culture medium prevents myricetin-induced decreases in mammary carcinoma cell growth | 87 |
| Figure 3.16 The levels of a double-stranded DNA damage marker, γ -H2AX, are increased in mammary carcinoma cells treated with myricetin, and the increase in γ -H2AX is prevented by NAC | 89 |

| | |
|---|-----|
| Figure 3.17 Extracellular H ₂ O ₂ is formed in cell culture medium in the presence of myricetin | 92 |
| Figure 3.18 SOD and catalase prevent myricetin-induced decreases in mitochondrial membrane stability | 94 |
| Figure 3.19 SOD and catalase prevent myricetin-induced mammary carcinoma cell death | 96 |
| Figure 3.20 Myricetin promotes p38 MAPK phosphorylation in mammary carcinoma cells | 98 |
| Figure 3.21 Inhibition of p38 MAPK does not prevent myricetin-induced mammary carcinoma cell death..... | 101 |
| Figure 4.1 Proposed model of myricetin-induced mammary carcinoma cell death | 117 |
| Appendix Figure 1 Z-VAD-fmk inhibits early apoptosis induced by artesunate . | 119 |
| Appendix Figure 2 Necrostatin-1 inhibits cell death induced by artesunate | 121 |
| Appendix Figure 3 T-cell proliferation is inhibited by p38 MAPK inhibitor III | 123 |
| Appendix Figure 4 Myricetin has a slight inherent fluorescence | 125 |

LIST OF TABLES

| | |
|---|----|
| Table 1.1 The effects of myricetin on different types of human cancer cell lines and mouse xenograft models of human cancer | 32 |
|---|----|

ABSTRACT

Myricetin is a dietary phytochemical found in a variety of fruits and vegetables. Myricetin has several anti-cancer effects on a variety of human cancer cells *in vitro* and *in vivo*, including bladder, pancreatic, and colorectal cancers; however, the effect of myricetin on breast cancer cells remains unclear. The goals of this study were to first determine if myricetin caused breast cancer cell death and then to establish the mechanisms underlying myricetin-induced breast cancer cell death. Myricetin decreased the viability of several human and mouse mammary carcinoma cells, including triple-negative breast cancer cells. Myricetin induced cell death of triple-negative breast cancer cells in a reactive oxygen species (ROS)-dependent manner. Myricetin-induced ROS caused decreased mitochondrial membrane stability, increased double-stranded DNA damage, and increased p38 MAPK phosphorylation, all of which can promote cell death. The myricetin-induced ROS was likely formed by myricetin autoxidation in cell culture medium to form H₂O₂. The relevance of myricetin autoxidation *in vivo* remains unknown. However, the potent anti-breast cancer effect of myricetin *in vitro* argues in favour of further investigation of myricetin as a possible breast cancer therapeutic.

LIST OF ABBREVIATIONS AND SYMBOLS USED

| | |
|-------------------------|--|
| °C | degrees Celsius |
| AIF | apoptosis inducing factor |
| Amplex Red | N-acetyl-3,7-dihydroxyphenoxazine |
| ANOVA | analysis of variance |
| Apaf-1 | apoptosis protease activation factor 1 |
| APS | ammonium persulfate |
| ATP | adenosine triphosphate |
| Bcl | B cell lymphoma |
| BSA | bovine serum albumin |
| CaCl ₂ | calcium chloride |
| Calpain | calcium-activated neural protease |
| CDK | cyclin dependent kinase |
| cDMEM | complete DMEM |
| Chk1 | checkpoint kinase 1 |
| cIAP1 | cellular inhibitor of apoptosis 1 |
| CM-H ₂ DCFDA | 2', 7'-dichlorofluorescein diacetate |
| CO ₂ | carbon dioxide |
| CYLD | cylindromatosis |
| CypA | cyclophilin A |
| DiOC ₆ | 3,3'-dihexyloxacarbocyanine iodide |
| DISC | death-inducing signaling complex |
| DMBA | dimethyl bezanthrane |
| DMEM | Dulbecco's modified Eagle's medium |

| | |
|-------------------------------|---|
| DMSO | dimethyl sulfoxide |
| DNA | deoxyribonucleic acid |
| DNAse | deoxyribonuclease |
| DTT | dithiothreitol |
| EDTA | ethylenediaminetetraacetic acid |
| EGCG | epigallocatechin-3-gallate |
| EGTA | ethylene glycol tetraacetic acid |
| EMT | epithelial-mesenchymal transition |
| ENDO G | endonuclease G |
| ERK | extracellular signal-regulated kinases |
| FACS | fluorescence-activated cell sorting |
| FADD | Fas-associated death domain |
| FBS | fetal bovine serum |
| FGM-2 | fibroblast growth medium-2 |
| H ₂ O ₂ | hydrogen peroxide |
| HEPES | N-2-hydroxyethylpiperazine-N'-2-ethanesulfonic acid |
| HER-2 | human epidermal growth factor 2 receptor |
| HMEpiC | human mammary epithelial cells |
| HRP | horseradish peroxidase |
| HtrA2 | high temperature requirement protein A2 |
| IAP | inhibitor of apoptosis protein |
| JNK | c-Jun N-terminal kinase |
| MAPK | mitogen-activated protein kinase |
| MAPKK | MAPK kinase |

| | |
|----------------------------------|--|
| MAPKKK | MAPK kinase kinase |
| MEpiCM | mammary epithelial cell medium |
| MKP | mitogen-activated protein kinase phosphatase |
| MLKL | mixed lineage kinase domain like |
| MMP | matrix metalloproteinase |
| MOMP | mitochondria outer membrane permeabilisation |
| MTP | mitochondrial transmembrane potential |
| Na ₂ HPO ₄ | disodium hydrogen phosphate |
| Na ₃ VO ₄ | sodium orthovanadate |
| NAC | N-acetylcysteine |
| NaCl | sodium chloride |
| NADPH | nicotinamide adenine dinucleotide phosphate |
| NaF | sodium fluoride |
| NaOH | sodium hydroxide |
| NF-κB | nuclear factor-κB |
| NOX | NADPH oxidase |
| NP-40 | nonidet P-40 |
| O ₂ ^{•-} | superoxide anion |
| •OH | hydroxyl radical |
| PAO | phenylarsine oxide |
| PARP | poly(ADP-ribose) polymerase |
| PBS | phosphate buffered saline |
| PI | propidium iodide |
| PI3K | phosphatidylinositol 3-kinase |

| | |
|-------------------|---|
| PMSF | phenylmethylsulfonyl fluoride |
| PR | progesterone receptor |
| PRR | pattern recognition receptor |
| PS | phosphatidylserine |
| PTEN | phosphatase and tensin homolog |
| PTP | protein tyrosine phosphatase |
| rhFGF-B | recombinant human fibroblast growth factor-B |
| RIPK1 | receptor-interacting protein kinase 1 |
| RNS | reactive nitrogen species |
| RO• | alkoxyl |
| RO ₂ • | peroxyl |
| ROS | reactive oxygen species |
| SDS | sodium dodecyl sulfate |
| SEM | standard error of the mean |
| SGLT1 | sodium-dependent glucose transporter |
| Smac | second mitochondria-derived activator of caspase |
| SOD | superoxide dismutase |
| TEMED | tetramethylethylenediamine |
| TNF | tumor necrosis factor |
| TNFR1 | TNF receptor 1 |
| TRADD | TNFR-associated death domain |
| TRAF2 | TNFR-associated factor 2 |
| TRAILR1 | TNF-related apoptosis-inducing ligand receptor 1 |
| TTBS | a solution of Tris-buffered saline and 0.05% Tween-20 |

| | |
|----------------|-------------------------------------|
| UV | ultraviolet |
| Z-VAD-fmk | N-benzyloxycarbonyl-Val-Ala-Asp-fmk |
| γ -H2AX | phosphorylated histone H2AX |

ACKNOWLEDGEMENTS

Over the past two and a half years there have been so many wonderful people who have helped me on the road to completing my degree. I am truly grateful for all the help, support, and guidance I have received throughout my time in the Hoskin lab. I feel very lucky to have had the opportunity to do research in the Hoskin lab and to have a supervisor as terrific as Dr. David Hoskin. I would like to thank Dave for accepting me into his lab and for being so supportive, patient, and encouraging, especially when my project did always go as planned.

I would like to thank my committee members Dr. Brent Johnston and Dr. Rob Liwski for their encouragement and great input throughout my degree.

I could not imagine having done my degree in any other lab but the Hoskin lab. Thank you to Anna, Laurence, Carolyn, Melanie, Leanne, Alicia, Javad, Henry, Dan, and all the members of the Hoskin lab past and present for creating a fantastic and fun learning environment, one I looked forward to coming to everyday. Thanks for all the laughs, cake, and timbits; if I was having a bad day I could always count on people in the lab to cheer me up. A huge thank you to Dr. Melanie Coombs for not only reading and editing my thesis, but for teaching me many techniques in the lab and for always being someone I could turn to for help. Thanks to Dr. Carolyn Doucette for being a great teacher in the lab and sharing your lab wisdom with me. Thank you to Dr. Anna Greenshields for being so patient with my constant questions.

Finally a big thank you to my friends and family for your support throughout my education, especially my mom for listening to me talk about my research when I had a bad day, even if you had no idea what I was talking about you were always there to support me.

CHAPTER 1

INTRODUCTION

1.1. Cancer

The word 'cancer' includes over 200 diverse diseases, but all begin similarly with normal cells accumulating mutations to become abnormal cells, which divide uncontrollably and can invade other tissues. Normal cells undergo a progressive process in which they undergo changes that cause them to become malignant (1, 2). The characteristics of cancer that allow tumor growth and metastasis were outlined by Hanahan and Weinberg in their framework for the hallmarks of cancer and consist of deregulation of cellular energetics, resistance of cell death, mutations and genome instability, evasion of immune detection and destruction, invasion of tissues (metastasis), initiation of angiogenesis, insensitivity to growth suppressors, self-sustaining of proliferative signaling, replicative immortality, and activation of tumor-promoting inflammation (3, 4). Although cancer mortality rates have declined since 1975, cancer incidence has increased and cancer remains a significant health problem worldwide and is a large burden on societal resources (5). It is estimated that 2 in 5 Canadians will develop cancer in their lifetime and 1 in 4 Canadians will die of cancer (6). In addition to the great burden that cancer has on the individual, cancer also has a substantial economic impact. In 2008 alone, the healthcare costs (direct and indirect) associated with malignant neoplasms was \$4.04 billion in Canada (7).

1.2 Breast Cancer

Breast cancer is the most common type of cancer for females with 1 in 9 Canadian women expected to develop breast cancer in their lifetime (6). The female breast cancer mortality rate has declined 43% since 1986 due to early

detection with increased screening and improved screening tools/treatments (6). Although the mortality rate has declined, breast cancer remains the second leading cause of cancer death in women with 1 in 30 Canadian women expected to die from breast cancer (6). Breast cancer is a heterogeneous cancer with several distinct pathological types that have different biological behaviors and treatment requirements. Breast cancer has traditionally been classified into three groups based on the morphology and site of development of the tumor: ductal and lobular carcinomas, which develop in the milk ducts and lobules, respectively, and inflammatory breast cancer (8). Breast cancer can be further grouped into three histopathological subtypes based on expression of the estrogen receptor (ER) and progesterone receptor (PR) for hormones and the Human Epidermal Growth Factor 2 Receptor (HER-2/*neu*). The three histopathological subtypes: ER- or PR-positive, HER-2/*neu* overexpressing, and triple-negative (lack expression of ER, PR, and HER-2/*neu*) are used to predict therapeutic outcomes (9–12). More recently, using patterns of gene expression and hierarchical clustering, breast cancer has been classified into seven major molecular subtypes: Luminal A, Luminal B, Luminal C, HER-2-enriched, Basal-like, Claudin low, and Normal Breast-like (13–15).

Several factors influence the type of treatment chosen for a breast cancer patient, including the stage of disease, grade of primary tumor, menopausal status and age of the patient, ER, PR and HER-2 status of the tumor, histologic type (ductal or lobular), invasion into lymphatics, and co-morbidities (16, 17). Treatment options consist of surgery, radiation, chemotherapy, endocrine/hormone therapy, and tissue-targeted therapy (trastuzumab, an anti-human HER-2 monoclonal antibody, is an example of a targeted therapy) (17–19). A combination of therapies is commonly used to help prevent recurrence and disease-specific death (17).

1.2.1 Triple-negative breast cancer

Triple-negative breast cancer is characterized by lack of (or low) expression of ER, PR, and HER-2 and represents approximately 15% of all invasive breast cancer; however, the prevalence varies by race and age with premenopausal and African-American populations of women having a higher prevalence of triple-negative breast cancer (20, 21). Triple-negative breast cancer is often categorized as basal-like, but the two are not synonymous since not all basal-like breast cancers are triple-negative and not all triple-negative breast cancers are basal-like (22). Triple-negative breast cancers are often higher grade and have a worse prognosis than other types of breast cancer (23) (20, 24). The risk of relapse within the first three years following diagnosis is high and the five-year survival rate is low compared to non-triple-negative breast cancer (24–26). Though triple-negative breast cancer is associated with a worse prognosis than ER-positive breast cancer, triple-negative breast cancer is actually more sensitive to anthracycline-based chemotherapy (27). It may therefore be easier to achieve a complete pathologic response to chemotherapy with triple-negative breast cancer, but if a complete pathologic response is not achieved then relapse is more likely to occur and lead to death, because if chemotherapy fails there are not any other treatments available (27). Compared to other types of breast cancer, adjuvant treatment options are more limited for triple-negative breast cancer, there are no targeted therapies, and chemotherapy is currently the only available clinical option (18, 28, 29). New treatment options and strategies are needed to combat this aggressive form of breast cancer.

This investigation focused on two triple-negative human breast cancer cell lines, MDA-MB-231 and MDA-MB-468, and also initially compared them to one ER- and PR-positive cell line (MCF-7) and one HER-2-overexpressing cell line (SK-BR-3) (30–33). All of the human breast cancer cell lines studied were originally derived from pleural effusions (34). In addition, two mouse mammary carcinoma cell lines, 4T1 and E0771, were studied.

1.3 Cell death

One of the goals of using chemotherapeutic drugs to treat cancer is to induce cancer cell death. The Nomenclature Committee on Cell Death proposed that cells should be considered dead if they meet any one of the following criteria: complete fragmentation (including the nucleus) of the cell into discrete bodies (apoptotic bodies) has occurred, the cell has lost its plasma membrane integrity *in vitro*, and/or adjacent cells have engulfed the fragments of the cell *in vivo* (35). It is recognized that there are several different forms of cell death, including apoptosis, necrosis, necroptosis, autophagic cell death, anoikis, cornification, mitotic catastrophe, parthanatos, pyroptosis, and ferroptosis (36). While there are several distinct cell death pathways, there are also similarities, redundancies, and cross-talk between these pathways and it is likely that several pathways are triggered at the same time. The different classifications of cell death can be determined using morphological and molecular criteria (36). Cell death may be accidental, as in necrosis, meaning that it is due to severe chemical, physical, or mechanical insults and cannot be prevented or modulated by pharmacologic interventions (37). Cell death may also be regulated, meaning that it involves molecular machinery in the cell that is genetically encoded and it can be modulated to an extent by pharmacologic intervention, for example apoptosis (37). The term programmed cell death is used to refer to regulated cell death that occurs during (post-) embryonic development, immune responses, and tissue homeostasis (37).

1.3.1 Apoptosis

The term 'apoptosis' was coined in 1972 by Kerr *et al.* to describe a form of regulated cell death with distinct morphological features such as nuclear and cytoplasmic condensation, shrinkage of the cell, plasma membrane blebbing, and disintegration of the cell into apoptotic bodies (38). While apoptosis can be

described in terms of morphological features, the molecular pathways involved in apoptosis have been characterized and can be used to describe apoptosis. There are two main pathways through which apoptosis can occur: the extrinsic pathway, which involves activation of receptors on the cell surface by extracellular signals, and the intrinsic (mitochondrial) pathway, which is activated by various intracellular stimuli (39). In both pathways proteins called caspases play an important role in inducing and carrying out the apoptotic process. Caspases are a large family of proteases that are conserved through evolution; in humans, several caspases, many which function in apoptosis, have been identified (40–42). Initiator caspases can play a role early in the apoptotic signaling pathway during which they activate downstream signaling molecules. Caspase-8 is an example of one such initiator caspase (43, 44). Effector caspases play a role downstream in the apoptotic cascade during which they act on various cellular substrates to execute apoptosis. Caspase-3, -6, -7 are effector caspases that are activated by upstream initiator caspases (43, 44).

The extrinsic apoptotic pathway (Figure 1.1) is activated when death ligands (members of the tumor necrosis factor superfamily) bind to death receptors on the cell surface such as Fas, TNF receptor 1 (TNFR1) and TNF-related apoptosis-inducing ligand receptor 1 (TRAILR1) (39, 45–47). Binding of the ligands to death receptors causes receptor trimerization and recruitment of adaptor molecules, such as the FAS-associated death domain (FADD), TNFR-associated death domain (TRADD) and TNFR-associated factor 2 (TRAF2), as well as recruitment of pro-caspase-8 to the intracellular cytoplasmic death domains of the death receptors (39, 45, 47, 48). Together, the intracellular cytoplasmic death domains along with FADD (or other adaptor molecules) and pro-caspase 8 form a complex called the death-inducing signaling complex (DISC) (39, 45). The formation of DISC causes the cleavage of pro-caspase-8 to activate caspase-8, which subsequently cleaves and activates downstream executioner caspases, such as caspases-3, -6, and/or -7, that carry out apoptosis (39, 45). Activated caspase-8 can also activate Bid (BH3-interacting domain death agonist), a pro-apoptotic member of the Bcl-2 family of proteins

that have either pro- or anti-apoptotic functions; activated Bid promotes mitochondria outer membrane permeabilization (MOMP) leading to a signaling cascade that activates apoptosis (45, 49, 50).

A variety of intracellular stress stimuli can activate the intrinsic apoptotic pathway (Figure 1.1), including nutrient deprivation, oxidative stress, DNA damage, and UV- and γ -irradiation (45, 51, 52). Pro-apoptotic members of the Bcl-2 family such as Bax and Bak act as sensors of stress stimuli (45, 53). Activated Bax and Bak contribute to pore formation in the mitochondrial outer membrane, which causes the release of pro-apoptotic proteins into the cytosol and a decrease in the mitochondrial membrane transmembrane potential (39, 53). The pro-apoptotic proteins released by MOMP include cytochrome c, second mitochondria-derived activator of caspase (Smac, also known as Diablo), and endonuclease G (45). Smac promotes apoptosis by binding to, and preventing the actions of, members of the inhibitors of apoptosis (IAP) family of proteins in the cytosol (45). When cytochrome c is released from the mitochondria it complexes with apoptosis protease activation factor 1 (Apaf-1) and the initiator caspase pro-caspase-9 to form the apoptosome (45, 54, 55). The apoptosome cleaves pro-caspase-9 to activate caspase-9, which subsequently can cleave and activate effector caspases (caspases-3, -6, and -7) that will cleave a wide variety of cellular targets leading to apoptosis (39, 45).

1.3.2 Necrosis/Necroptosis

Another form of cell death is necrosis, which is morphologically different from apoptosis. The morphological features of necrosis include swelling of the cytoplasm and cytoplasmic organelles, rupture of the plasma membrane and release of intracellular contents, and, unlike apoptosis, nuclei remain mostly intact (35, 56). Necrosis has typically been considered a form of cell death that occurs in an unregulated manner; however, there are now several studies that have identified mechanisms for regulated necrosis (56–59). A chemical inhibitor of regulated necrosis called necrostatin-1, which inhibits receptor-interacting

protein kinases, was found and the process of regulated necrosis was subsequently termed necroptosis (60). Induction of necroptosis has been associated with the activation of death receptors, the best characterized of which is necroptosis induced via the TNFR1 pathway (Figure 1.1) (56). Depending on the stimulus, cell type, and cell activation state, TNFR1 signaling can promote apoptosis, nuclear factor- κ B (NF- κ B) signaling, or necroptosis (56, 61). Upon binding of TNF to TNFR1 several proteins are recruited to the cytoplasmic portion of TNFR1, including receptor-interacting protein kinase 1 (RIPK1), cellular inhibitor of apoptosis 1 and 2 (cIAP1 and cIAP2, both of which are E3 ligases), TRADD, TRAF2 and TRAF5; together, these proteins form complex I (56, 61, 62). The E3 ligases cIAP1 and cIAP2 catalyze the polyubiquitination of RIPK1, which can act as a docking site for additional proteins involved in NF- κ B signaling to activate the NF- κ B pathway (56). Alternatively, the enzyme cylindromatosis (CYLD) can remove ubiquitin from RIPK1, thus allowing RIPK1 to complex with RIPK3, TRADD, FADD and caspase-8 to form complex II (56, 61, 63). If caspase-8 is active it will cleave RIPK1 and RIPK3, thereby promoting apoptosis (64). If caspase-8 is inhibited by pharmacological means or depleted or deleted by genetic means, then RIPK1 and RIPK3 remain active and promote necroptosis (58, 65). The mechanisms underlying RIPK1 and RIPK3 execution of necroptosis are unclear; however, it appears that RIPK3 interacts with the pseudokinase mixed lineage kinase domain like (MLKL) (66); this complex induces necroptotic cell death through a variety of mechanisms, including reactive oxygen species (ROS), reactive nitrogen species (RNS), apoptosis inducing factor (AIF), lysosomal membrane permeabilization, and poly(ADP-ribose) polymerase (PARP) cleavage (56, 57, 61, 67). In addition to activation by death receptors, there are other pathways that can promote cell death by necroptosis; however, the mechanisms involved in these pathways have yet to be fully elucidated. Pattern recognition receptors (PRRs) such as toll-like receptors can promote necroptosis, and there is also a form of necroptosis that involves alkylating DNA damage and release of AIF from the mitochondria (56, 68, 69). Another form of regulated cell death is pyroptosis, which occurs when

pores form in the plasma membrane in a caspase 1-dependent manner, resulting in dissipation of ionic gradients and osmotic pressure that lead to release of cytosolic contents (70).

1.3.3 Caspase-independent cell death involving the mitochondria

There are several regulated modes of cell death that are independent of caspase activation, one of which is necroptosis since to date there are no reports of caspase activation during necroptosis (66). Cellular stress stimuli can promote MOMP that causes cell death independently of caspase activation (36). When the mitochondrial outer membrane becomes permeabilized several proteins are released into the cytosol that can promote caspase-independent cell death. These proteins include AIF, endonuclease G (ENDOG), and high temperature requirement protein A2 (HtrA2, also known as OMI) (71). In addition, disruption of the mitochondrial outer membrane interferes with its normal functions in cell energetics, leading to depleted ATP that also promotes cell death (72). The HtrA2 protein can promote apoptosis by binding to and inhibiting members of the IAP family, but can also promote caspase-independent cell death by acting as an effector protein via its serine protease activity (73, 74). Upon its release from the mitochondria ENDOG can translocate to the nucleus where it can cause DNA fragmentation, thereby promoting cell death (75). AIF is an important mitochondrial protein involved in promoting caspase-independent cell death (71). When AIF is released from the mitochondria it translocates to the nucleus where, potentially along with ENDOG, AIF causes chromatin condensation and high molecular weight DNA loss; this process is referred to as AIF-mediated necroptosis (68, 69). Following translocation of AIF to the nucleus, recent studies have shown that AIF binds to phosphorylated histone H2AX (γ -H2AX), which accumulates at sites of double stranded DNA breaks, as well as the endonuclease cyclophilin A (CypA) to form a complex that causes DNA degradation leading to necroptosis (76). Release of AIF from the mitochondria can be stimulated in several ways, including by activated Bax and excessive

calcium influx that results in PARP1 overactivation (72). Increases in intracellular calcium due to ER stress promote activation of cytosolic proteases known as calpains (calcium-activated neutral proteases), which then cause AIF release from the mitochondria (77). Lysosomal permeabilization can also cause AIF release from the mitochondria due to lysosomal proteases released into the cytoplasm (71). Cathepsin D, a lysosomal protease, induces AIF release from the mitochondria (78). Additionally, ROS may cause AIF release from the mitochondria indirectly because of ROS-induced lysosomal permeability (79). Another form of cell death that involves AIF release is parthanatos, which is dependent on PARP1 activation (80). Parthanatos is triggered when DNA damage causes activation of PARP1, leading to poly(ADP-ribose) (PAR) synthesis and binding of PAR to AIF, which triggers AIF release from the mitochondria and translocation to the nucleus (80).

1.4 ROS

ROS are a group of partially reduced metabolites of oxygen molecules that can have a wide variety of effects on cell functions, including stimulation of signaling pathways for metabolism, intracellular signal transduction, proliferation, differentiation, metabolism, and cell death (81, 82). The effect(s) that ROS have on cells depends on the duration and amount of ROS generated, the type of cells involved and the cellular context (82). ROS, which are generated during normal cellular metabolism processes and inflammation, are very reactive molecules that can interact with biological molecules. ROS include the superoxide anion ($O_2^{\cdot-}$), hydrogen peroxide (H_2O_2), and hydroxyl radicals ($\cdot OH$), peroxy (RO_2^{\cdot}), and alkoxy ($RO\cdot$) (83). Cells have several antioxidant systems to regulate ROS levels and protect against ROS to maintain the redox (reduction-oxidation) balance, including the glutathione system, the thioredoxin system, peroxiredoxins, the enzymes SOD and catalase, and ROS-scavenging vitamins E and C (84). When excess ROS are produced to the extent that it overwhelms the capacity of cellular antioxidant systems, the cell is said to be under oxidative stress (83).

Excessive ROS can damage cellular proteins, lipids, and DNA, which leads to cell death (83). Extracellular sources of ROS include various drugs, pollutants, and radiation; intracellular sources of ROS include mitochondria, endoplasmic reticulum, and NADPH complexes (85, 86). The major source of intracellular ROS generation is the mitochondrial electron transport chain, which produces electrons that react with oxygen to form ROS (84, 87, 88). The main type of ROS formed by the mitochondria is superoxide, which can spontaneously dismutate to H_2O_2 , or be converted to H_2O_2 by SOD in the mitochondrial matrix or by SOD in the cytoplasm (85, 89).

1.4.1 The role of ROS in cell signaling

Although ROS are often thought of as damaging to cells, ROS are also important in cell signaling, during which ROS may act as a secondary intracellular messenger or change protein structure and function by altering important amino acid residues (83). In particular, H_2O_2 has several features that allow it to function as an intracellular messenger, i.e., it can freely diffuse, it is uncharged and small, and it can be quickly synthesized and destroyed (89, 90). A variety of extracellular cell signaling stimuli that include cytokines, hormones and neurotransmitters induce intracellular H_2O_2 formation, which can subsequently affect the functions of transcription factors, kinases, and phosphatases (90–93). It is now recognized that at sub-cytotoxic levels H_2O_2 is a ubiquitous intracellular signaling messenger that oxidizes the cysteine residues of proteins (90). In cells stimulated with growth factors, members of the NOX family of NADPH oxidases produce H_2O_2 , which oxidizes protein tyrosine phosphatases (PTPs), as well as the tumor suppressor PTEN (also a PTP), to reversibly inactivate them and trigger downstream signaling events (94–97). H_2O_2 may also promote protein phosphorylation during cell signaling by activating protein tyrosine kinases; for example, H_2O_2 oxidizes the tyrosine kinase Src, causing it to become activated (98). H_2O_2 is also important for propagating signals from death receptors, such as TNFR1, during apoptosis (89).

Transcription of genes can be activated by ROS in several ways (99). ROS inhibition of phosphatases promotes kinase-mediated activation of transcription factor, such as NF- κ B, and their translocation to the nucleus (99). ROS also inhibits degradation of transcription factors resulting their accumulation in the nucleus; for example, ROS inhibits degradation of the hypoxia-inducible factor 1 α transcription factor (99). ROS also causes transcription of genes by oxidizing DNA (99). ROS can oxidize bases in the promoter of the vascular endothelial growth factor, which enhances binding of transcription factors to the promoter (100). Additionally, ROS are involved in transcriptional activation downstream of several receptors, including the androgen and oestrogen receptors, by causing formation of DNA breaks in regulatory regions of target genes (101).

ROS can also activate or mediate mitogen-activated protein kinase (MAPK) signaling pathways that are involved in biological processes that include apoptosis, inflammation, cell growth and differentiation, and responses to environmental stresses (83). There are three main types of MAPK pathways in mammalian cells: the c-Jun N-terminal kinases (JNKs), the extracellular signal-regulated kinases (ERKs), and the p38 MAPKs (83). Activation of MAPKs involves a 3-tiered system in which a MAPK kinase kinase (MAPKKK) phosphorylates and activates a MAPK kinase (MAPKK), which in turn phosphorylates and activates one or more MAPKs (102). Many different stimuli can activate MAPKs; however, JNKs and p38 MAPKs are usually activated in response to stress stimuli, while ERKs are activated in response to growth factors (103, 104). The p38 MAPK pathway can be activated by a number of different stress signals, including inflammatory cytokines and oxidative stress (102). There are four p38 MAPK isoforms: p38 MAPK α , p38 MAPK β , p38 MAPK γ , and p38 MAPK δ that differ in tissue distribution (most tissues express the α and β isoforms, while the expression of the γ and δ isoforms is more limited) and substrate specificity (105). Activated p38 MAPK proteins that translocate to the nucleus phosphorylate several different targets, such as transcription factors and kinases that are involved in many processes, including

cell proliferation, migration, differentiation, and cell death (83). The activation of p38 MAPK in cancer cells can have pro- or anti-tumorigenic effects, depending on the type of stimulus and the cell type (102). In many cancers, including breast cancer, the activity of p38 MAPK α is often upregulated, while in other types of cancer, such as liver cancer, the activity of p38 MAPK α is downregulated (102, 106–108). Some studies have shown the p38 MAPK activation can promote cancer cell apoptosis and inhibit proliferation, while other studies have found that p38 MAPK activation can be anti-apoptotic and actually promote cancer cell proliferation (109, 110). In breast cancer, p38 MAPK activates several transcription factors and proteins that promote cell invasion and metastasis (102, 111, 112). Alternatively, p38 MAPK signaling may also have anti-breast cancer effects. The negative regulators of p38 MAPK, known as mitogen-activated protein kinase phosphatases (MKPs), have been linked to breast cancer resistance to several chemotherapeutic drugs, as well as oxidative-stress induced cell death (113). Overexpression of MKPs in breast cancer *in vitro* causes inhibition of p38 MAPK signaling and increases resistance to hydrogen peroxide-induced cell death, indicating that p38 MAPK signaling is important for ROS-induced cell death (114).

1.4.2 ROS and cancer

ROS can be pro- or anti-tumorigenic (Figure 1.2), depending on the type of ROS, dose, site of ROS production, and duration. As mentioned earlier, ROS can activate several signaling pathways, including the p38 MAPK pathway, which may promote or inhibit tumor growth. ROS can cause direct oxidative DNA damage and also damage proteins that lead to structural changes in DNA (115–117). Continual exposure of normal cells to sub-cytotoxic levels of ROS over a long period of time may lead to somatic mutations and promote the malignant transformation of normal cells (116, 117). ROS can also contribute to tumorigenesis by causing mutations and functional changes in the tumor suppressors such as p53 and PTEN (97, 118). Chronic inflammation promotes

tumorigenesis via ROS that regulate inflammatory signaling (for example, ROS is important for signaling induced by the inflammatory cytokine TNF) (119, 120). Both exogenous and endogenous sources of ROS can induce cell proliferation in several different types of cancer, including breast cancer (85, 121–124). In breast cancer cells, ROS can promote increased NF- κ B activity and expression of c-Myc and heme oxygenase-1, which all enhance cell proliferation (124). There are some ROS-scavenging drugs that have anti-cancer effects, several of which are in clinical trials for cancer treatment, and might also be important for cancer prevention (85).

While ROS can have a tumor-promoting effect, especially at low levels, it can also be anti-tumorigenic. Activation of the extrinsic pathway of apoptosis generates ROS, which is important for propagating signals from death receptors to downstream signaling molecules for induction of apoptosis (92, 125). The intrinsic pathway of apoptosis is activated by a variety of stresses, including ROS, that promote MOMP causing apoptosis, or necroptosis (85). Several studies have shown that exposure of cancer cells to ROS directly or to drugs that cause ROS production can induce several types of cancer cells to undergo apoptosis (85, 126–128). ROS can modulate anti-apoptotic proteins, many different kinases, cell survival proteins, and transcription factors such as NF- κ B to promote cell death (85). Although ROS can promote cancer cell proliferation, ROS can also inhibit cancer cell proliferation (85). ROS can activate (by phosphorylation) various proteins involved in inhibiting cell cycle progression such as checkpoint kinase 1 (Chk1) and Chk2 (129). Additionally, in breast cancer cells, knockdown of redox proteins leads to increased ROS levels, causing a decrease in NF- κ B-dependent cell proliferation (130).

Unlike normal cells, cancer cells experience a continual pro-oxidative state (partly due to their increased metabolic activity) that causes them to have elevated ROS levels, leading to perpetual oxidative stress (84, 131–133). Cancer cells therefore have adapted antioxidant systems and increased pro-survival molecules to manage the constant oxidative stress (134). The difference in ROS levels between normal and cancer cells can be exploited therapeutically. Since

cancer cells have higher basal levels of ROS, a relatively modest increase in ROS could put them over their ROS tolerance and cause them to die, while a modest increase in ROS may remain below the cytotoxic tolerance threshold for normal cells (84). There are many drugs that promote ROS generation and many current chemotherapeutic drugs induce ROS in cancer patients (84, 85). For example, procarbazine (used for treatment of Hodgkin's and non-Hodgkin's lymphomas and primary brain tumors), doxorubicin (used for treatment of breast, thyroid, and gastric cancer), cisplatin (used in lung and ovarian cancer), and docetaxel (used in breast, gastric, lung, and prostate cancer) are just a few of many chemotherapeutic drugs that induce ROS formation and are approved anti-cancer drugs by the U.S. Food and Drug Administration (85). Another form of cancer treatment that induces cancer cell death by ROS is the use of ionizing radiation (135). The dose of ROS-inducing drugs and/or radiation must be carefully regulated to avoid doses that are sub-cytotoxic and could therefore be protumorigenic.

1.5 Phytochemicals

Phytochemicals are 'plant' chemicals that are non-nutrient bioactive compounds in foods such as vegetables, fruits, and whole grains (136). Phytochemicals are usually not essential for plant growth and survival, but they are considered secondary metabolites that have diverse functions such as UV protection, protection from microbial infection and herbivores, attractants for pollinators and seed dispersing animals, signaling molecules for the formation of nitrogen-fixing root nodules, and an allelopathic role (137–139). Humans ingest phytochemicals as part of their diet, and while phytochemicals are not essential for short-term health, there is a large body of evidence suggesting that they have favorable effects on human health in the long term, in part due to their potent antioxidant activity (136, 140). There are many epidemiological studies showing that higher intake of fruits, vegetables, and whole grains containing high levels of phytochemicals is associated with a reduced incidence of different cancers and

chronic diseases such as type II diabetes, cardiovascular disease, and impaired cognitive function (141–146).

More than 8,000 structurally diverse phytochemicals have been reported (137). Phytochemicals can be classified based on their structure as phenolics, carotenoids, alkaloids, organosulfur compounds, and nitrogen-containing compounds, and each of these groups can be further broken down into smaller, more specific groups (Figure 1.3) (136). The phenolics are the largest and best studied group of phytochemicals with a common feature of at least one aromatic ring bearing at least one hydroxyl group (136, 147). Of the several different classes of phenolics, the largest group is the flavonoids. The typical structure of flavonoids consists of two aromatic rings linked by three carbons (136, 137). Flavonoids are the most abundant phenolics in human diets; it is estimated that approximately two thirds of phenolics in the human diet are flavonoids (136). The estimated daily intake of flavonoids for humans ranges from 20 mg to 650 mg, with one report suggesting as high as 1 g (143, 148–152). Estimating dietary intake must be carefully interpreted because there is no agreement on the best method to analyze intake of different polyphenols, and many factors influence the formation of flavonoids in plants, including environmental conditions, light, processing and storage, degree of ripeness, and plant genetics (139, 153). Flavonoids are found in a wide variety of fruits and vegetables, as well as in beverages such as wine, tea, coffee, and cocoa (153). The flavonoids can be further classified into flavonols (e.g., quercetin and myricetin), flavones (e.g., apigenin, luteolin), flavanols (also known as catechins, e.g., epicatechin and epigallocatechin gallate), flavanones (e.g., naringenin and hesperitin), anthocyanidins (e.g., cyanidin and malvidin), and isoflavanoids (e.g., genistein and daidzein) (136).

In plant-based foods, flavonoids are primarily found as glycosylated conjugates (although some do exist in aglycone form), and this glycosylation influences their metabolism (140). The exact mechanism(s) of flavonoid absorption by intestinal cells are unclear, although the nature of the glycosylation in flavonoid conjugates may dictate the site of absorption (137, 140, 154, 155).

Following ingestion, the majority of flavonoids (especially aglycones) are thought to be absorbed into the bloodstream in the small intestine, but some are absorbed in the colon (137). Flavonoid conjugates can be hydrolyzed by enzymes (glycosidases) that are part of the intestinal brush border (156). Following removal of the sugar residue the flavonoid can passively diffuse across the brush border of the small intestine and be taken up by intestinal cells (156). Intact flavonoid conjugates can also be taken up into cells by active transporters, such as the sodium-dependent glucose transporter (SGLT1), and once in cells they can be cleaved by cytoplasmic glycosidases (157, 158). Once the flavonoid conjugates have been hydrolyzed to the free aglycone they are further modified and conjugated by glucuronidation, methylation, and/or sulfation (137, 140). The resulting metabolites then enter the bloodstream where they travel to the liver and are further metabolized (137, 159). Flavonoids that are resistant to the enzymes in the small intestine are not absorbed by the small intestine and pass into the colon where intestinal microflora play an important role in their absorption (160). Intestinal microflora enzymes cleave the conjugate flavonoids into smaller molecules, including phenolic acids and hydroxycinnamates that can then be absorbed and then metabolized by the liver (140, 161, 162). The rate extent of intestinal absorption is determined by the chemical structure of the flavonoid, although there are variations in absorption between individuals (154).

Phytochemical bioavailability (the fraction of a substance that is available in the human body for physiological functions) following ingestion of plant-based foods varies between phytochemicals and depends on their absorption and the dietary source (154). In feeding studies, measurable concentrations of isoflavones were found in human plasma despite that fact that isoflavones undergo considerable degradation in the gut (153, 163–165). Additionally, when human studies were conducted with raisin supplementation in healthy volunteers the majority of phytochemicals present in the raisins were present in human serum 1 h after ingestion, at levels that would protect serum from oxidation; this study indicated that ingestion of a plant-based food can result in bioavailable and bioactive levels of phytochemicals in human serum (166). For the flavonol

quercetin, bioavailability may vary depending on the dietary source; for example, the bioavailability of quercetin from red wine and apples was found to be much lower than from fried onions or black tea (153, 167, 168). The plasma concentration of most flavonoids decreases 1-2 h (elimination half-life) after absorption in the small intestine (140). Quercetin actually has an elimination half-life of close to 24 h, which is at least partially due to its affinity for plasma albumin (140, 168–170). One strategy that is being pursued to increase bioavailability and activity of phytochemicals for therapeutic use is nanoparticle technology (171). Nanotechnology can improve bioavailability of phytochemicals by protecting them from being degraded thereby increasing their stability, increase their solubility in aqueous solutions, increase circulation time and retention in tissues, and improve target specificity (171)

There have been many *in vitro* studies showing that flavonoids have anti-inflammatory properties, scavenge free radicals, alter enzyme activity, inhibit cell growth and proliferation, modulate cell death, and have antibiotic properties (143, 153, 166). All of the properties of phytochemicals described *in vitro* could contribute to the favorable effects of flavonoid consumption on the incidence of chronic diseases and cancer observed in epidemiological studies (137, 139, 141).

1.6 Phytochemicals and Cancer

There are many epidemiological studies that indicate consumption of fruits, vegetables, and whole grains containing phytochemicals is associated with a reduced risk of many types of cancer (141, 172–175). One study estimated that people with low fruit and vegetable intake have twice the risk of developing cancer compared to individuals with a high fruit and vegetable intake (172). For breast cancer, a low intake of flavonoids is associated with a higher cancer risk while a Mediterranean-style diet (one high in fruits, vegetables, and fish and low in red meat) is associated with a lower risk of developing breast cancer (176, 177). One of the mechanisms by which phytochemicals could play a role in

cancer prevention is by limiting ROS-induced DNA mutations and/or induction of signaling pathways that promote cell proliferation (136, 178, 179).

Phytochemicals can limit ROS production through their direct antioxidant activity or by inducing expression of antioxidant systems within cells (136, 178, 179).

There is great interest in using the anti-cancer properties of phytochemicals to develop new cancer therapeutics. Between 1940 and 2002, approximately 69% of drugs approved for treatment of cancer were natural products or derived from knowledge of the bioactive properties of natural products; for example, paclitaxel, docetaxel, and vincristine are all derived from plants (174, 180, 181).

Phytochemicals represent a good option for developing new therapeutics because they are considered safe, are easily obtained, do not have significant toxic effects for long-term therapy, and are often cytotoxic for cancer cells but not normal cells (174, 182–184). The structure of a phytochemical is important for its anti-cancer properties and different types of cancer may be more sensitive to certain structures (185). Both *in vitro* and *in vivo* studies with cancer cells lines have revealed that phytochemicals have a wide array of anti-cancer activities. Flavonoids can induce apoptosis of a variety of cancer cell types, as well as inhibit proliferation of cancer cells (186–190). The antioxidant activity of flavonoids is important for their anti-cancer effects but it is also recognized that at high doses many phytochemicals can have pro-oxidant properties that promote cancer cell death (191–194). Flavonoids can also modulate the expression of proteins involved in regulating the cell cycle; flavonoids can arrest cell cycle progression at different stages, causing cell proliferation to be inhibited (183, 195–198). Signal transduction and gene expression can be inhibited by flavonoids (199–202). Flavonoids can also inhibit angiogenesis and induce expression of tumor suppressor genes (136, 202–206). Invasion and metastasis of cancer cells can be prevented by flavonoids (207). Several intracellular proteins (cadherins, slug, vimentin, snail, and ZEB1) that are important for epithelial-mesenchymal transition (EMT), a process that is essential for metastasis, are modulated by flavonoids (208–213). Expression of matrix metalloproteinases (MMPs), which play a role in metastasis by degrading the

extracellular matrix surrounding tumor cells, can be inhibited by flavonoids (214–217). Two phytochemicals that have been studied extensively for their anti-cancer properties are epigallocatechin-3-gallate (EGCG) and resveratrol (218–221).

Green tea is a beverage that is consumed worldwide and its consumption has been associated with reduced cancer incidence (218, 222). The components of green tea that are largely responsible for its cancer preventative properties are a group of flavonoids called catechins (flavanols), of which the major and most active catechin is EGCG (218). EGCG inhibits proliferation and induces apoptosis in a variety of cancer cell types, including breast, lung, and colon cancer both *in vitro* and *in vivo* (218, 219, 223, 224). The activation of NF- κ B, which upregulates expression of proteins such as anti-apoptotic Bcl-2 proteins, is inhibited by EGCG, which also promotes stabilization of the p53 tumor suppressor (225). EGCG also induces expression of pro-apoptotic proteins such as Bak and Bax that contribute to mitochondrial membrane permeability (226). Inhibition of cancer cell proliferation by EGCG is caused by induction of cell cycle arrest through EGCG modulation of cell cycle proteins including cyclins and cyclin dependent kinases (CDKs) (218, 227–229). EGCG can act as an antioxidant preventing ROS-induced damage to cells; however, EGCG can also have pro-oxidative activities (218, 226, 230, 231). EGCG-induced apoptosis is the result of EGCG-generated ROS and activation of caspase-3 and caspase-9 (226). Cell death induced by EGCG can also be promoted by activation of the JNK and p38 MAPK signaling pathways (226). EGCG can also inhibit cancer cell invasion and metastasis by inhibiting proteins necessary for EMT, e.g., vimentin, β -catenin, slug, and snail (232).

Resveratrol (3, 4', 5-trihydroxystilbene) is a phytochemical that belongs to the stilbene class of phenolic phytochemicals (233). Resveratrol is found in a variety of foods such as red grapes, peanuts, berries, and red wine (221, 233). Studies have shown that resveratrol has anti-cancer effects for several types of cancer, including breast, colon, skin, esophageal, gastric, pancreatic, and prostate cancer (220). Resveratrol can modulate Fas ligand and the Fas receptor

to induce apoptosis and, like EGCG, can inhibit NF- κ B signaling to promote apoptosis in a variety of cancer cell types (234–236). Expression of both survivin and induction of the Wnt signaling pathway are inhibited by resveratrol, which promotes cancer cell death and/or inhibits cancer cell proliferation (237–239). Resveratrol, like EGCG, can modify the expression and actions of cell cycle proteins, including cyclin D1, CDK2, and CDK4, to inhibit cell proliferation (240, 241). Cancer cell invasion and metastasis can be limited by resveratrol as resveratrol decreases expression of MMPs, such as MMP-2 and MMP-9 (242, 243). One problem with the use of resveratrol as a therapeutic agent is that its bioavailability is relatively low; however, in mice topical application of resveratrol inhibits UVB-induced skin damage and reduces the incidence of skin cancer (244, 245). In addition, prophylactic administration of resveratrol to rats leads to a decreased incidence of carcinogen-induced esophageal and intestinal tumors, indicating that resveratrol may be useful in preventing cancer (245).

1.7 Myricetin and cancer

Myricetin is a phytochemical belonging to the flavonol class of flavonoids (Figure 1.3), and is found in foods and beverages such as red grapes, broccoli, cabbage, chili peppers, garlic, guava, berries, honey, black tea, green tea, and red wine (Figure 1.4) (246–249). Several studies have shown that myricetin may be beneficial for a variety of diseases and overall health, including improvement of bone health and prevention of osteoporosis, protection against several conditions associated with diabetes (oxidative stress in erythrocytes, diabetic nephropathy, hyperglycemia), improvement of male gamete function, cardioprotection against myocardial infarction, and prevention and treatment of cancer (250–258). There is little epidemiological data examining the relationship between myricetin and cancer because it is difficult to measure intake of a specific phytochemicals in the diet, but there are studies showing that intake of foods high in flavonols is associated with a decreased risk of breast cancer (259). A study by Knekt *et al.* that examined intake of several flavonoids and risk of

different cancers in Finland found that high intake of myricetin was associated with lower prostate cancer risk (141). The average daily intake of myricetin for a person with a balanced diet is estimated to be approximately 1.5 mg (136). It is thought that metabolism of myricetin, following ingestion, is dependent on intestinal microflora (260). In humans who consumed cranberry syrup, myricetin metabolites, as well as native myricetin, were detected in their urine (261).

Both *in vitro* and *in vivo* studies have revealed that myricetin is active against a number of different cancers (Table 1.1), including colorectal, bladder, lung, oral, skin, esophageal, brain, and pancreatic cancer, as well as leukemia (262–269). Myricetin is cytotoxic for several human cancer cell lines, including the human promyeloleukemic cell line HL-60, in which myricetin causes apoptosis (269–271). Myricetin induced caspase-3 and caspase-9 activation and decreased anti-apoptotic Bcl-2 protein expression, while increasing pro-apoptotic Bcl-2 protein (Bax and Bad) expression in HL-60 cells (269, 271). Myricetin also caused MOMP and release of cytochrome c from the mitochondria, thereby promoting apoptosis (269). These studies suggested that myricetin-induced apoptosis is not ROS-dependent since myricetin does not significantly increase ROS levels in HL-60 cells (269–271). Importantly, myricetin did not alter the viability of normal blood cells (269). However, in A549 human lung cancer cells, myricetin-induced cytotoxicity was dependent on ROS, as well as inhibition of the thioredoxin system, which is important for antioxidant function and maintenance of cell viability (272). In human bladder cancer cells, myricetin-induced apoptosis also involved activation of the p38 MAPK signaling pathway and inhibition of the phosphatidylinositol 3-kinase (PI3K) signaling pathway (263, 268). Induction of cell death by myricetin may also involve AIF release from the mitochondria, which can lead to AIF-mediated necroptosis (262). Myricetin can also inhibit cancer cell proliferation by causing cell cycle arrest in different stages of the cell cycle, depending on the cancer cell type, via modulation of CDKs and cyclins that are important for cell cycle regulation (250, 263, 265, 272). Cancer cell migration and invasion are also inhibited by myricetin. In medulloblastoma cells, myricetin inhibits hepatocyte growth factor-induced actin re-organization that is essential

for cell migration (267). Myricetin also inhibits migration and invasion of cancer cells by inhibiting the ERK and NF- κ B signaling pathways, and inhibiting expression and activity of MMPs (250, 263–265, 267). In addition to having intrinsic chemotherapeutic properties, myricetin enhances the action of other cancer therapeutics. For example, myricetin enhances the suppression of human lung cancer cell growth by X-ray treatment both *in vitro* and in mouse xenograft models (273). In addition, myricetin enhances intestinal absorption of cancer chemotherapeutic drugs tamoxifen and doxorubicin in rats; this suggests that lower doses of chemotherapeutic drugs could be given if used in combination with myricetin (274, 275).

There have been very few studies examining the effects of myricetin on breast cancer. A study by Rodgers and Grant shows that myricetin has no effect on the growth of MCF-7 human breast cancer cells and causes increased intracellular glutathione content (276). In contrast, Kuntz et al. found myricetin to inhibit the growth of MCF-7 cells (277). In a model of breast cancer using female Wistar rats exposed to dimethyl beanthracene (DMBA, a procarcinogen that selects for breast cancer in female Wistar rats) in order to induce carcinogenesis, oral myricetin increased SOD levels in plasma and breast tissue, thereby preventing DMBA-induced oxidative damage and DMBA-induced tumor formation (278).

1.8 Rationale and Objectives

This study focuses on the effects of myricetin on triple-negative breast cancer cells. There are several studies indicating the myricetin has anti-cancer properties but few studies have examined the effects of myricetin on breast cancer cells, and there are no studies examining the effects of myricetin on the triple-negative subset of breast cancer cells. Given that treatment options for triple-negative breast cancer are limited and the prognosis is worse for triple-negative breast cancer patients compared to patients with other breast cancer subsets, new treatment strategies are needed. In addition, the mechanisms by

which myricetin induces cancer cell death remain unclear and seem to vary depending on the type of cancer being studied (269, 272). The objectives of this study were to first determine if myricetin could induce triple-negative breast cancer cell death, and secondly, to determine the mechanism(s) involved in myricetin-induced death of triple-negative breast cancer cells.

Figure 1.1. The apoptotic and necroptotic cell death pathways. *Extrinsic apoptotic pathway:* binding of Fas ligand (FasL) to the Fas receptor promotes the formation of DISC (death-inducing signaling complex) containing FADD, pro-caspase 8, and the cytoplasmic domain of the Fas receptor. DISC cleaves pro-caspase-8 to active caspase-8, which subsequently cleaves and activates caspase-3/6/7 that then execute apoptosis. Caspase-8 can also activate Bid that can promote intrinsic apoptosis. *Intrinsic apoptotic pathway:* cell stress stimuli activate pro-apoptotic proteins, such as Bax and Bak that cause pore formation in the outer mitochondrial membrane, leading to mitochondrial outer membrane permeabilization (MOMP). Cytochrome C (Cty C) released from the mitochondria forms a complex with Apaf-1 and pro-caspase-9 called the apoptosome. The apoptosome activates caspase-9, which activates caspase-3/6/7 that promote apoptosis. Smac released from the mitochondria inhibits anti-apoptotic proteins (IAPs), while apoptosis-inducing factor (AIF) released from the mitochondria can promote necroptosis. *Necroptotic pathway:* Binding of TNF α to TNFR1 promotes formation of complex I containing TRADD, RIPK1, TRAF, and ciAP. RIPK1 and TRAF are ubiquitinated by ciAP which promotes signaling through NF- κ B (not shown). If CYLD is present it causes de-ubiquitination of RIP1 and TRAF promoting formation of complex II. Complex II consists of RIP1 and RIP3 kinases, FADD, TRADD, and caspase-8. If caspase-8 is active it cleaves and inactivates RIP1 and RIP3, and then it will activate apoptosis. If caspase-8 activity is inhibited then RIP1 and RIP3 will be active and will promote necroptosis.

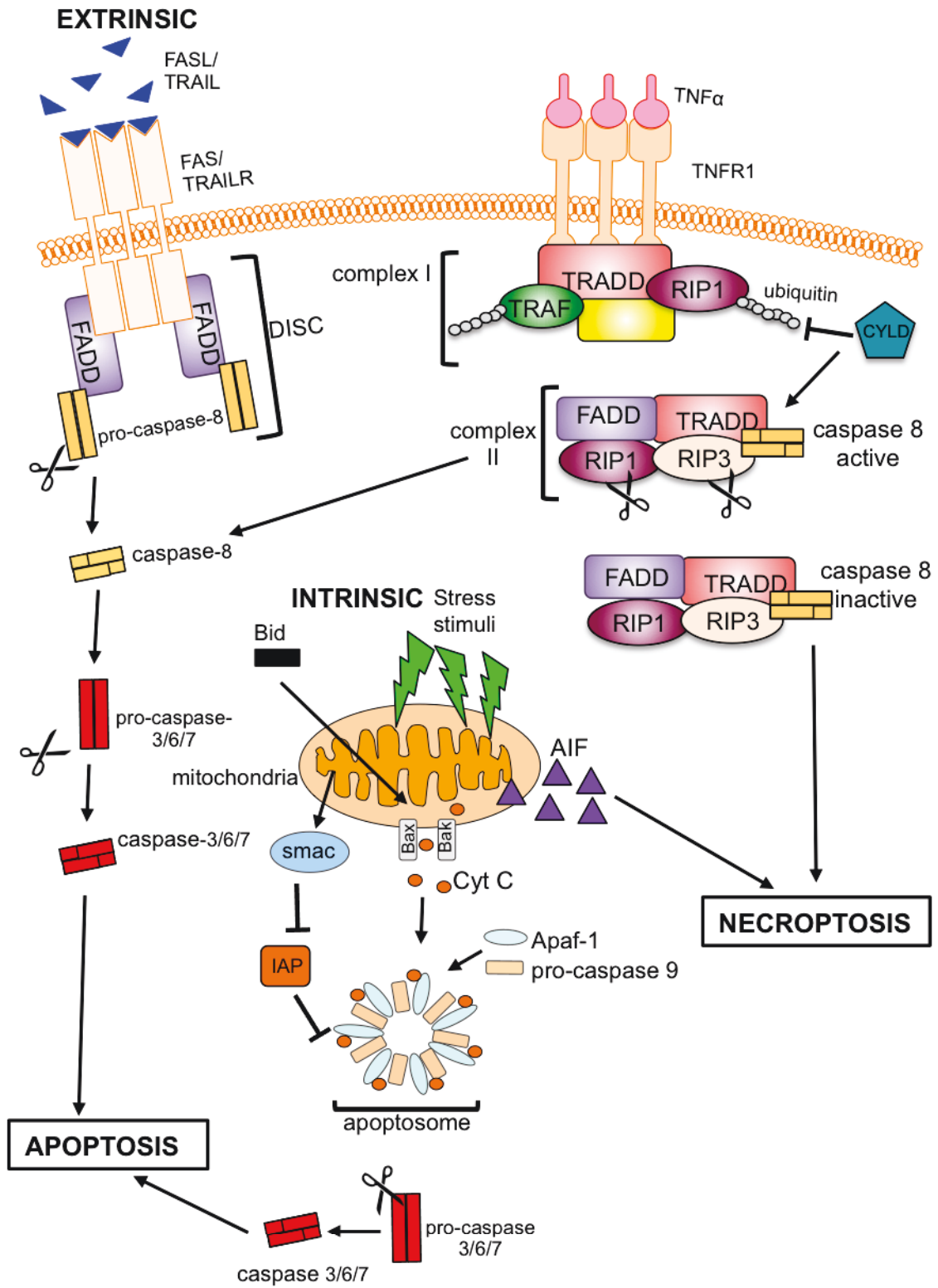


Figure 1.1

Figure 1.2. The effects of ROS on cancer. Depending on the type and level of ROS, ROS can be pro- or anti-tumorigenic. A low level of ROS usually promotes tumor development and growth, while a high level of ROS tends to inhibit tumor growth by causing cell death.

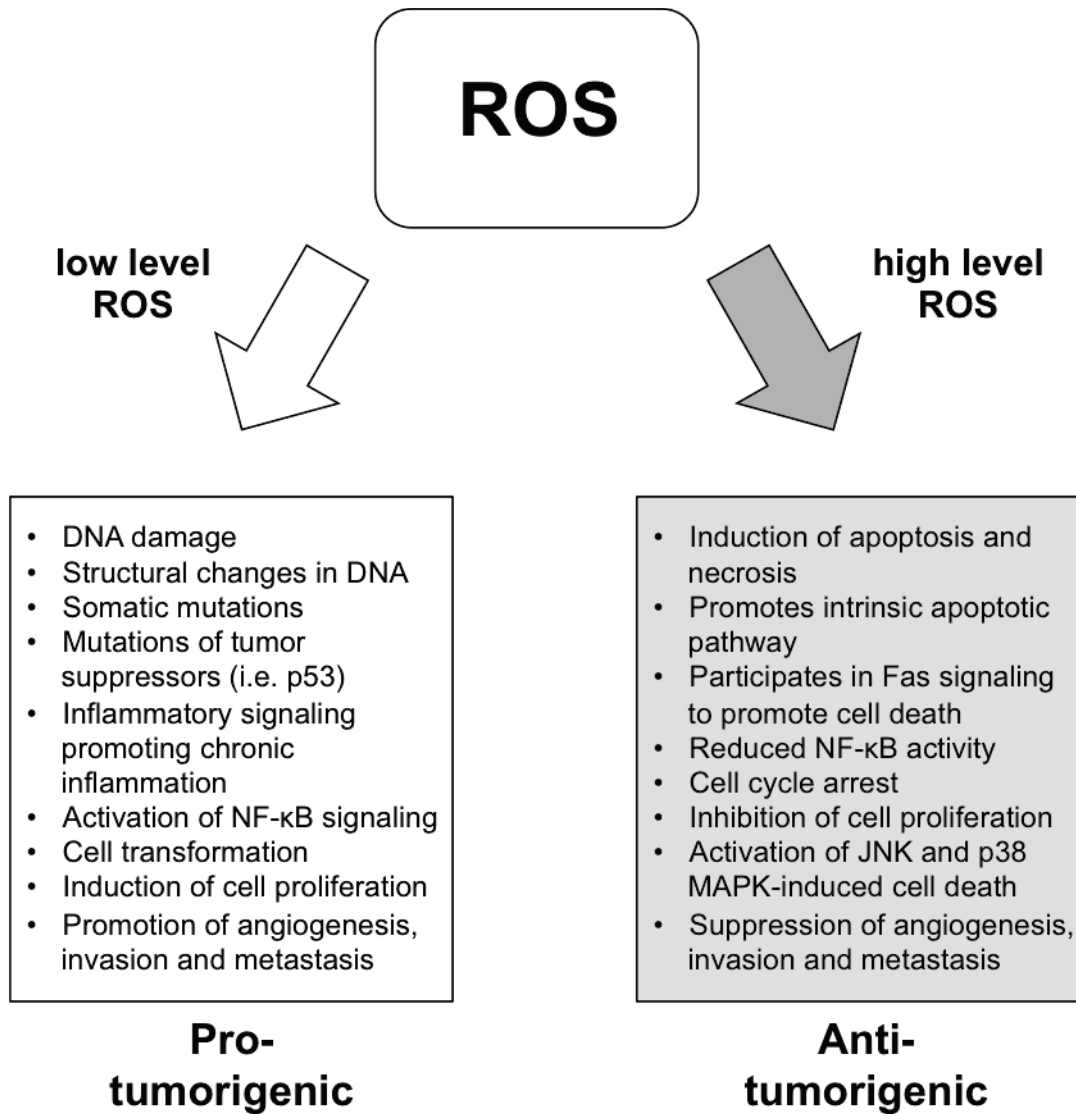


Figure 1.2

Figure 1.3. Classification of phytochemicals. Phytochemicals can be classified into different groups based on their structure. The major class of dietary phytochemicals are the phenolics. Flavonoids are the most common phenolics in the human diet. Myricetin belongs to the flavonol group of flavonoids.

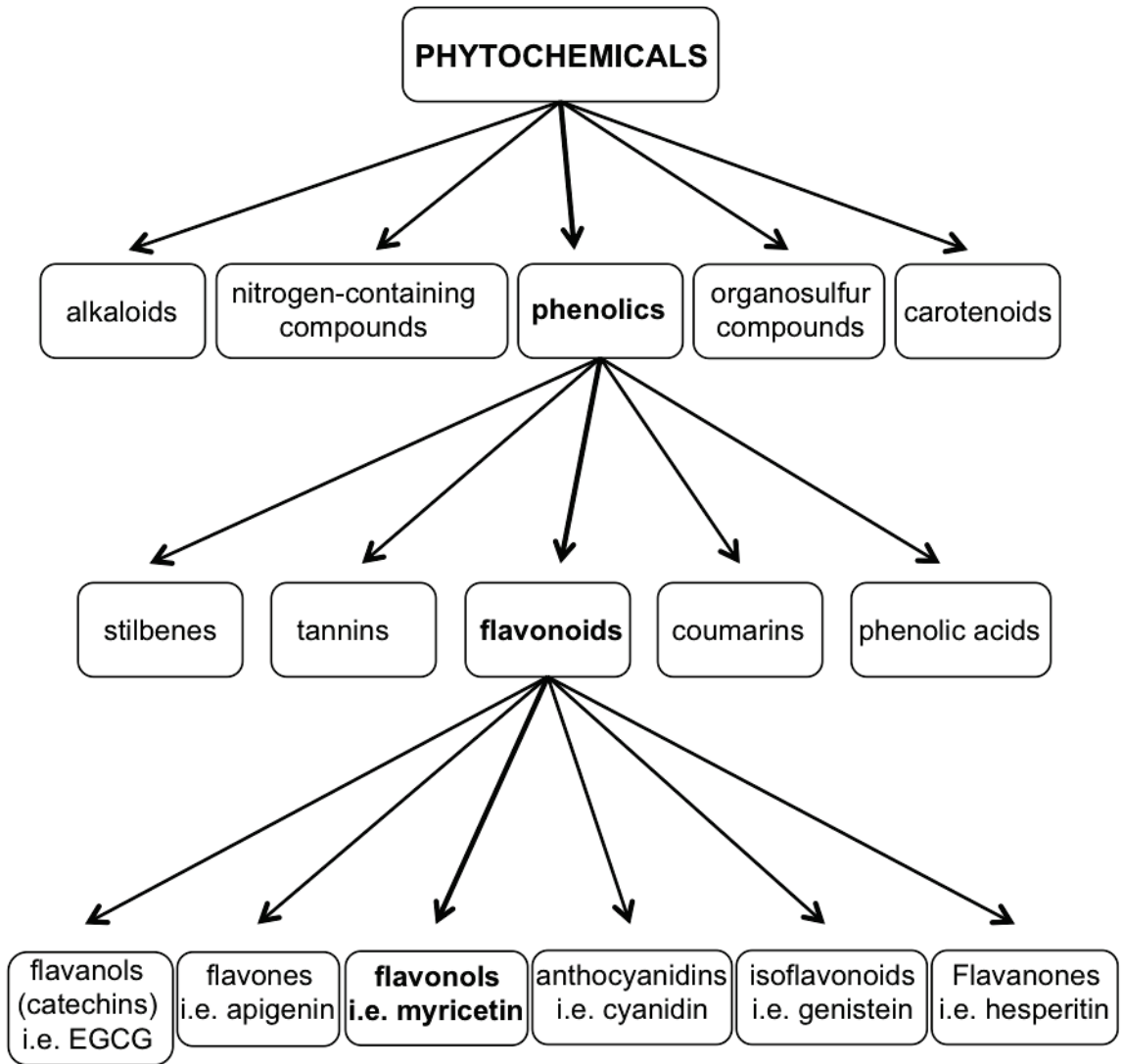


Figure 1.3

Figure 1.4. The chemical structure of myricetin. The chemical structure of myricetin is typical for phenolics, which contain at least one aromatic ring bearing one hydroxyl group. More specifically, myricetin is typical of the flavonoid class of phenolics, which contain two aromatic rings linked by three carbons.

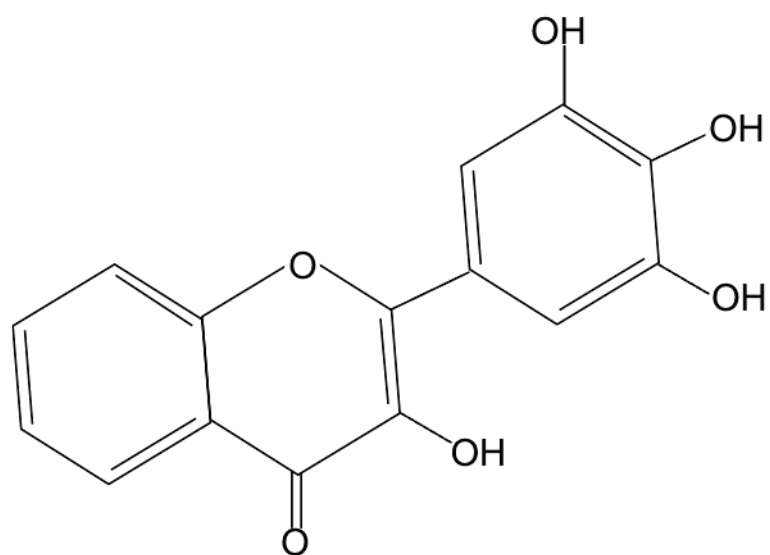


Figure 1.4

Table 1.1. The effects of myricetin on different types of human cancer cell lines and mouse xenograft models of human cancer.

| Cancer type | Effects of myricetin treatment | References |
|--------------------|---|-------------------|
| Bladder | <p>↑apoptosis, ↓proliferation, ↑ G2/M cell cycle arrest ↓ migration, ↑ p38 MAPK, ↓ Akt phosphorylation, ↓ MMP-9, ↓ tumor growth <i>in vivo</i></p> | (258) |
| Colorectal | <p>↑ Apoptosis, ↑ Bax and Bak, ↓ proapoptotic Bcl-2, ↑ AIF release</p> | (257) |
| Esophageal | <p>↓ proliferation, ↑ apoptosis, ↓ invasion and migration, ↑ G1 cell cycle arrest, ↓ tumor growth <i>in vivo</i></p> | (245) |
| Leukemia | <p>↑ apoptosis ↑ Caspase-3 and Caspase-9 activation ↑ Cytochrome C release ↓ prop-apoptotic Bcl-2 ↑ Bax and Bad</p> | (264-266) |
| Lung | <p>↓ viability, ↑ ROS, ↓ thioredoxin system, ↓ migration and invasion, ↓ MMP-2, ↓ ERK signaling, ↓ NF-κB signaling</p> | (259, 267) |
| Medulloblastoma | <p>↓ migration, ↓ HGF-induced actin reorganization</p> | (262) |
| Pancreatic | <p>↑ apoptosis, ↓ Akt phosphorylation, ↓ tumor growth <i>in vivo</i></p> | (263) |

CHAPTER 2

MATERIALS AND METHODS

2.1. Cell lines and primary cells

MDA-MB-468 human breast carcinoma cells were generously provided by Dr. P. Lee (Dalhousie University, Halifax, NS), Dr. S. Drover (Memorial University of Newfoundland, St. John's, NL) provided MDA-MB-231 human breast carcinoma cells, and Dr. Jean Marshall (Dalhousie University) provided 4T1 mouse mammary carcinoma cells. E0771 mouse mammary carcinoma cells were provided by Dr. Jun Wang (Dalhousie University). MCF-7 and SK-BR-3 human mammary carcinoma cells were provided by Dr. K Goralski and Dr. G. Dellaire (Dalhousie University), respectively. Normal human mammary epithelial cells (HMEpiC) were purchased from ScienCell Research Laboratories (San Diego, CA). Normal human dermal fibroblasts were purchased from Lonza Inc. (Walkersville, MD).

2.2. Reagents

Myricetin, Dulbecco's Modified Eagle Medium (DMEM), phenol red-free DMEM, phosphate buffered saline (PBS), dimethyl sulfoxide (DMSO), Triton-X-100, phosphatase substrate, sodium acetate, phenylmethylsulfonyl fluoride (PMSF), β -mercaptoethanol, 30% w/v H_2O_2 , super oxide dismutase (SOD), catalase, N-acetylcysteine (NAC), sodium deoxycholate, Nonidet P-40 (NP-40), aprotinin, leupeptin, sodium fluoride (NaF), pepstatin A, dithiothreitol (DTT), phenylarsine oxide (PAO), and bovine serum albumin (BSA) were purchased from Sigma-Aldrich Canada Ltd. (Oakville, ON). L-glutamine, fetal bovine serum (FBS), 1 M N-2-hydroxyethylpiperazine-N'-2-ethanesulfonic acid (HEPES) buffer, 10,000 U/ml penicillin/10,000 μ g/ml streptomycin solution, 3,3'-dihexyloxacarbocyanine iodide ($DiOC_6$), 0.25% trypsin-EDTA or TrypLE™

Express, Amplex® Red, horseradish peroxidase (HRP), propidium iodide (PI), and 2', 7'-dichlorofluorescein diacetate (DCFDA) were purchased from Life technologies (Burlington, ON). Mammary Epithelial Cell Medium (MEpiCM) and accompanying supplements were purchased from ScienCell Research Laboratories (San Diego, CA). Fibroblast Growth Medium-2 (FGM-2) and appropriate supplements were purchased from Lonza Inc. (Walkersville, MD). Sodium hydroxide (NaOH) was purchased from Fisher Scientific (Ottawa, ON). Annexin-V-FLUOS was purchased from Roche Diagnostics (Laval, QC). Sodium chloride (NaCl), ethylene glycol tetraacetic acid (EGTA), Tris base, Tween-20, sodium dodecyl sulfate (SDS), acrylamide/bis-acrylamide (29:1, 30% solution), tetramethylethylenediamine (TEMED), ammonium persulfate (APS), and glycine were purchased from Bio-Shop Canada Inc. (Burlington, ON). Ethylene diamine tetraacetic acid (EDTA) and disodium hydrogen phosphate (Na_2HPO_4) were purchased from EM 46 Industries Inc. (Hawthorne, NY). Sodium orthovanadate (Na_3VO_4) and calcium chloride (CaCl_2) were purchased from EMD Chemicals, Inc. (Gibbstown, NJ). Foxp3 fixation/permeabilization concentrate and diluent, and 10x permeabilization buffer were purchased from eBioscience, Inc. (San Diego, CA). p38 MAPK inhibitor III was purchased from EMD Millipore (Etobicoke, ON).

2.3. Antibodies

Rabbit anti-phospho-p38 MAPK (pTpY180/182) antibody was purchased from Invitrogen. Rabbit anti-p38 MAPK antibody was purchased from Cell Signaling Technology (Beverly, MA). Primary goat anti-actin antibody (I-19), and the secondary antibodies HRP-conjugated bovine anti-goat and HRP-conjugated donkey anti-rabbit were purchased from Santa Cruz Biotechnology (Santa Cruz, CA). Anti-Human/Mouse phospho-H2AX (S139) eFluor® 660 and Mouse IgG1 K isotype control eFluor® 660 were purchased from eBioscience.

2.4. Culture medium and conditions

Breast carcinoma cells were maintained in a humidified 10% CO₂ incubator at 37°C and cultured in DMEM supplemented with 2 mM L-glutamine, 100 U/ml penicillin, 100 µg/ml streptomycin, 10% heat-inactivated (56°C for 30 min), FBS and 5 mM HEPES buffer (pH 7.4); from this point on it is referred to as complete DMEM (cDMEM). HMEpiC were maintained in a humidified 5% CO₂ incubator at 37°C and cultured in MEpiCM supplemented with a supplied penicillin/streptomycin solution and mammary epithelial cell growth supplement mixture (ScienCell Research Laboratories). Human dermal fibroblasts were cultured in Fibroblast Growth Medium-2 (FGM-2) containing supplements from the supplier (Lonza Inc.) that included 2% FBS, recombinant human insulin, recombinant human fibroblast growth factor-B (rhFGF-B), gentamicin sulfate and amphotericin-B. Breast carcinoma cells and human dermal fibroblasts were grown in 75 mm² tissue culture flasks (Corning Inc., Tewksbury, MA) and were passaged at 70-80% confluency using 0.25% trypsin-EDTA or TrypLE™ Express (Life technologies, Oakville, ON). HMEpiC were cultured in 75 cm² tissue culture flasks coated with 0.015 mg/ml poly-L-lysine (ScienCell Research Laboratories) for 1 h and washed with sterile H₂O prior to culturing. Both human dermal fibroblasts and HMEpiC were cultured for a maximum of 8-10 passages. The vehicle used for myricetin was DMSO; the myricetin stock was made up at 100 mM in DMSO and stored at -80°C.

2.5. Cell seeding

All cell lines used were adherent and were therefore seeded 1 d before treatment to allow them to adhere to tissue culture plates and flasks. For all experiments and all cell types, cells were treated in cDMEM. For all experiments involving NAC (used at 10 mM), Z-VAD-fmk (50 µM), necrostatin-1 (40 µM), sodium pyruvate (100 µM or 1 mM), SOD (5 U/ml) and catalase (30 U/ml), and p38 MAPK inhibitor III (10 µM), the respective compounds were added at least

30 min prior to treatment with myricetin; these compounds were not washed from the cells prior to myricetin treatment. Concentrations of these compounds were based on published (279) and unpublished work by members of my lab (Dr. Melanie Coombs and Dr. Carolyn Doucette) indicating that these concentrations were non-cytotoxic and had functional activity.

2.5.1. Human breast carcinoma cells

For acid phosphatase and Amplex Red® assays, cells were seeded in triplicate or quadruplicate in 96-well flat bottom plates at 5×10^3 cells/well in 100 μ l of medium. For annexin-V-FLUOS/PI staining, 3,3'-Dihexyloxacarbocyanine iodide (DiOC₆) staining and γ -H2AX antibody staining, cells were seeded in 6-well flat bottom plates at 1×10^5 cells/well for 4 h treatments and 5×10^4 cells/well for 24 and 48 h treatments in 2 ml of medium. For DCFDA staining, cells were seeded at 1×10^5 cells/well in 6-well flat bottom plates in 2 ml of medium. For western blotting, cells were seeded in 75 cm² flasks at 7×10^5 cells/flask in 10 ml of medium.

2.5.2. Mouse mammary carcinoma cells

For acid phosphatase assays, mouse mammary carcinoma cells were seeded at 3×10^3 cells/well in 96 well plates in 100 μ l of medium. For annexin-V-FLUOS/Propidium iodide staining and DiOC₆ staining, cells were seeded in 6-well plates at 2×10^4 cells/well in 2 ml of medium.

2.5.3. Human dermal fibroblasts

Cells were seeded at 5×10^3 cells/well in 96-well flat bottom plates in 100 μ l of medium for acid phosphatase assays. Cells were seeded in FGM-2, which was removed prior to myricetin treatment, and treated with myricetin in cDMEM.

2.5.4. Human mammary epithelial cells (HMEpiC)

For acid phosphatase assays, cells were seeded at 5×10^3 cells/well in Corning CellBIND 96-well flat bottom plates in 100 μ l of medium. Cells were seeded in MEpiCM, which was removed prior to myricetin treatment, and treated with myricetin in cDMEM.

2.6. Acid Phosphatase Assay

An acid phosphatase colorimetric assay was used to determine the phosphatase activity (an indicator of cell number) in cell cultures exposed to various treatments at different time points (24, 48, and 72h). The acid phosphatase assay quantifies relative cell number based on the conversion of *p*-nitrophenyl phosphate (pNPP) to *p*-nitrophenyl by cytosolic acid phosphatase (280). The *p*-nitrophenyl product is yellow under basic conditions and has an absorbance of 405 nm, which is measured as an indicator of cell number. When the desired time point was reached, 96-well plates were centrifuged at $1400 \times g$ for 5 min. The supernatant was discarded and the cells were washed twice with 1X PBS. Following the PBS washes, 100 μ l of fresh PBS and 100 μ l of phosphatase buffer (4 mg/ml phosphatase substrate, 0.1% Triton X-100 and 0.2 M sodium acetate, pH 5.5) were added to each well and cells were incubated for 2 h at 37°C in a humidified 10% CO₂ incubator. After 2 h, 10 μ l of 1 N NaOH was added to each well to stop the chemical reaction and plates were shaken at 550 rpm for 3 min on a Microplate Genie (Montreal Biotech Inc., Montreal, QC). Absorbance was measured at 405 nm using an Expert 96 microplate reader (Biochrom ASYS, Cambridge, UK). The percent phosphatase activity decrease was calculated using the equation $(1 - (\text{experimental reading} / \text{medium control reading})) \times 100$. The percent phosphatase activity decrease was used as an indicator of total cell number with a greater decrease in phosphatase activity indicating the presence of fewer cells.

2.7. Amplex® Red assay

Amplex® Red (N-acetyl-3,7-dihydroxyphenoxazine) assays were used to measure formation of H₂O₂ by myricetin in cell culture medium in the presence and absence of cells. In the presence of H₂O₂ the HRP-catalyzed oxidation of Amplex® Red, a colorless and non-fluorescent compound, to the red and fluorescent product resorufin can be measured (281). The reaction stoichiometry of Amplex® Red and H₂O₂ is 1:1 (281). For cell-free experiments, 100 µl of myricetin in phenol red-free cDMEM was added to 96-well flat bottom plates in triplicate. A master mix containing Amplex® Red and HRP in phenol red-free cDMEM (Sigma) was added to the 96-well plates at 100 µl/well for a final concentration per well of 25 µM Amplex® Red and 0.005 U/ml HRP. H₂O₂ was used as a positive control (0.1 mM). Plates were incubated for 4 h at 37°C in a humidified 10% CO₂ incubator and after 4 h absorbance was measured at 570 nm using an Expert 96 microplate reader. Plates were then incubated for 24 h at 37°C in a humidified 10% CO₂ incubator and absorbance was measured at 570 nm. For experiments with human breast carcinoma cells were seeded at 5 × 10³ cells/well in a 96-well flat bottom plate 1 d prior to treatment with myricetin and the experiments were carried out as described above.

2.8. Flow Cytometry

For all experiments fluorescence data was acquired for 1 × 10⁴ counts per sample using a FACSCalibur flow cytometer with BD CellQuest™ software (version 3.3, BD Biosciences, Mississauga, ON). Myricetin is inherently fluorescent (Appendix Figure 4), but this fluorescence was considered negligible compared to the large shifts in fluorescence observed in myricetin-treated cells that were also treated with DiOC₆, DCFDA, or anti-phospho-H2AX eFluor® 660. Where appropriate, myricetin-treated cells alone were included as a control. FCS Express software (version 3.0, De Novo Software, Thornhill, ON) was used to analyze the data.

2.8.1. Annexin-V-FLUOS/PI staining

Annexin-V-FLUOS/PI staining was used to determine apoptosis in breast carcinoma cells treated with myricetin. In healthy cells, phosphatidylserine (PS) is found on the cytoplasmic side of the inner leaflet of the plasma membrane (282). During the early phases of apoptosis PS translocates to the outer leaflet of the plasma membrane where it is exposed on the external surface of the cell (282). Annexin-V is a protein that binds phospholipids in a Ca^{2+} -dependent manner and has a high affinity for binding PS (283); therefore, binding of fluorochrome-tagged Annexin-V can be used as a marker of early apoptosis. PI is a fluorescent DNA intercalating agent that only enters cells when the cell membrane becomes permeable, such as when the cells are undergoing necrosis. Fluorochrome-tagged Annexin V can be used to stain cells in conjunction with PI staining to distinguish non-apoptotic cells (Annexin-V⁻/PI⁻) from cells undergoing apoptosis (Annexin-V⁺/PI⁻) and necrosis (Annexin V⁺/PI⁺), as measured by flow cytometry (284). Cells were treated with myricetin in cDMEM, or for experiments involving NAC and SOD/catalase cells were treated in serum-free DMEM to prevent any artifacts resulting from SOD and catalase present in serum. After 24 or 48 h treatment with the indicated concentrations of myricetin, NAC, SOD/catalase, p38 inhibitor, or necrostatin-1 the medium from each sample was removed and transferred to 5 ml round bottom tubes. To lift cells from the tissue culture plate 1 ml of TrypLE ExpressTM was added to each sample and plates were incubated in a humidified 10% CO₂ incubator at 37°C for 3-5 min. The cells were removed from the tissue culture plates and placed in the 5 ml tubes containing their respective medium. Samples were centrifuged at 500 × g for 5 min, supernatants were discarded, and cells re-suspended in 1 ml of 1X PBS. Cells were centrifuged for 5 min at 500 × g, supernatants were discarded, and cells resuspended in 50 µl of Annexin-V-FLUOS/PI labeling buffer which contained 5 mM CaCl₂, 10 mM HEPES, 140 mM NaCl, 2% Annexin-V-FLUOS reagent (v/v) (Roche Diagnostics) and 1 µg/ml PI (Life Technologies). Samples were incubated for 15 min at room temperature, 0.45 ml of labeling buffer was added

to each sample and samples were analyzed by flow cytometry. As proper controls, unstained, Annexin-V-FLUOS single-stained and PI single-stained samples were included to compensate for the overlapping emission spectra of Annexin-V-FLUOS and PI during analysis by flow cytometry.

2.8.2. DiOC₆ staining

The DiOC₆ assay was used to measure mitochondrial transmembrane potential (MTP). Healthy mitochondria have a high MTP and the inner mitochondrial membrane is negatively charged (285). As a result, cationic, lipophilic fluorescent probes such as DiOC₆ will localize to the mitochondrial matrix with a high MTP and form fluorescent aggregates (285). In mitochondria with reduced membrane stability, the MTP is lowered and charge distribution is altered in a way that prevents DiOC₆ from localizing to the mitochondrial matrix; this results in reduced fluorescence (285). Cells were treated with myricetin in cDMEM, or for experiments involving NAC and SOD/catalase, cells were treated in serum-free DMEM to prevent any artifacts resulting from SOD and catalase present in serum. After 4 or 24 h treatment with indicated concentrations of myricetin, NAC, or SOD/catalase, medium was removed from each sample and placed in 5 ml round-bottom tubes. Cells were then lifted from the tissue culture plate using 1 ml TrypLE ExpressTM added to each sample, and incubating plates for 3-5 min in a humidified 10% CO₂ incubator at 37°C. Cells were then transferred from tissue culture plates to the 5 ml round-bottom tubes containing their corresponding medium. Samples were centrifuged for 5 min at 500 × g, supernatants were discarded and cells were re-suspended in 1 ml of cDMEM or serum-free DMEM. Cells were stained with 40 nM DiOC₆ for 30 min at 37°C in a humidified 10% CO₂ incubator. Cell fluorescence was measured by flow cytometric analysis. FCS Express was used to analyze the decrease in fluorescence intensity to determine the % decrease in mitochondrial membrane stability.

2.8.3. DCFDA assay

To assess levels of reactive oxygen species in cells following myricetin treatment the DCFDA assay was used. DCFDA is a non-fluorescent compound that is cell permeable and can be used as a probe for intracellular ROS. When DCFDA enters cells it is cleaved by intracellular esterases to the cell impermeable product H₂DCF (286). If ROS is present in the cells H₂DCF is oxidized to DCF which is fluorescent and can be detected by flow cytometry; therefore, the more ROS present the more DCF is formed and a greater fluorescence is observed (286). After allowing cells to adhere to tissue culture plates overnight, the medium was removed and cells were washed once with 1XPBS. The PBS was removed and cells were stained with 5 μM DCFDA in phenol red-free, serum-free medium for 30 min at 37°C in a humidified 10% CO₂ incubator. After 30 min the stain was removed and cells were washed once with PBS. Cells were then treated with indicated concentrations of myricetin and NAC for 4 h in phenol red-free DMEM supplemented with 1% FBS. After 4 h, medium was removed from each sample and placed in a 5 ml round-bottom tubes. Cells were then lifted from the tissue culture plate using 1 ml TrypLE Express™ added to each sample, and incubating plates for 3-5 min at 37°C in a humidified 10% CO₂ incubator. Cells were then transferred to the 5 ml round-bottom tubes containing their corresponding medium. Samples were centrifuged for 5 min at 500 × g, supernatants were discarded and cells were re-suspended in 350 μl cold 1X PBS. Samples were kept on ice and cellular fluorescence was measured by flow cytometry. For analysis by flow cytometry 1 × 10⁴ live cell counts were measured.

2.8.4. Intracellular antibody staining for γ-H2AX

To determine DNA damage in cells following myricetin treatment, levels of γ-H2AX, a marker of double-stranded DNA damage (287), were assessed. After allowing the cells to adhere to tissue culture plates overnight, the medium was

replaced and the cells were treated with the indicated concentrations of myricetin and NAC. After 4 h, medium was removed from each sample and placed in a 5 ml round-bottom tube. Cells were then lifted from the tissue culture plate using TrypLE Express™ added to each sample, and incubating plates for 3-5 min in a humidified 10% CO₂ incubator at 37°C. Cells were then transferred from tissue culture plates to the 5 ml round-bottom tubes containing their respective medium. Samples were centrifuged for 5 min at 500 × g and supernatants were discarded. The cells were resuspended in PBS, centrifuged for 5 min at 500 × g and the supernatant was discarded. A fixation/permeabilization working solution was made from a 1:3 dilution of fixation/permeabilization concentrate to fixation/permeabilization diluent. The cells were suspended in 0.5 ml of the working solution and stored at 4°C overnight. After overnight incubation, 1X permeabilization buffer was added to each sample and samples were centrifuged for 5 min at 500 × g and the supernatant was discarded. The cells were resuspended in 100 µl of 1X permeabilization buffer containing the diluted anti-human/mouse γ-H2AX fluorochrome-conjugated antibody, or the mouse IgG1 K fluorochrome-conjugated isotype antibody and incubated at room temperature for 30 min. Then, 1X permeabilization buffer was added to each sample and the samples were centrifuged for 5 min at 500 × g and the supernatant was discarded. The previous step was repeated once more and after the supernatant was discarded the cells were resuspended in FACS buffer. Cell fluorescence was measured by flow cytometry and FCS Express was used to analyze shifts in fluorescence that corresponded to increased γ-H2AX levels.

2.9. Protein isolation

Cells treated with indicated concentrations of myricetin only, or a combination of myricetin and NAC for 30 min or 3 h were lifted from tissue culture flasks using 3 ml TrypLE Express™ added to each sample. Flasks were incubated in a humidified 10% CO₂ incubator at 37°C for 3-5 min. Samples were transferred to tubes and centrifuged for 5 min at 500 × g and 4°C. The

supernatant was removed, cells were re-suspended in 1 ml of cold PBS and centrifuged for 5 min at $500 \times g$ and 4°C . The supernatant was then removed and cells were resuspended in 50 μl of cold lysis buffer comprised of 150 mM NaCl, 5 mM EDTA, 5 mM EGTA, 0.25% w/v sodium deoxycholate, 50 mM Tris-HCl (pH 7.5), 50 mM Na_2HPO_4 and 0.1% v/v NP-40, also containing phosphatase and protease inhibitors (1 mM PMSF, 100 μM Na_3VO_4 , 10 $\mu\text{g}/\text{ml}$ aprotinin, 5 $\mu\text{g}/\text{ml}$ leupeptin, 10 mM NaF, 5 $\mu\text{g}/\text{ml}$ pepstatin A, 1 mM DTT, and 10 μM PAO). Samples were incubated on ice for 15 min and centrifuged for 10 min at $14,000 \times g$ and 4°C . The supernatant containing the cellular proteins was collected for each sample and stored at -80°C for a maximum of 4 days before protein quantification.

2.10. Protein quantification

A colorimetric Bradford assay (288) was used to measure and equalize the total cell protein in all samples. For protein quantification, 5 μl of each sample was added to 1 ml of Biorad Protein Assay Dye that was diluted 1 in 5 in ddH₂O. To generate a protein standard curve, a range of BSA concentrations (2.5-80 $\mu\text{g}/\text{ml}$) were used. Each sample diluted in protein assay dye was added in triplicate or quadruplicate to 96-well flat bottom plates and absorbance was measured at 570 nm using an Expert 96 microplate reader. Using the protein standard curve, the amount of protein in each sample was calculated and the samples diluted to equalize the amount of protein in all samples. The protein samples were denatured at 95°C for 5 min in SDS-PAGE sample loading buffer (15% v/v β -mercaptoethanol, 200 mM Tris HCl [pH 6.8], 6% w/v SDS, 0.01% w/v bromophenol blue, and 30% v/v glycerol) and stored at -80°C .

2.11. Western blotting

Equal amounts of protein samples (10 μg) and pre-stained Bio-Rad protein ladder were separated on a 12% polyacrylamide gel (12% acrylamide,

0.1% w/v sodium dodecyl sulfate [SDS], 375 mM Tris-HCl [pH 8.8], 0.15% v/v tetramethylethylenediamine [TEMED], and 0.1% w/v ammonium persulfate [APS]) with a 4% acrylamide stacking gel (4% acrylamide, 0.1% w/v SDS, 125 mM Tris-HCl [pH 6.8], 0.15% v/v TEMED, and 0.1% APS). Proteins were resolved at 200 V in SDS-PAGE running buffer (0.1% v/v SDS, 200 mM glycine, and 20 mM Tris-HCl [pH 8.3]) for 1h. Protein was transferred from the gel to a nitrocellulose membrane using the iBlot[®] dry blotting system (Life Technologies) according to the manufacturer's instructions. Membranes were blocked in 5% w/v fat-free milk in Tris-buffered saline (20 mM Tris-HCl [pH 7.6], 200 mM NaCl) with 0.05% v/v Tween-20 (TTBS) at room temperature for 1 h or at 4°C overnight. Following blocking, the membranes were washed with TTBS and incubated with the indicated primary antibody overnight at 4°C or for 1 h at room temperature. The membranes were washed in TTBS for 30 min, with the wash being changed every 5 min, and incubated with the indicated HRP-conjugated secondary antibody for 1 h at room temperature. Membranes were washed again for 30 min in TTBS then incubated with enhanced chemiluminescence reagents (GE Healthcare) for 1 min. Membranes were exposed to X-ray film (Sci-Med Inc., Truro, NS), which was developed using a Kodak X-OMAT 1000A automated X-Ray developer. To account for variations in protein loading, membranes were also probed for actin. To quantify the intensity of each protein band by densitometry, ImageJ software (version 1.45, National Institutes of Health, Bethesda, MD) was used. For each sample two blots were run, one blot for phospho-protein and one for total protein. Actin was probed for on both blots and for analysis the intensity of the phospho- and total proteins were divided by their corresponding actin intensities. The ratio of actin-normalized phospho-protein to actin-normalized total-protein was determined and the ratio for each sample was normalized to the ratio for the media at the appropriate time points.

2.12. Statistical analysis

Statistical analysis was conducted using GraphPad Prism analysis software (GraphPad Software Inc., La Jolla, CA). Statistical comparisons were performed using one-way analysis of variance (ANOVA) with the Tukey-Kramer multiple comparisons post-test. When the p value was less than 0.05 data were considered significantly different (denoted by *). Data were considered not significantly different (denoted by ns) when the p value was greater than 0.05.

CHAPTER 3

RESULTS

3.1. Myricetin reduces mammary carcinoma cell phosphatase activity

Previous studies of myricetin have shown that myricetin has cytostatic and cytotoxic effects for a variety of cancer cell lines (263, 265–267, 269, 270), but there are very few studies examining its effect on mammary carcinoma cell growth. A range of concentrations of myricetin were used to treat a panel of human and mouse mammary carcinoma cell lines and the effect of myricetin on total cell number was assessed using phosphatase activity as an indicator of relative viable cell number. Less phosphatase activity (or a greater decrease in percent phosphatase activity) indicated that less cells were present. Myricetin treatment caused a decrease in phosphatase activity in a dose-dependent manner for all human and mouse mammary carcinoma cell lines tested after 24 h (Figure 3.1). A decrease in phosphatase activity indicated that myricetin was either having a cytotoxic or cytostatic effect on the mammary carcinoma cells. For the purposes of this study the subsequent data focuses on the MDA-MB-231 and MDA-MB-468 triple negative breast cancer cell lines, as they were shown to be sensitive to myricetin in Figure 3.1 (A and B); additionally the effect of myricetin on 4T1 mouse mammary carcinoma cells was determined. On the basis of the data shown in Figure 3.1, concentrations of 25 and 50 μM myricetin were chosen for subsequent experiments.

The effect of myricetin on normal human cells was investigated using HMEpiC and human dermal fibroblasts. The phosphatase activity in HMEpiC was decreased by myricetin treatment after 24 h in a dose-dependent manner (Figure 3.2A), similar to the effect of myricetin on mammary carcinoma cells (Figure 3.1). Human dermal fibroblasts appeared to be less sensitive to myricetin treatment. In contrast to HMEpiC, when human dermal fibroblasts were treated with myricetin for 24 h, the phosphatase activity was not decreased with most concentrations of

myricetin tested, except for a concentration of 10 μM myricetin that caused a 10-15% decrease in phosphatase activity, which was significant compared to the vehicle (Figure 3.2B).

Several phytochemicals have been reported to have cytostatic and cytotoxic effects on mammary carcinoma cells (289–293). The sensitivity of mammary carcinoma cells to myricetin was compared to their sensitivity to two other phytochemicals, resveratrol and epigallocatechin gallate (EGCG), which are known to have inhibitory effects on cell viability and growth. Acid phosphatase assays were used to measure phosphatase activity of mammary carcinoma cells treated for 24 h with myricetin, resveratrol, or EGCG. All three phytochemicals tested caused decreases in phosphatase activity, indicating that the number of cells present was decreased (Figure 3.3). For both MDA-MB-231 and MDA-MB-468 cell lines myricetin and EGCG caused similar decreases in phosphatase activity, for example at 50 μM myricetin or EGCG there was approximately a 75% decrease in phosphatase activity (Figure 3.3). Compared to resveratrol, myricetin had a greater inhibitory effect on phosphatase activity, for example at 50 μM there was approximately a 75% decrease with myricetin compared to a 15-25% (depending on the cell line) decrease with resveratrol (Figure 3.3). The effect of myricetin on mammary carcinoma cell number was also compared to the effects of two conventional breast cancer chemotherapeutic drugs, doxorubicin and docetaxel. Myricetin, doxorubicin, and docetaxel all caused similar dose-dependent decreases in MDA-MB-231 and MDA-MB-468 cell phosphatase activity, indicating decreases in cell number (Figure 3.4).

3.2. Myricetin is cytotoxic to mammary carcinoma cells

The acid phosphatase assay does not distinguish between growth inhibitory and cytotoxic effects, so to determine whether the decrease in phosphatase activity observed with myricetin treatment (Figure 3.1) was due to increased cytotoxicity, an apoptosis assay was conducted. MDA-MB-468 cells were treated with myricetin and images of the cells after 24 h of treatment were

acquired. Myricetin treatment resulted in less cells present in the images acquired, and the cells that were present were much smaller than vehicle-treated cells, suggesting that they were undergoing cell death (Figure 3.5). To further determine whether myricetin induced mammary carcinoma cell death, the MDA-MB-231 and MDA-MB-468 human mammary carcinoma cell lines were treated with myricetin for 24 or 48 h and stained with Annexin-V-FLUOS/PI. Using flow cytometry to measure Annexin-V-FLUOS/PI staining, 50 μ M myricetin was found to induce significant late apoptosis/necrosis (approximately 50% of cells were undergoing late apoptosis/necrosis) in MDA-MB-231 cells after both 24 and 48 h of treatment (Figure 3.6A-C), while 25 μ M myricetin did not induce significant early or late apoptosis/necrosis in MDA-MB-231 cells (Figure 3.6A-C). In contrast, MDA-MB-468 cells treated with 50 μ M myricetin showed significant early apoptosis (approximately 25% of cells at 24 h and 50% at 48 h) and late apoptosis/necrosis (60% of cells at 24h and 25% at 48 h) at both 24 and 48 h of myricetin treatment (Figure 3.6D-F). MDA-MB-468 cells treated with 25 μ M myricetin underwent significant early apoptosis at 24 (about 20% of cells) and 48 h (about 25% of cells) (Figure 3.6E, F). Whether or not myricetin caused mouse mammary carcinoma cells to die by apoptosis was also investigated. The mouse mammary carcinoma 4T1 cell line was treated with myricetin for 24 h and stained with Annexin-V-FLUOS/PI. Myricetin caused significant early apoptosis (20% of cells) and late apoptosis/necrosis (60% of cells) of 4T1 cells, but only at the 50 μ M concentration (Figure 3.7).

3.3. Myricetin causes a loss of mammary carcinoma cell mitochondrial membrane integrity.

The Annexin-V-FLUOS/PI staining data indicated that myricetin caused mammary carcinoma cell apoptosis. Apoptosis and cell death can be promoted by changes to the mitochondria; therefore whether or not myricetin caused changes to the mitochondria was examined. Mammary carcinoma cells were treated with myricetin and stained with DiOC₆ as an indicator of changes in

mitochondrial membrane potential. Flow cytometry was used to measure DiOC₆ staining, where a loss of DiOC₆ staining signified a decrease in mitochondrial membrane stability (the greater the decrease in mitochondrial membrane stability, the greater the loss in mitochondrial membrane potential). When MDA-MB-231 and MDA-MB-468 cells were treated with myricetin significant decreases in mitochondrial membrane stability were observed as early as 4 h following treatment (Figure 3.8). In MDA-MB-231 cells 50 μ M of myricetin caused significant decreases in mitochondrial membrane stability at 4 h (approximately a 60% decrease in mitochondrial membrane stability) and 24 h (85% decrease in mitochondrial membrane stability) (Figure 3.8A, B). Similarly, in MDA-MB-468 cells 50 μ M myricetin caused a significant decrease in mitochondrial membrane stability (approximately 25%) at 4 h (Figure 3.8C, D). At 24 h both 25 (60% decrease) and 50 μ M (90% decrease) myricetin caused a significant decrease in mitochondrial membrane stability of MDA-MB-468 cells (Figure 3.8C, D). The mitochondrial membrane stability was also significantly decreased (75%) in the mouse mammary carcinoma 4T1 cell line in cells treated for 24 h with 50 μ M myricetin (Figure 3.9). To determine the cell death pathways that were involved in myricetin-induced mammary carcinoma cell death, the involvement of caspases and RIPK1 in myricetin-induced cell death was studied. MDA-MB-231 and MDA-MB-468 cells were pre-treated with the pan-caspase inhibitor Z-VAD-fmk or the RIPK1 inhibitor necrostatin-1 (Nec-1) and then treated with myricetin for 24 h. The cells were stained with Annexin-V-FLUOS/PI and apoptosis was determined by flow cytometry. For both the MDA-MB-231 (Figure 3.10A) and MDA-MB-468 (Figure 3.10B) cells, pre-treatment with Z-VAD-fmk or Nec-1 did not alter myricetin-induced early apoptosis or late apoptosis/necrosis (both of the inhibitors were determined to be functionally active, see Appendix Figure 1 and 2). This data suggested that myricetin-induced cell death was independent of caspase and RIPK1 activation.

3.4. Myricetin induces accumulation of intracellular reactive oxygen species (ROS), which promotes mammary carcinoma cell death.

Several phytochemicals have cytotoxic effects by causing accumulation of intracellular ROS that leads to cell death (231, 291, 294). To determine if myricetin caused intracellular accumulation of ROS in mammary carcinoma cells prior to causing cell death, the DCFDA assay was used to determine early ROS production. MDA-MB-231 and MDA-MB-468 cells were stained with DCFDA, a detector of intracellular ROS, and treated with myricetin for 4 h. Myricetin (50 μ M) caused significant accumulation of intracellular ROS in approximately 60% of MDA-MB-231 (Figure 3.11A, B) and 65% of MDA-MB-468 (Figure 3.11C, D) cells after 4 h of treatment. Pre-treatment with the antioxidant NAC significantly inhibited accumulation of intracellular ROS in mammary carcinoma cells treated with myricetin (Figure 3.11).

Myricetin increased intracellular ROS, but the impact of ROS in myricetin-induced cell death remained unknown. To determine the role of myricetin-induced intracellular ROS in cell death, mammary carcinoma cells were incubated with NAC, then treated with myricetin and stained with Annexin-V-FLUOS/PI. If ROS was important for myricetin-induced cell death then the presence of an antioxidant should prevent myricetin-induced cell death. Treatment with NAC completely inhibited early apoptosis and late apoptosis/necrosis for both MDA-MB-231 (Figure 3.12A, B) and MDA-MB-468 (Figure 3.12C,D) cells treated with myricetin for 24 h. NAC also prevented the death of 4T1 mouse mammary carcinoma cells treated with myricetin for 24 h (Figure 3.13). This data demonstrated that ROS were important for myricetin-induced mammary carcinoma cell death.

Myricetin was shown to cause decreases in mammary carcinoma cell mitochondrial membrane stability (Figure 3.8, 3.9) and induce intracellular ROS (Figure 3.11), so the role of myricetin-induced ROS in mammary carcinoma cell mitochondrial stability was determined. Mammary carcinoma cells were treated with NAC and myricetin for 4 and 24 h, and then stained with DiOC₆ to determine

mitochondrial membrane stability. NAC completely prevented myricetin-induced decreases in mammary carcinoma mitochondrial membrane stability at both 4 and 24 h following treatment for both the MDA-MB-231 (Figure 3.14A) and MDA-MB-468 (Figure 3.14B) cells.

To further confirm that myricetin-induced changes in mammary carcinoma cells were due to ROS, another antioxidant (sodium pyruvate) was added to mammary carcinoma cells and the cells were treated with myricetin. The acid phosphatase activity of myricetin and sodium pyruvate treated mammary carcinoma cells was assessed. For both MDA-MB-231 and MDA-MB-468 cells a lower (100 μ M) and higher (1 mM) concentration of sodium pyruvate inhibited myricetin-induced decreases in phosphatase activity (Figure 3.15). Complete inhibition of myricetin-induced decreases in phosphatase activity was observed with 1 mM sodium pyruvate whereas 100 μ M sodium pyruvate caused a 15-35% reduction in myricetin-induced phosphatase activity, depending on the concentration of myricetin used (Figure 3.15). This indicated that myricetin-induced decrease in phosphatase activity was due to ROS.

3.5. Myricetin causes ROS-dependent DNA damage in mammary carcinoma cells.

Because myricetin caused increased intracellular ROS accumulation (Figure 3.11), and ROS can directly cause DNA damage, the amount of DNA damage in myricetin-treated mammary carcinoma cells was investigated. To measure DNA damage, a marker of double-stranded DNA damage, γ -H2AX, was used (287). Mammary carcinoma cells were treated with myricetin for 4 h and then stained with fluorochrome-labeled anti- γ -H2AX antibody. Flow cytometry was used to measure the frequency of cells with an increased level of γ -H2AX. Myricetin caused significant increase in γ -H2AX levels in both MDA-MB-231 and MDA-MB-468 cells as shown in Figure 3.16, approximately 65% of myricetin-treated cells had increased γ -H2AX compared to 10% of vehicle-treated cells. When mammary carcinoma cells were treated with NAC in combination with

myricetin, the myricetin-induced increase in γ -H2AX was significantly inhibited in both MDA-MB-231 and MDA-MB-468 cells (Figure 3.16); taken together, these data indicated the myricetin-induced ROS promoted DNA damage in mammary carcinoma cells.

3.6. Myricetin forms extracellular ROS in cell culture medium.

Certain phytochemicals have been found to form ROS in cell culture medium in the absence of cells (295–297). To determine if myricetin formed ROS in cell culture medium, an Amplex® Red assay, which specifically detects H_2O_2 , was used. Myricetin was diluted in cell culture medium and Amplex® Red assay reaction mixture containing Amplex® Red and HRP was added to the medium. In the presence of H_2O_2 , Amplex® Red reagent gets converted to resorufin, which can be detected by measuring absorbance at 570 nm. Myricetin caused significant conversion of Amplex® Red to resorufin in cell culture medium (Figure 3.17A), indicating the presence of H_2O_2 in culture medium containing myricetin. When MDA-MB-468 cells were added to the Amplex® Red assay the results were similar to when no cells were present, i.e., myricetin induced similar conversion of Amplex® Red to resorufin (Figure 3.17B). These results demonstrated that myricetin forms ROS in cell culture medium independently of the presence of mammary carcinoma cells.

To determine if the extracellular ROS formed by myricetin in cell culture medium was involved in myricetin-induced decreases in mitochondrial membrane stability, mammary carcinoma cells were treated with myricetin and a mixture of super oxide dismutase (SOD) and catalase. SOD is an enzyme that catalyzes the reduction of super oxide anions to H_2O_2 , while catalase is an enzyme that catalyzes the decomposition of H_2O_2 to H_2O and O_2 . Neither enzyme is able to cross the cell membrane and will therefore only act on extracellular ROS. Cells treated with SOD/catalase and myricetin were stained with DiOC₆ to determine the mitochondrial membrane stability in the treated cells. SOD/catalase

completely inhibited myricetin-induced decreases in mitochondrial membrane stability in both MDA-MB-231 and MDA-MB-468 cells (Figure 3.18).

Since myricetin-induced cell death in mammary carcinoma cells was dependent on ROS (Figure 3.12), I next determined whether or not the extracellular ROS formed by myricetin was responsible for cell death. MDA-MB-231 and MDA-MB-468 cells were treated with SOD/catalase and myricetin, and then stained with Annexin-V-FLUOS/PI to measure cell death. SOD/catalase treatment significantly inhibited myricetin-induced early apoptosis and late apoptosis/necrosis in both MDA-MB-231 and MDA-MB-468 cells (Figure 3.19) to a similar degree as NAC (Figure 3.12). Taken together, the data from Figures 3.18 and 3.19 indicate that myricetin-induced mammary cell death was due to ROS formed in the extracellular environment by myricetin.

3.7. Myricetin causes p38 MAPK activation in mammary carcinoma cells.

Several signaling pathways can be activated in cells that are under oxidative stress, including the p38 MAPK signaling pathway (83). To determine if myricetin caused p38 MAPK activation in mammary carcinoma cells, MDA-MB-231 and MDA-MB-468 cells were treated with myricetin and cell lysates were obtained for western blot analysis. In mammary carcinoma cells treated with myricetin for 30 min or 3 h there was significant phosphorylation of p38 MAPK (Figure 3.20). In addition, MDA-MB-468 cells that were treated with both myricetin and NAC showed significantly inhibited myricetin-induced p38 MAPK phosphorylation (Figure 3.20C, D). In contrast, when MDA-MB-231 cells were treated with myricetin and NAC, the NAC did not inhibit myricetin-induced p38 MAPK phosphorylation (Figure 3.20A, B).

Activation of the p38 MAPK signaling pathway can promote cell apoptosis (110). Since the p38 MAPK pathway was activated in myricetin-treated mammary carcinoma cells, the role of this pathway in myricetin-induced cell death was examined. MDA-MB-231 and MDA-MB-468 cells were treated with a p38 MAPK

inhibitor and myricetin, and then were stained with Annexin-V-FLUOS/PI to determine cell death. The p38 MAPK inhibitor used was shown to be active at inhibiting the p38 MAPK pathway, as it significantly inhibited T cell proliferation (Appendix Figure 3). When mammary carcinoma cells were treated with the p38 inhibitor and myricetin there was no effect on myricetin-induced early apoptosis or late apoptosis/necrosis (Figure 3.21). This data demonstrated that while the p38 MAPK pathway may be activated in myricetin-treated mammary carcinoma cells, it is not necessary for myricetin-induced cell death.

Figure 3.1. Myricetin reduces mammary carcinoma cell phosphatase activity. (A-F) Human mammary carcinoma cell lines (A) MDA-MB-231, (B) MDA-MB-468, (C) MCF-7, (D) SK-BR-3 and mouse mammary carcinoma cell lines (E) 4T1 and (F) E0771 were incubated with the indicated concentrations of myricetin for 24 h. The acid phosphatase colorimetric assay was used to measure cell number, and at 24 h the cells were lysed and acid phosphatase substrate was incubated with the lysate for 2 h. The percent phosphatase activity decrease is relative to the medium control. The data shown are the mean of 3 or 4 independent experiments \pm SEM; * denotes $p < 0.05$ and ns denotes not significant compared to DMSO vehicle control as determined by ANOVA with the Tukey-Kramer multiple comparisons post-test.

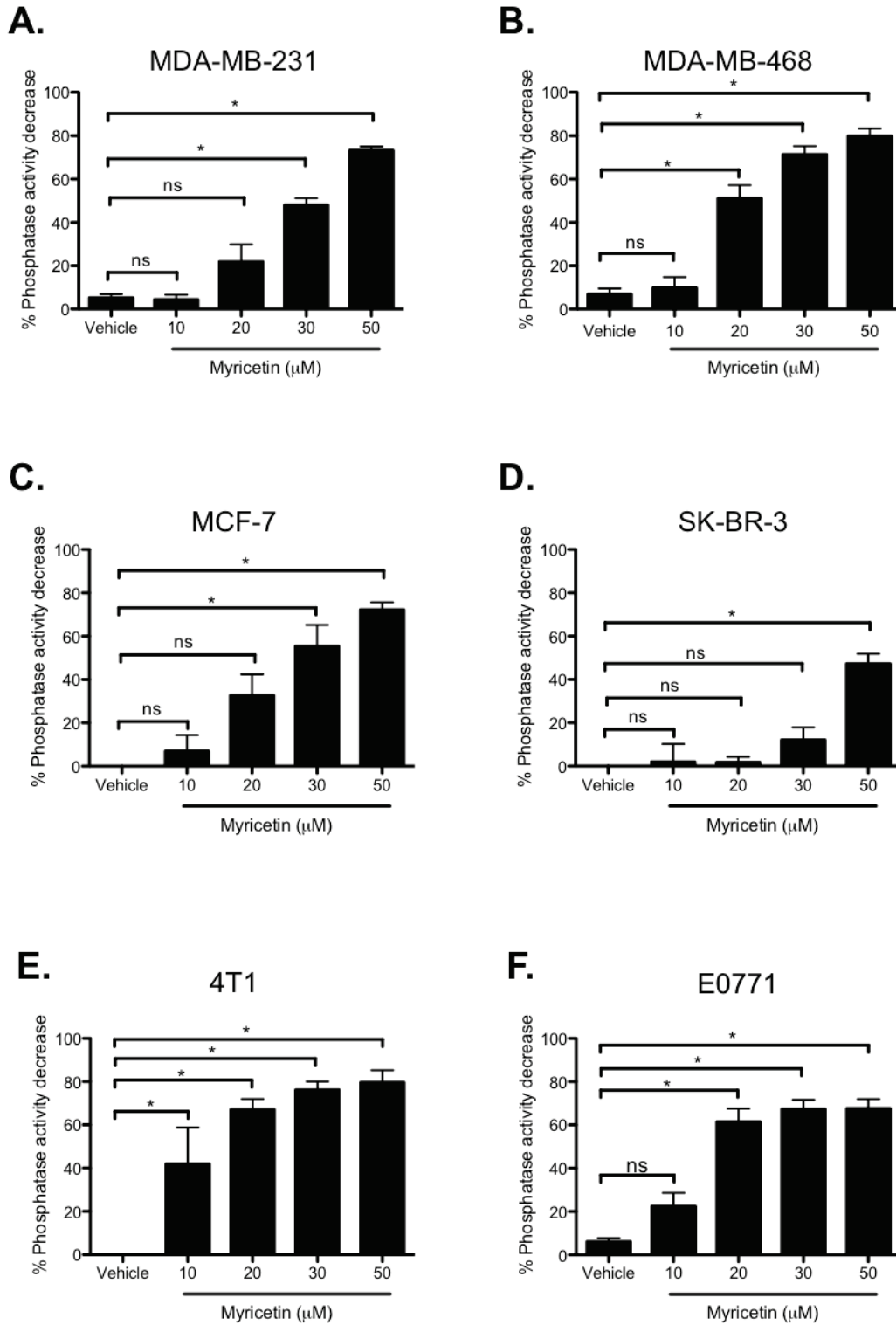
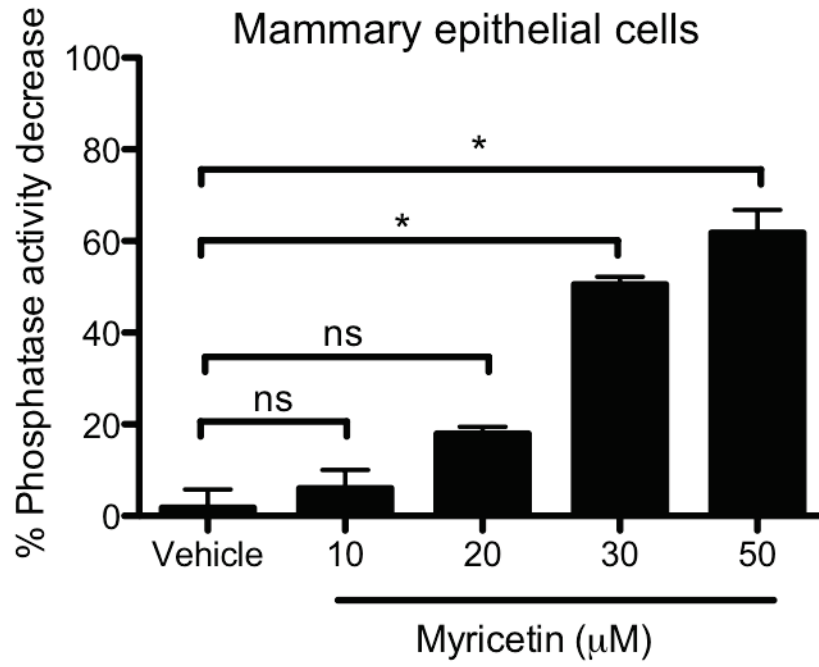


Figure 3.1

Figure 3.2. Myricetin reduces human mammary epithelial cell, but not human dermal fibroblast cell phosphatase activity. (A) Primary human mammary epithelial cells and (B) primary human dermal fibroblasts were incubated with the indicated concentrations of myricetin for 24 h. The acid phosphatase colorimetric assay was used to measure cell number, and at 24 h the cells were lysed and acid phosphatase substrate was incubated with the lysate for 2 h. The percent phosphatase activity decrease is relative to the medium control. The data shown are the mean of 3 independent experiments \pm SEM; * denotes $p < 0.05$ and ns denotes not significant compared to DMSO vehicle control as determined by ANOVA with the Tukey-Kramer multiple comparisons post-test.

A.



B.

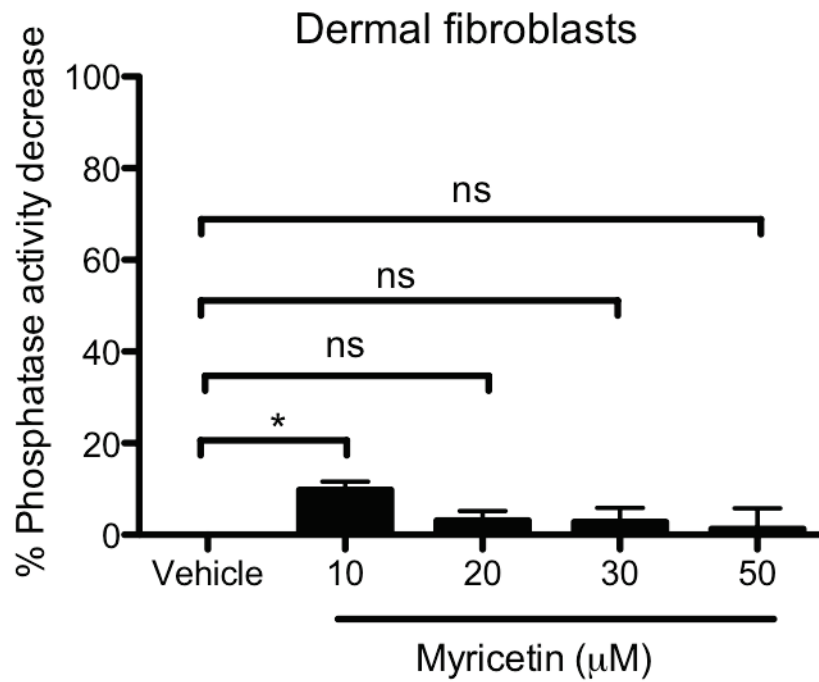


Figure 3.2

Figure 3.3. The effect of myricetin on mammary carcinoma cell phosphatase activity is similar to the effects on phosphatase activity seen with EGCG, and greater than the effect of resveratrol. (A) MDA-MB-231, (B) MDA-MB-468, and (C) 4T1 cells incubated with the indicated concentrations of myricetin, EGCG, or resveratrol for 24 h. The acid phosphatase colorimetric assay was used to measure cell number, and at 24 h the cells were lysed and acid phosphatase substrate was incubated with the lysate for 2 h. The percent phosphatase activity decrease is relative to the medium control. The data shown are the mean of 3 or 4 independent experiments \pm SEM; * denotes $p < 0.05$ and ns denotes not significant compared to myricetin as determined by ANOVA with the Tukey-Kramer multiple comparisons post-test.

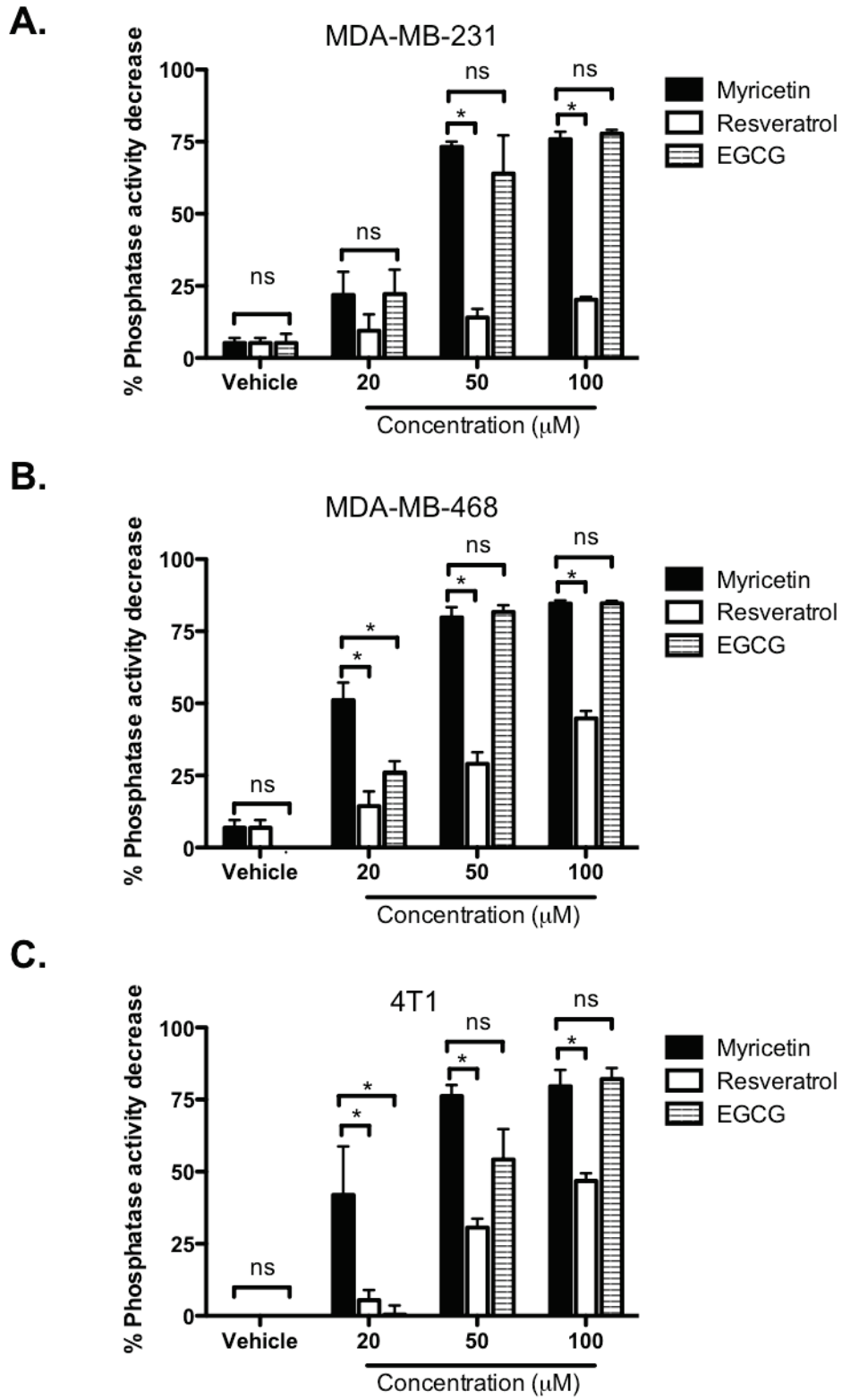


Figure 3.3

Figure 3.4. The dose-dependent inhibitory effect of myricetin on mammary carcinoma cell phosphatase activity is similar to the effects of conventional chemotherapeutic drugs. MDA-MB-231 (**A**) and MDA-MB-468 (**B**) cells were incubated with the indicated concentrations of myricetin, doxorubicin, or docetaxel for 24, 48, or 72 h. Concentrations of doxorubicin and docetaxel were chosen based on previous work by Dr. Melanie Coombs in my lab (unpublished). The acid phosphatase colorimetric assay was used to measure cell number, and at the indicated time point the cells were lysed and acid phosphatase substrate was incubated with the lysate for 2 h. The percent phosphatase activity decrease is relative to the medium control. The data shown are the mean of 3 independent experiments \pm SEM; * denotes $p < 0.05$ and ns denotes not significant compared to DMSO vehicle (myricetin and docetaxel) or H₂O vehicle (doxorubicin) as determined by ANOVA with the Tukey-Kramer multiple comparisons post-test.

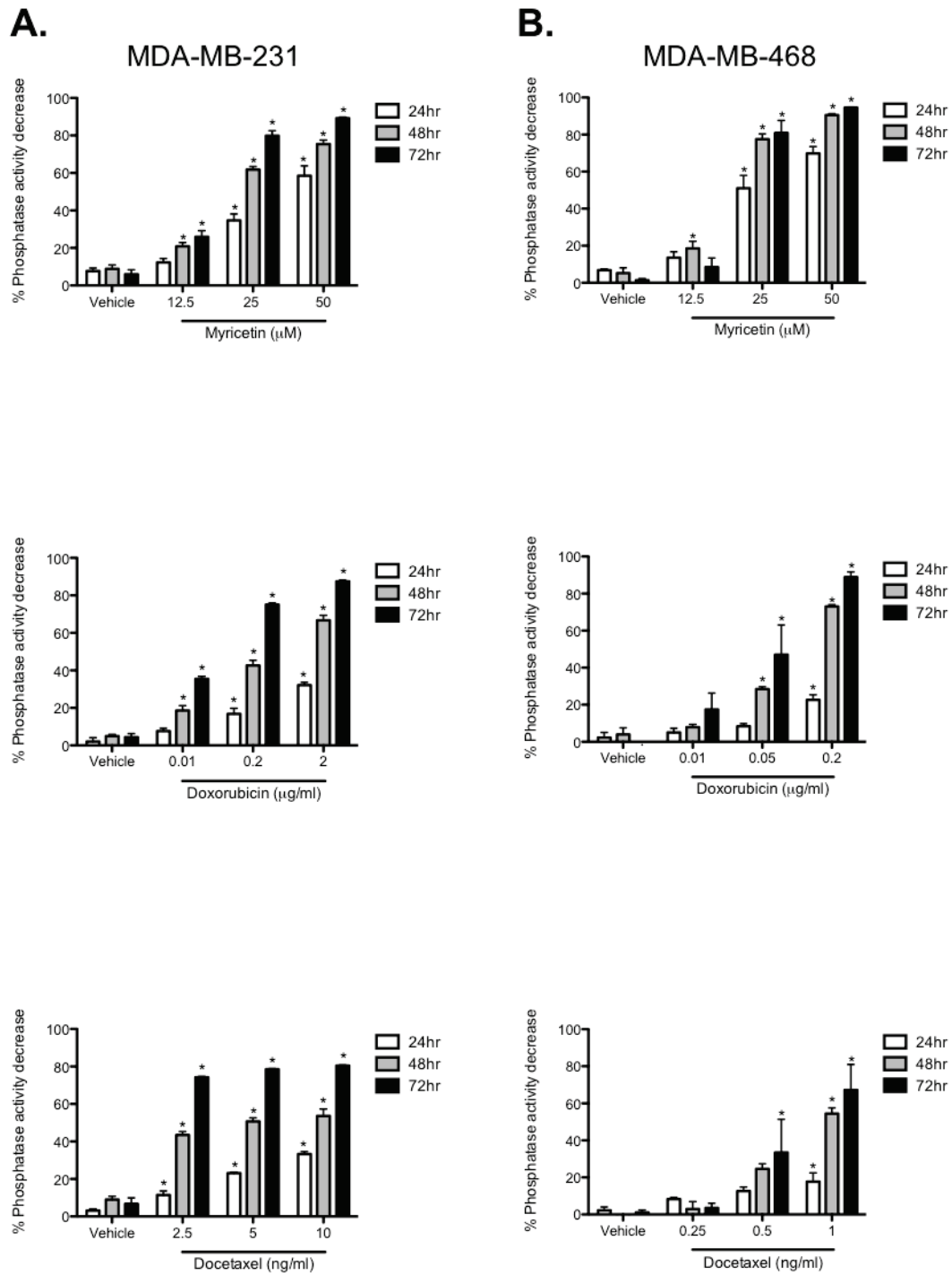
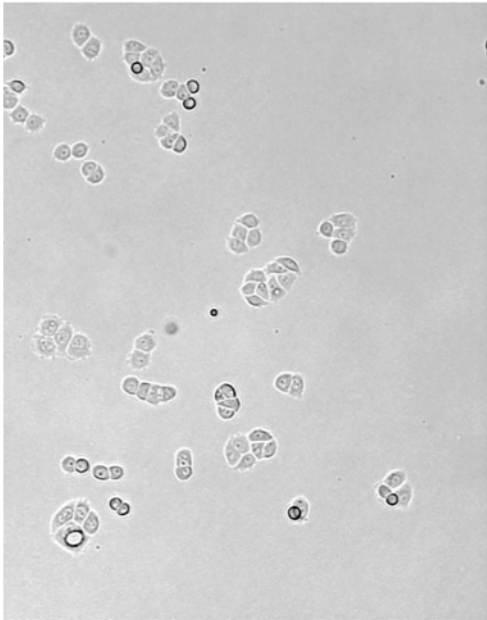


Figure 3.4

Figure 3.5. Myricetin reduces mammary carcinoma cell number and size.

MDA-MB-468 cells were treated with vehicle (DMSO) or myricetin for 24 h and then images of the cells were captured using a Nikon[®] Digital Sight camera (Nikon Canada Inc, Mississauga, ON, Canada) head connected to a Nikon[®] Eclipse t1500 microscope at 200× magnification. Images are representative of 3 independent experiments.

Vehicle



50 μ M Myricetin

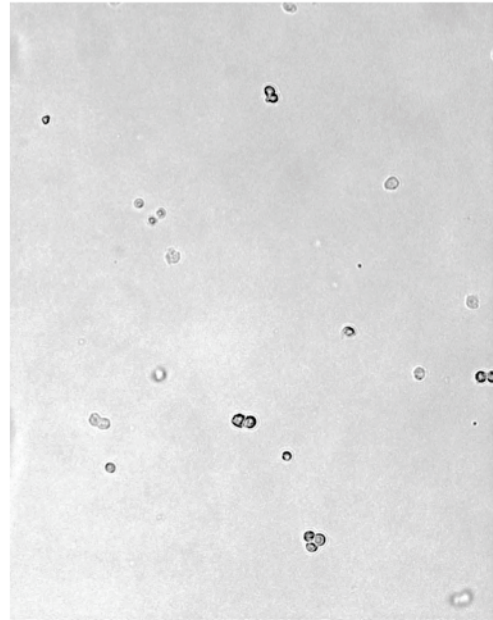


Figure 3.5

Figure 3.6. Myricetin induces human mammary carcinoma cell death. (A), (B), (C) MDA-MB-231 and (D), (E), (F) MDA-MB-468 human mammary carcinoma cells were incubated with the indicated concentrations of myricetin for 24 or 48 h. The cells were stained with Annexin-V-FLUOS/PI and fluorescence was measured by flow cytometry. The percent of cells undergoing early apoptosis and late apoptosis were based on the percent of cells that were Annexin-V only positive (early apoptosis) and the cells that were both Annexin-V and PI positive (late apoptosis/necrosis). Data shown are (A), (D) flow cytometry dot plots from one representative experiment at 24 h (B), (E) the mean early and late apoptosis/necrosis of cells treated for 24 h and (C), (F) for 48 h from 3 independent experiments \pm SEM; * denotes $p < 0.05$ compared to DMSO vehicle (myricetin-treated cells in early apoptosis were compared to the early apoptosis vehicle-treated cells and myricetin-treated cells in late apoptosis/necrosis were compared to the late apoptosis/necrosis vehicle-treated cells).

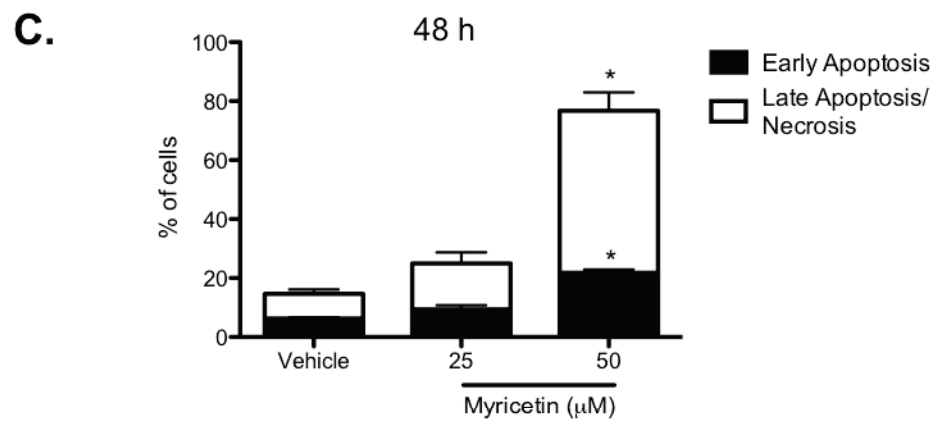
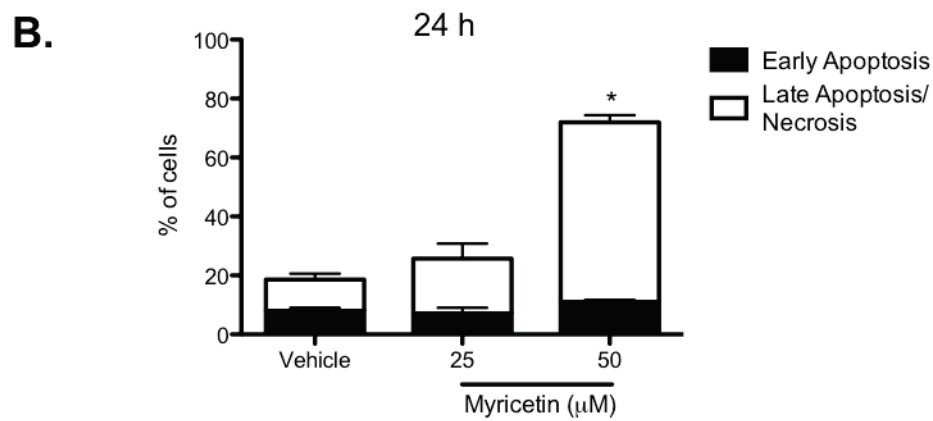
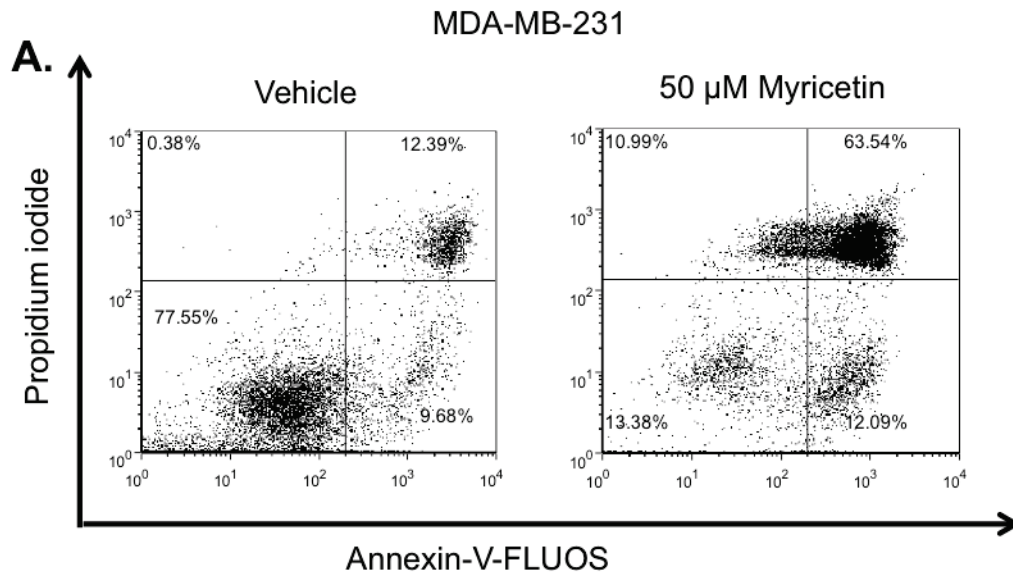


Figure 3.6

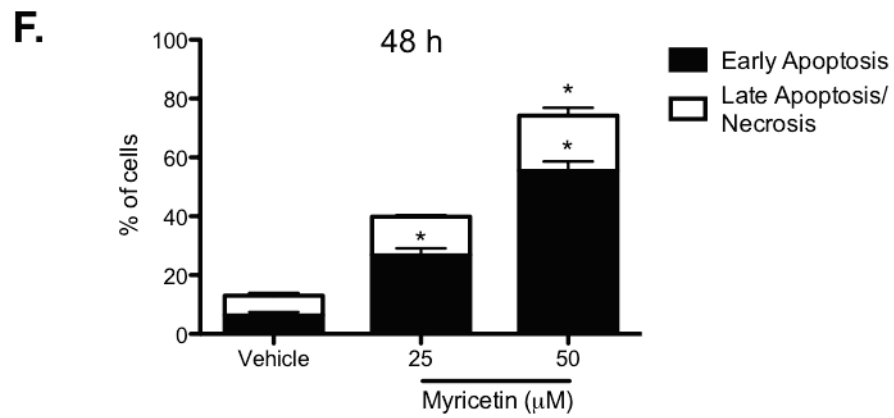
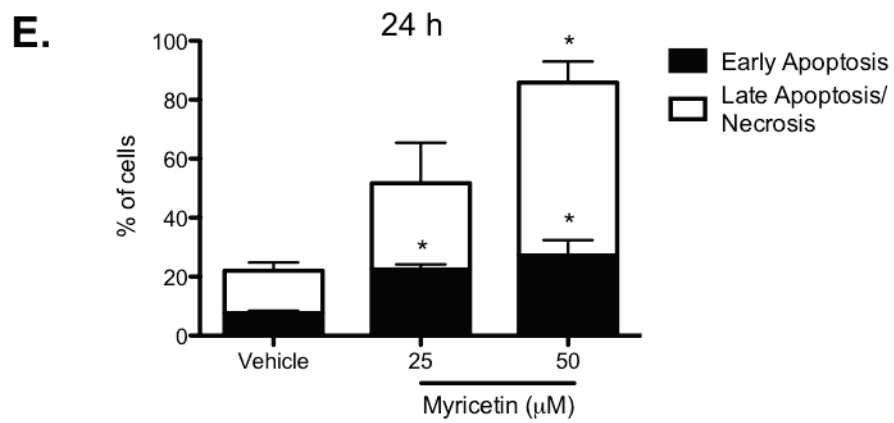
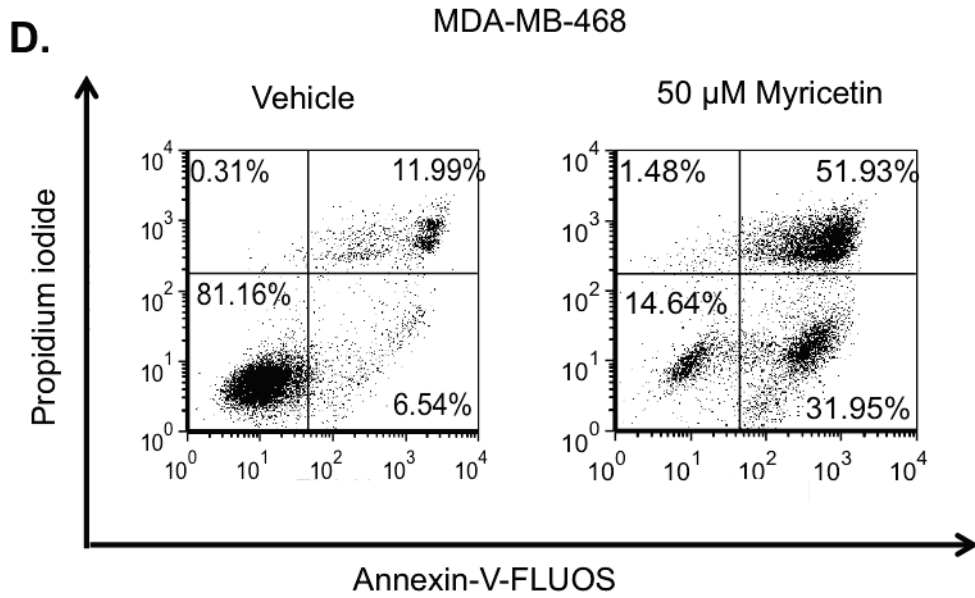


Figure 3.6 (continued)

Figure 3.7. Myricetin induces mouse mammary carcinoma cell death. 4T1 mouse mammary carcinoma cells were incubated with the indicated concentrations of myricetin for 24 h. The cells were stained with Annexin-V-FLUOS/PI and fluorescence was measured by flow cytometry. The percent of cells undergoing early apoptosis and late apoptosis were based on the percent of cells that were Annexin-V only positive (early apoptosis) and the cells that were both Annexin-V and PI positive (late apoptosis/necrosis). Data shown are **(A)** flow cytometry dot plots from one representative experiment at 24 h, **(B)** the mean early and late apoptosis/necrosis of cells treated for 24 h from 3 independent experiments \pm SEM; * denotes $p < 0.05$ compared to DMSO vehicle (myricetin-treated cells in early apoptosis were compared to the early apoptosis vehicle-treated cells and myricetin-treated cells in late apoptosis/necrosis were compared to the late apoptosis/necrosis vehicle-treated cells).

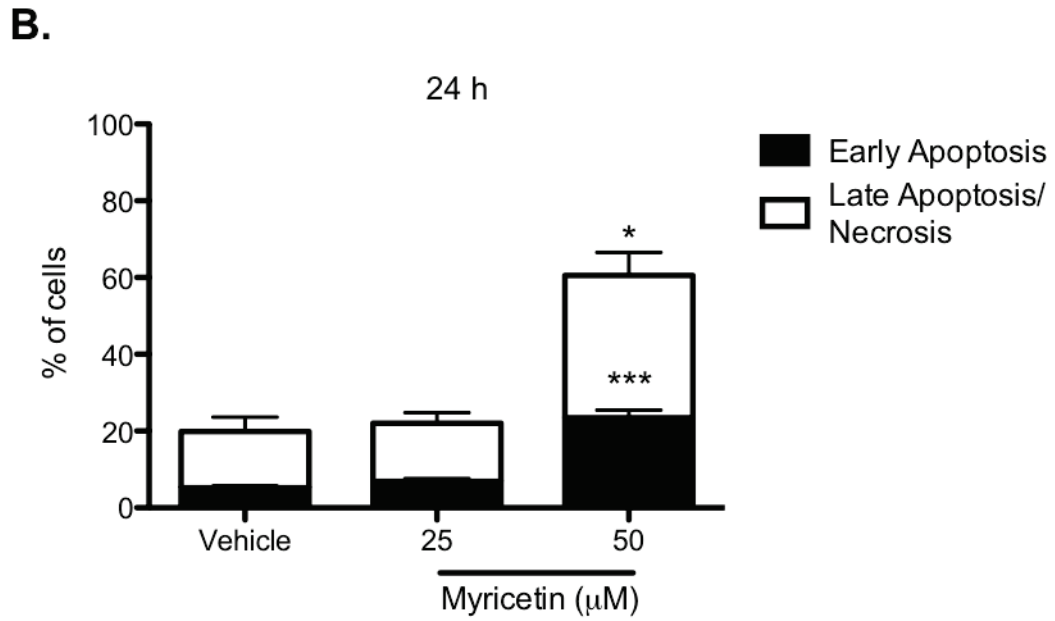
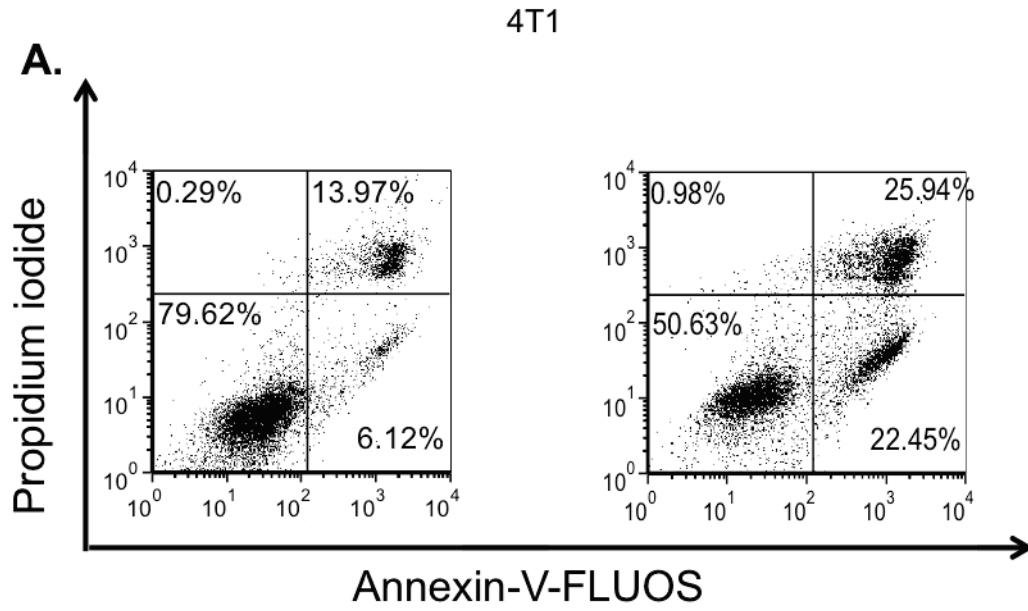


Figure 3.7

Figure 3.8. The stability of the mitochondrial membrane in human mammary carcinoma cells is decreased by myricetin. (A), (B) MDA-MB-231 and (C), (D) MDA-MB-468 human mammary carcinoma cells were incubated with the indicated concentrations of myricetin for 4 or 24 h. The cells were stained with DiOC₆ and fluorescence was measured by flow cytometry. The percent mitochondrial membrane decrease is indicated by decreased fluorescence (leftward shift in DiOC₆ staining intensity). Data shown are (A), (C) flow cytometry histogram plots from one representative experiment at 24 h, (B), (D) the mean percent mitochondrial membrane stability decrease of cells treated for 4 h (left) and for 24 h (right) from 3 or 4 independent experiments \pm SEM; * denotes $p < 0.05$ and ns denotes not significant compared to DMSO vehicle.

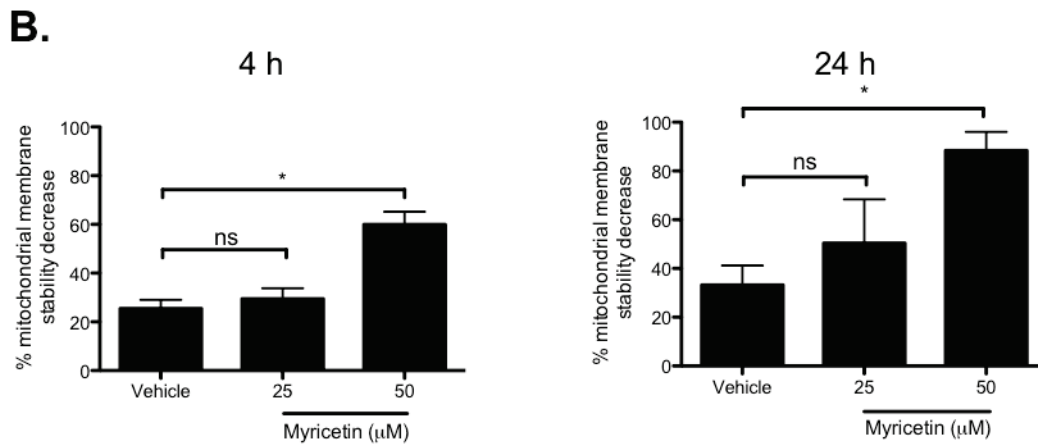
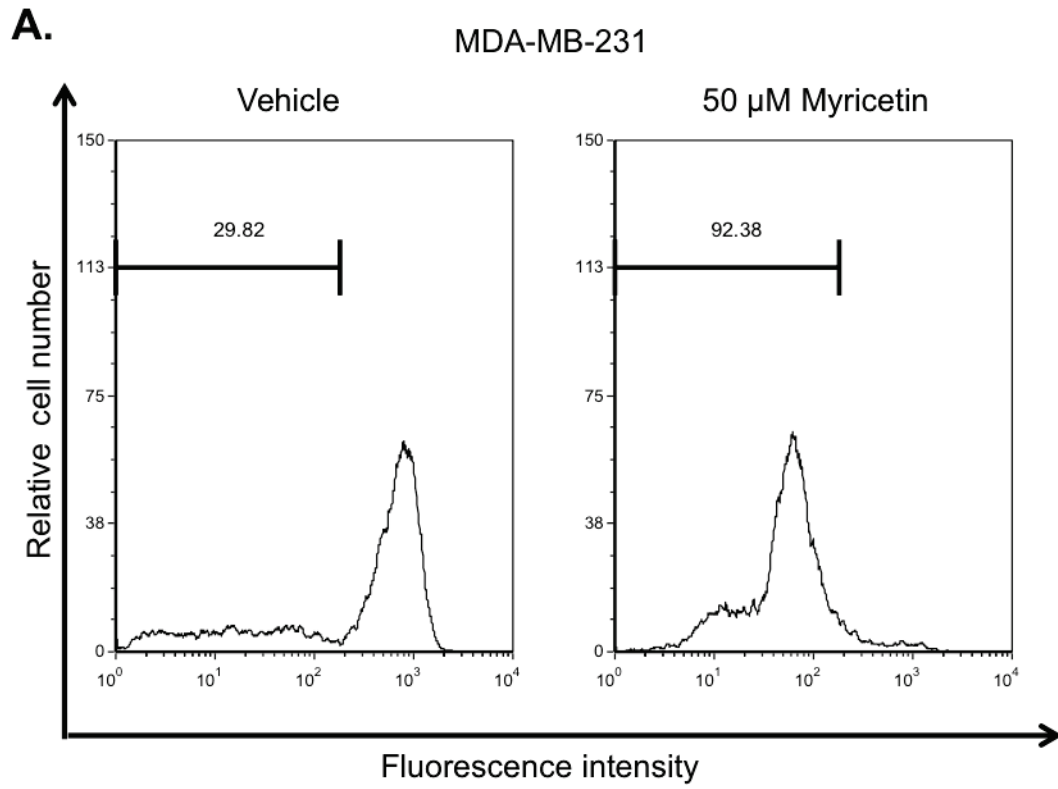


Figure 3.8

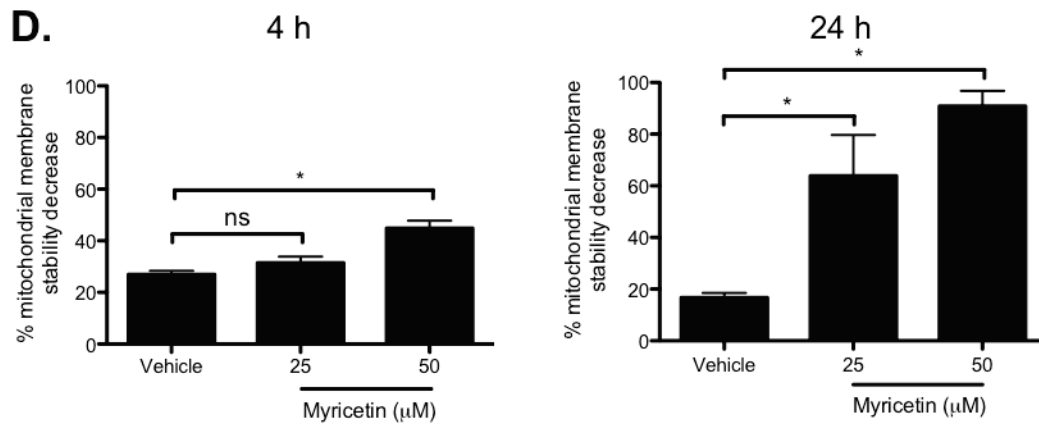
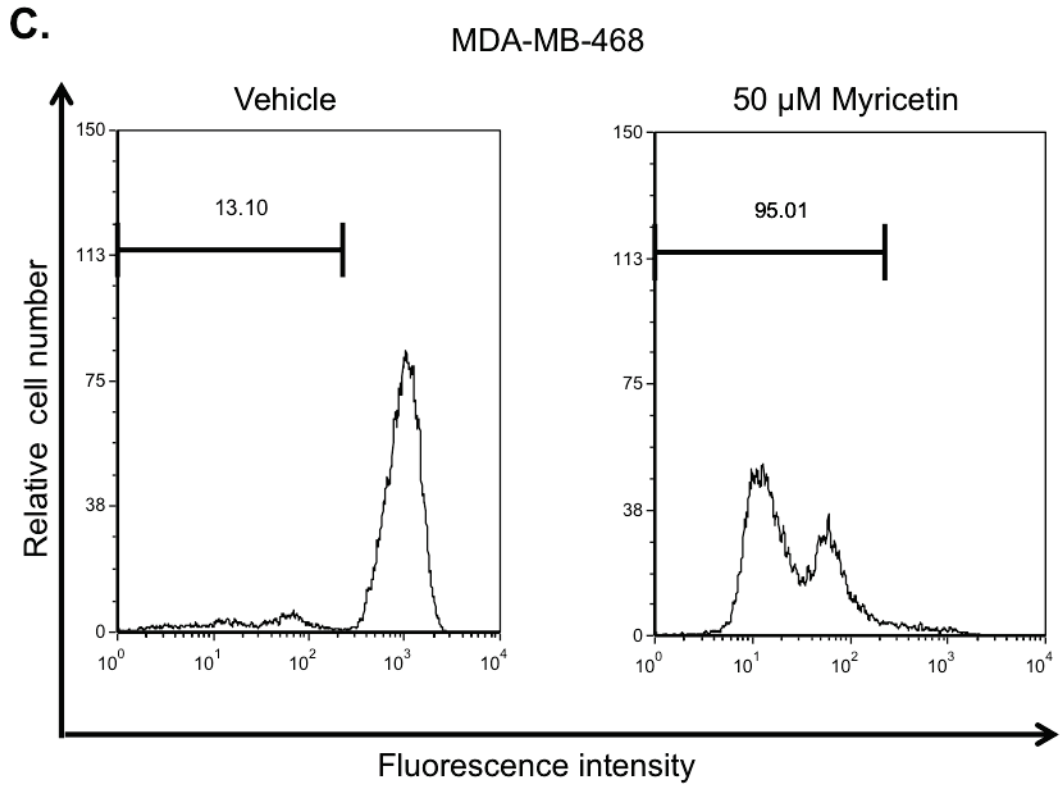


Figure 3.8 (continued)

Figure 3.9. The stability of the mitochondrial membrane in mouse mammary carcinoma cells is decreased by myricetin. 4T1 mouse mammary carcinoma cells were incubated with the indicated concentrations of myricetin for 24 h. The cells were stained with DiOC₆ and fluorescence was measured by flow cytometry. The percent mitochondrial membrane decrease is indicated by decreased fluorescence (leftward shift in DiOC₆ staining intensity). Data shown are **(A)** flow cytometry histogram plots from one representative experiment and **(B)** the mean percent mitochondrial membrane stability decrease from 3 or 4 independent experiments \pm SEM; * denotes $p < 0.05$ and ns denotes not significant compared to DMSO vehicle.

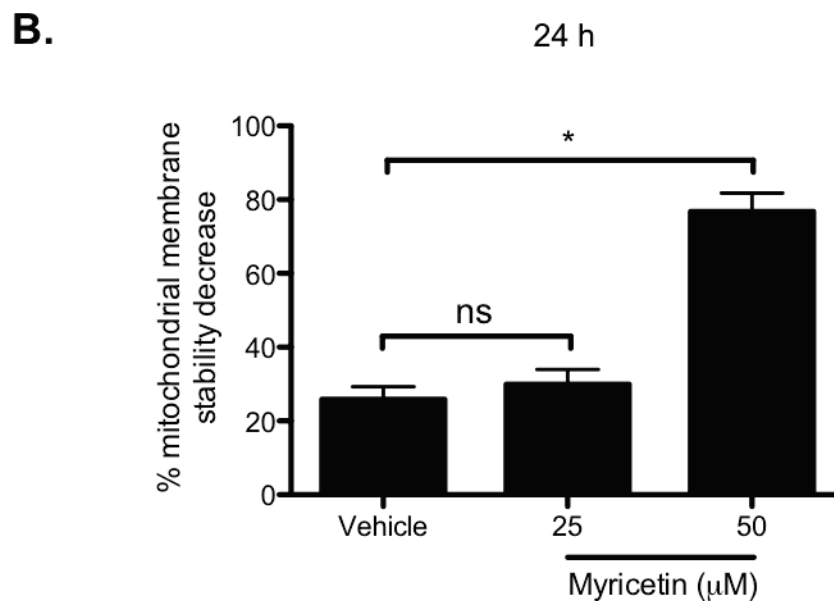
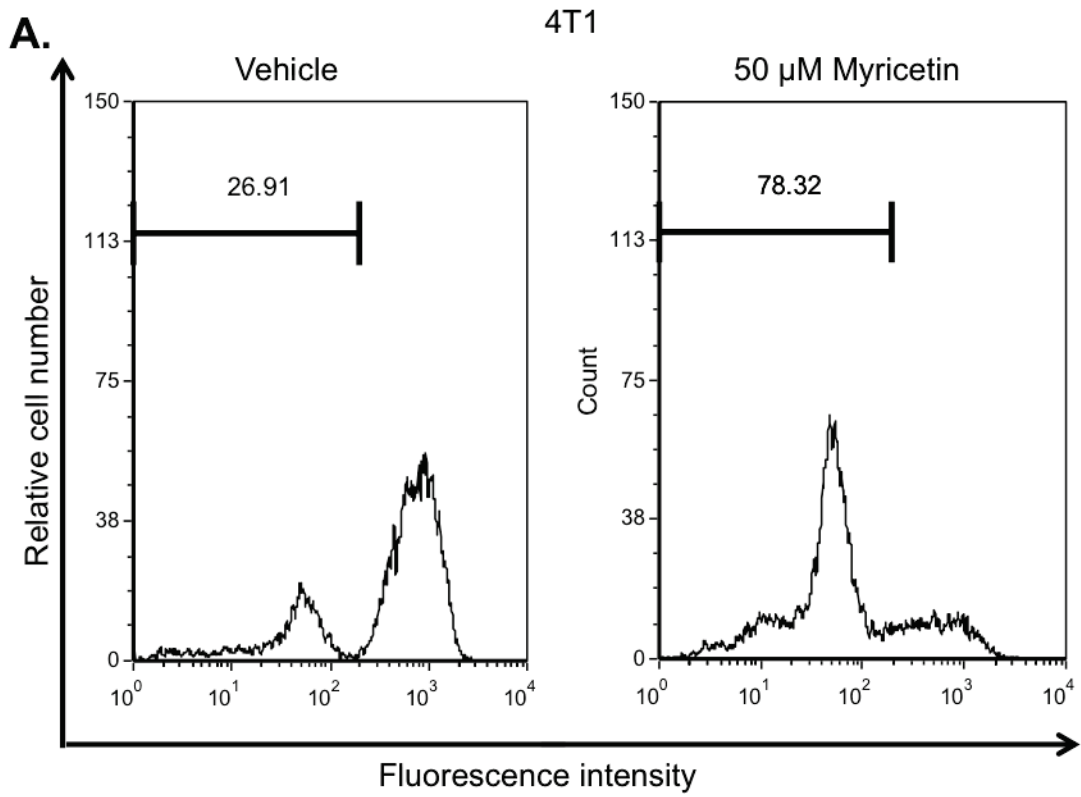
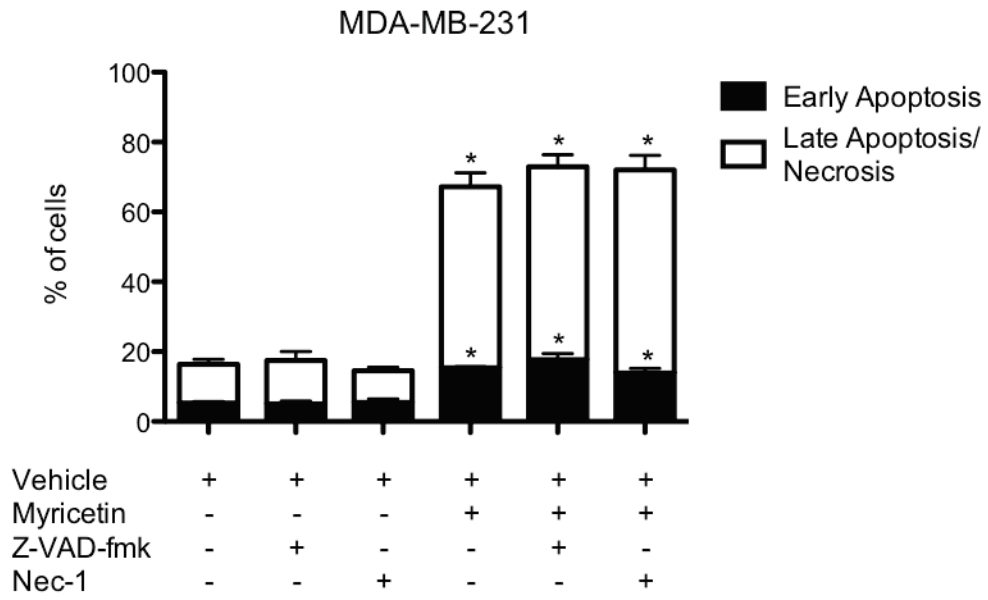


Figure 3.9

Figure 3.10. Myricetin-induced mammary carcinoma cell death is caspase-independent and RIPK1-independent. (A) MDA-MB-231 and (B) MDA-MB-468 mammary carcinoma cells were incubated with Z-VAD-fmk (caspase inhibitor) or necrostatin-1 (RIPK1 inhibitor) for 30 min prior to myricetin treatment; cells were then incubated with myricetin for 24 h. The cells were stained with Annexin-V-FLUOS/PI and fluorescence was measured by flow cytometry. The percent of cells undergoing early apoptosis and late apoptosis were based on the percent of cells that were Annexin-V only positive (early apoptosis) and the cells that were both Annexin-V and PI positive (late apoptosis/necrosis). Data shown are the mean early and late apoptosis/necrosis of cells treated for 24 h from 3 independent experiments \pm SEM; * denotes $p < 0.05$ compared to DMSO vehicle (myricetin-treated cells in early apoptosis were compared to the early apoptosis vehicle-treated cells and myricetin-treated cells in late apoptosis/necrosis were compared to the late apoptosis/necrosis vehicle-treated cells).

A.



B.

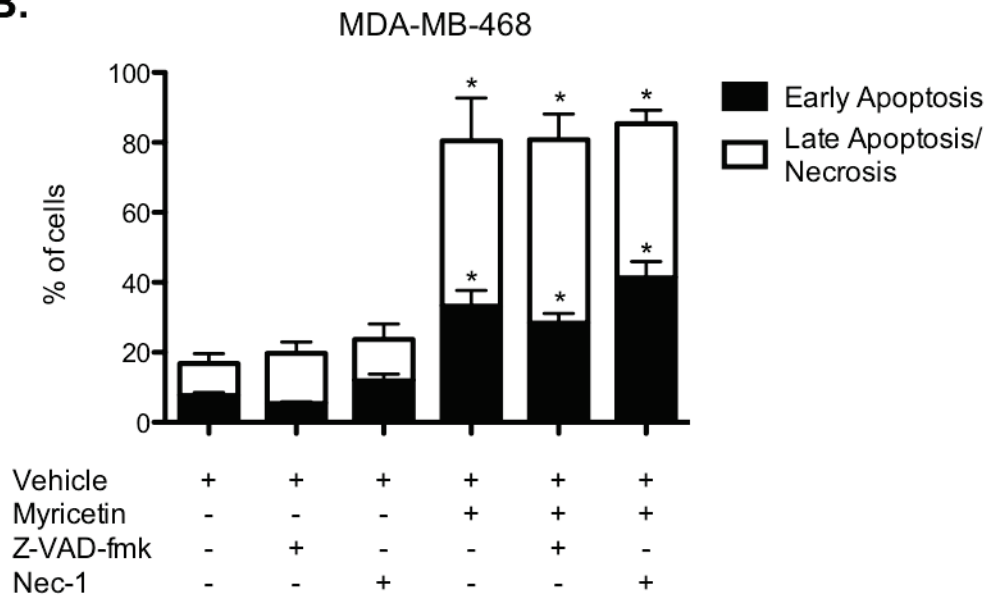


Figure 3.10

Figure 3.11. Intracellular ROS levels are increased in mammary carcinoma cells treated with myricetin. (A), (B) MDA-MB-231 and (C), (D) MDA-MB-468 cells were stained with H₂DCFDA, incubated with or without the antioxidant NAC for 30 min, and were then incubated with the indicated concentrations of myricetin for 4 h. H₂O₂ treated cells were used as a positive control. Fluorescence was measured by flow cytometry. The percent of cells positive for increased ROS is indicated by increased fluorescence (a rightward shift in DCFDA staining intensity). Data shown are **(A)** flow cytometry histogram plots from one representative experiment for MDA-MB-231, **(B)** the mean percent of MDA-MB-231 cells that are ROS positive from 3 independent experiments \pm SEM **(C)** flow cytometry histogram plots from one representative experiment for MDA-MB-468, **(D)** the mean percent of MDA-MB-468 cells that are ROS positive from 3 independent experiments \pm SEM; * denotes $p < 0.05$ and ns denotes not significant compared to DMSO vehicle.

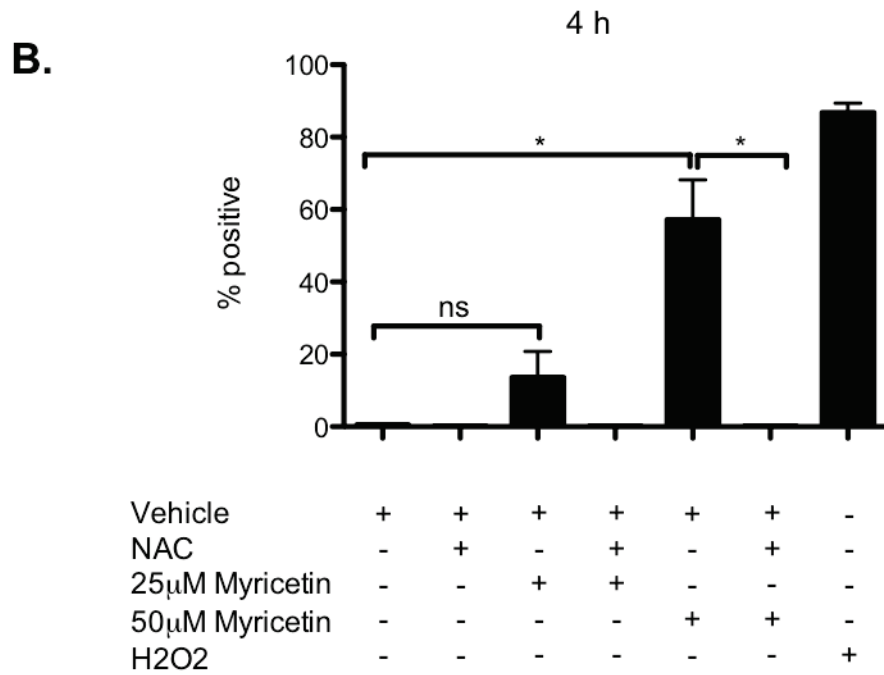
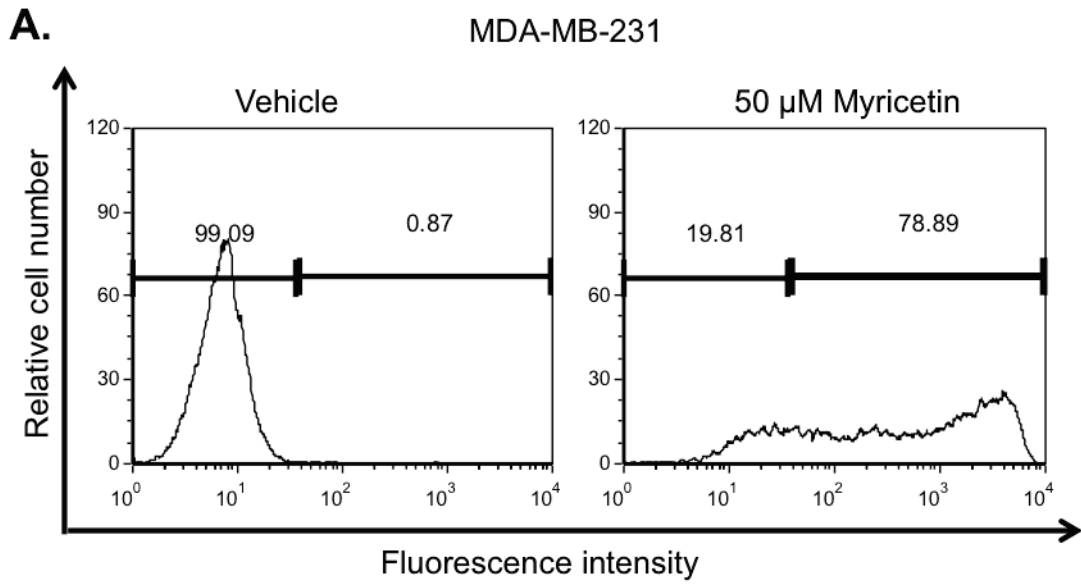


Figure 3.11

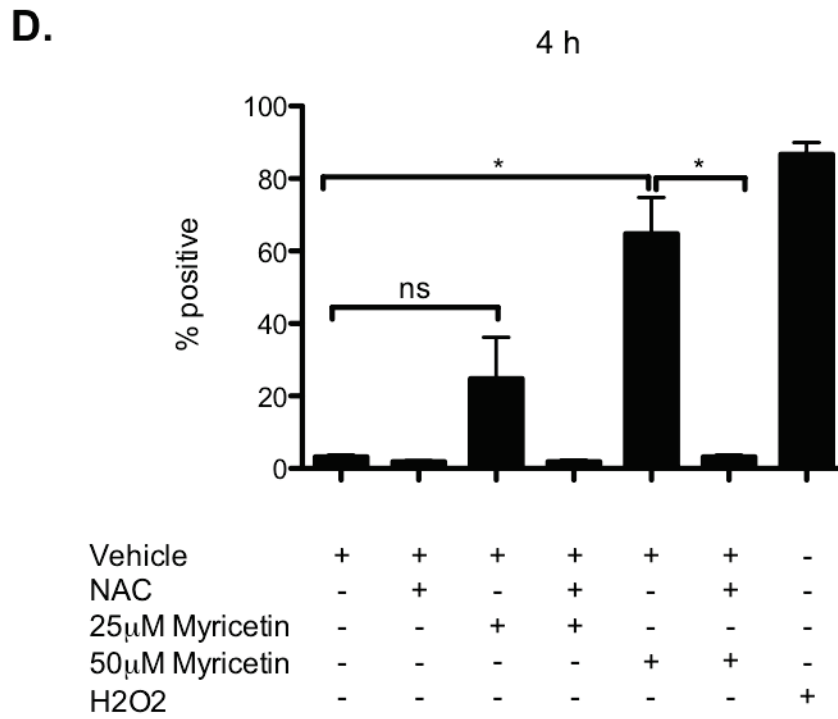
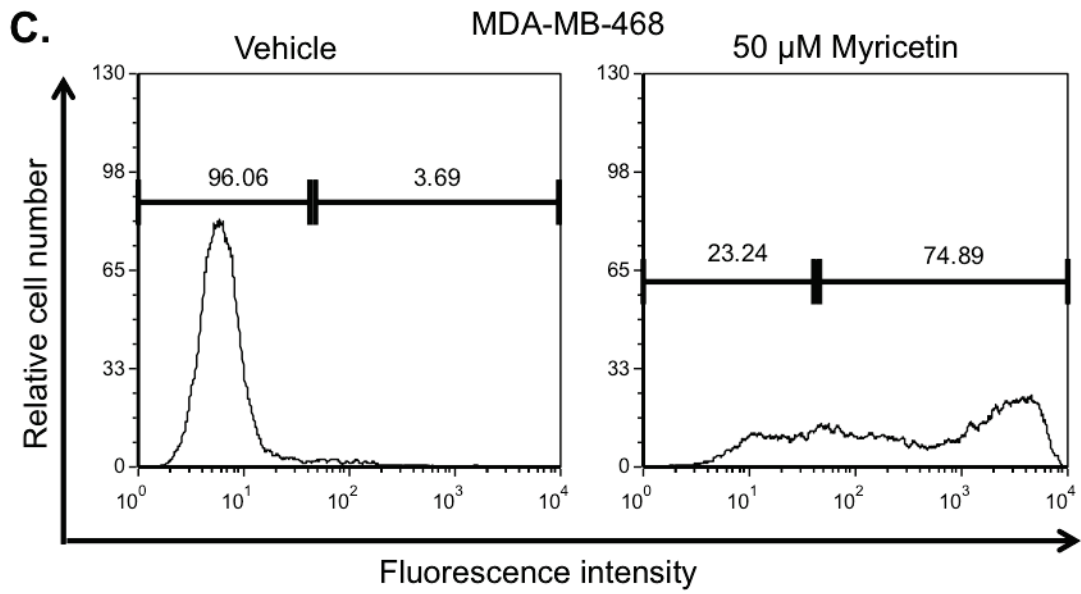


Figure 3.11 (continued)

Figure 3.12. NAC prevents myricetin-induced human mammary carcinoma cell death. (A), (B) MDA-MB-231 and (C), (D) MDA-MB-468 cells were incubated for 30 min with NAC and were then incubated with 50 μ M myricetin for 24 h. The cells were stained with Annexin-V-FLUOS/PI and fluorescence was measured by flow cytometry. The percent of cells undergoing early apoptosis and late apoptosis were based on the percent of cells that were Annexin-V only positive (early apoptosis) and the cells that were both Annexin-V and PI positive (late apoptosis/necrosis). Data shown are (A), (C) flow cytometry dot plots from one representative experiment and (B), (D) the mean early and late apoptosis/necrosis of cells from 3 independent experiments \pm SEM; * denotes $p < 0.05$ compared to DMSO vehicle and # denotes $p < 0.05$ compared to myricetin + NAC treated cells. For the statistical analysis the percent of cells undergoing early apoptosis for each treatment condition was compared separately from the percent of cells undergoing late apoptosis/necrosis for each condition.

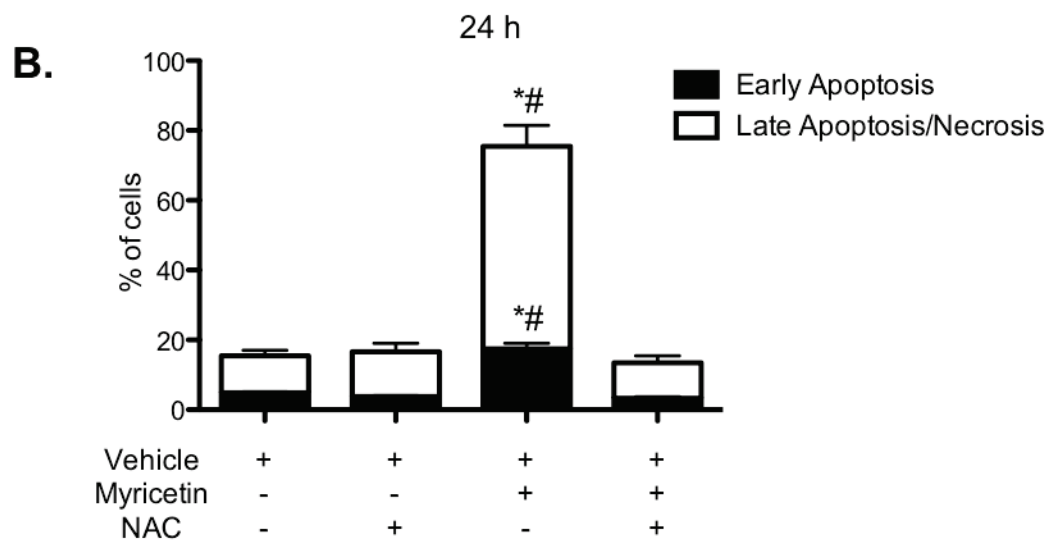
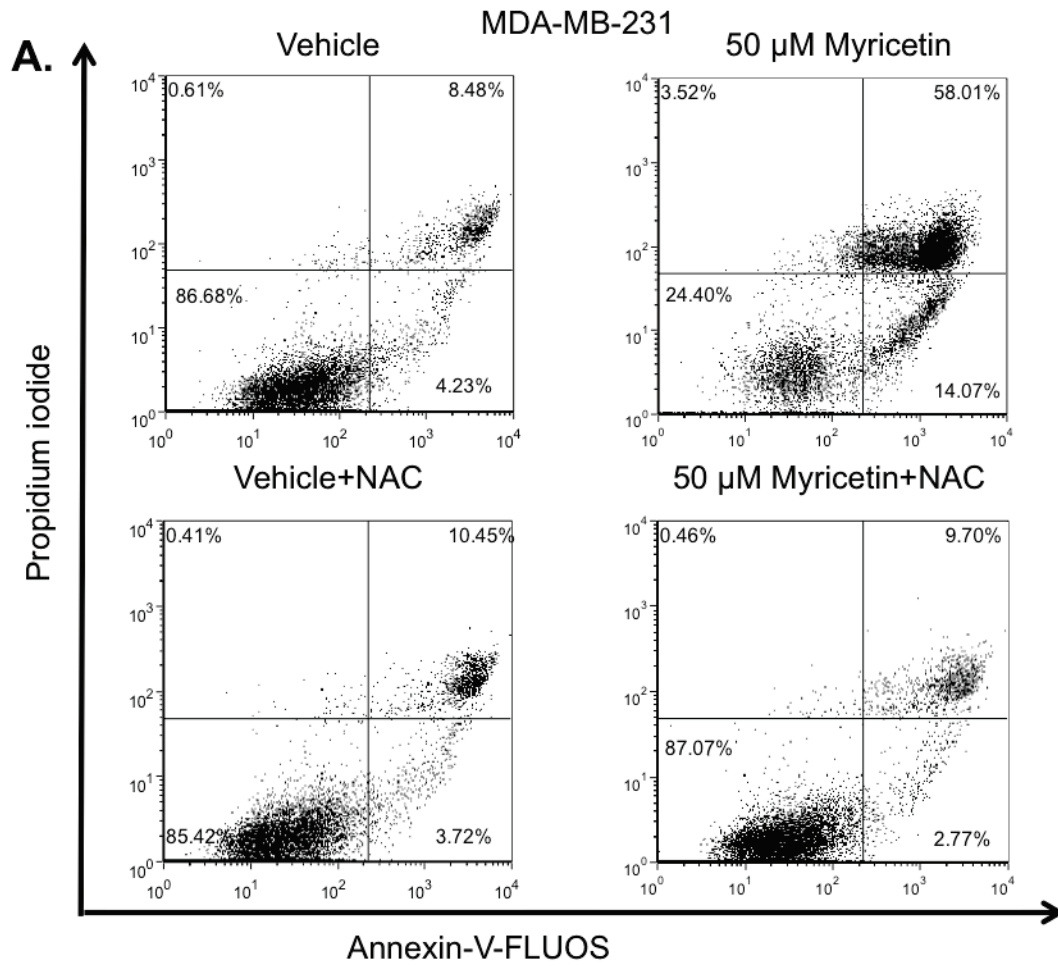


Figure 3.12

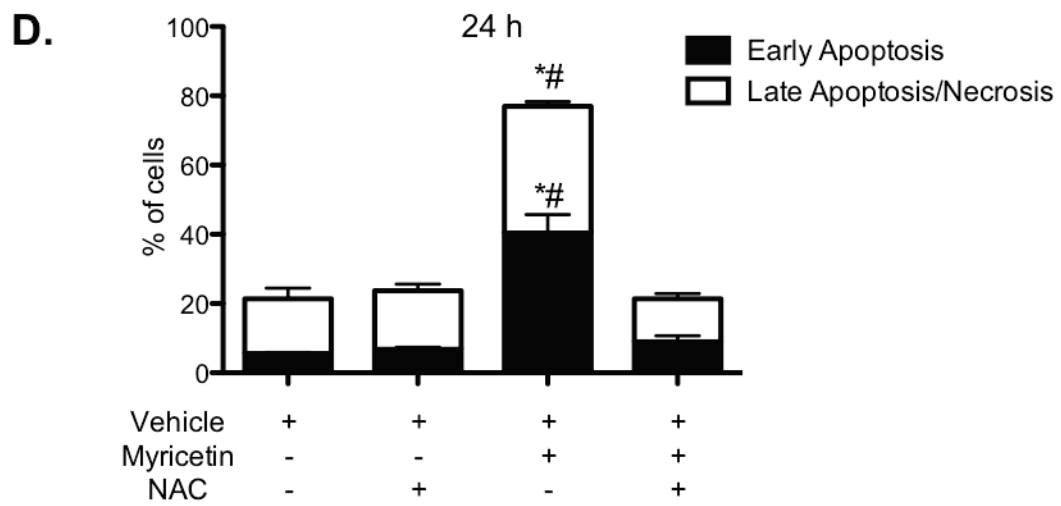
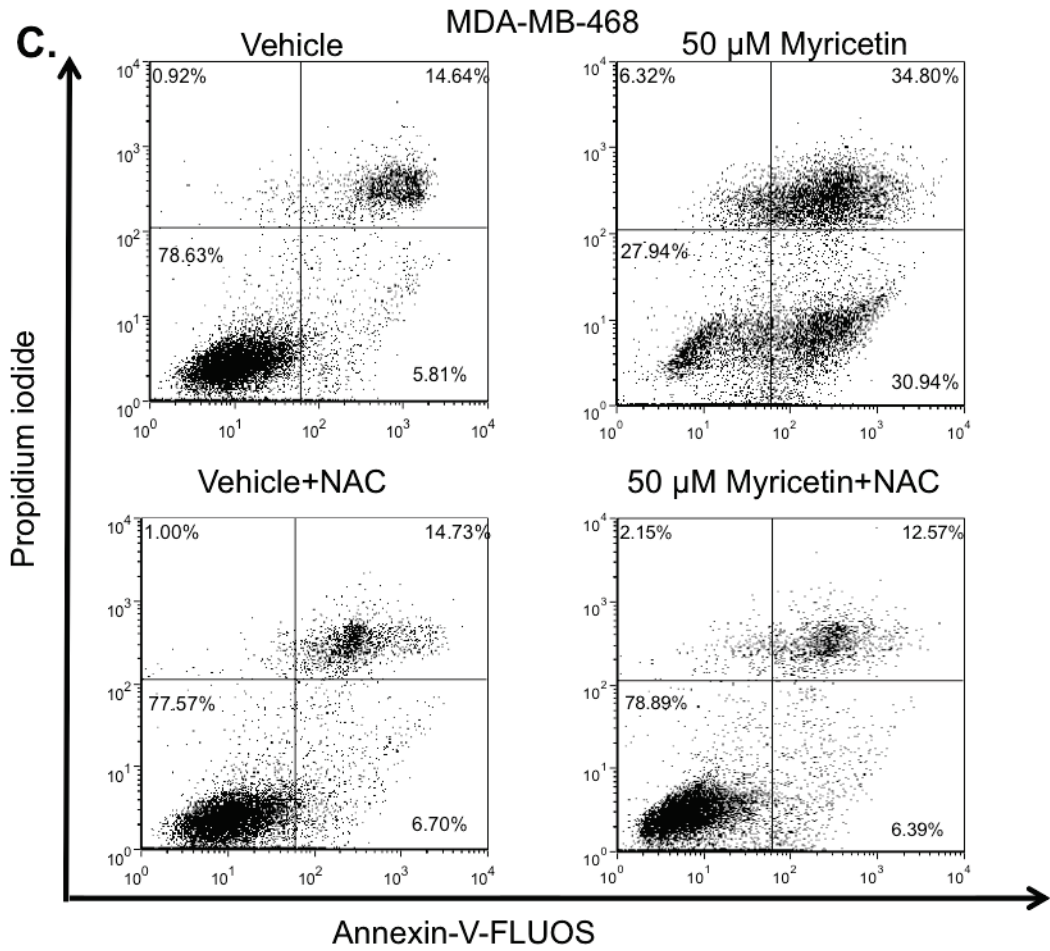


Figure 3.12 (continued)

Figure 3.13. NAC prevents myricetin-induced mouse mammary carcinoma cell death. 4T1 cells were incubated for 30 min with NAC and were then incubated with 50 μ M myricetin for 24 h. The cells were stained with Annexin-V-FLUOS/PI and fluorescence was measured by flow cytometry. The percent of cells undergoing early apoptosis and late apoptosis were based on the percent of cells that were Annexin-V only positive (early apoptosis) and the cells that were both Annexin-V and PI positive (late apoptosis/necrosis). Data shown are **(A)** flow cytometry dot plots from one representative experiment and **(B)** the mean early and late apoptosis/necrosis of cells from 3 independent experiments \pm SEM; * denotes $p < 0.05$ compared to DMSO vehicle and # denotes $p < 0.05$ compared to myricetin + NAC treated cells. For the statistical analysis the percent of cells undergoing early apoptosis for each treatment condition was compared separately from the percent of cells undergoing late apoptosis/necrosis for each condition.

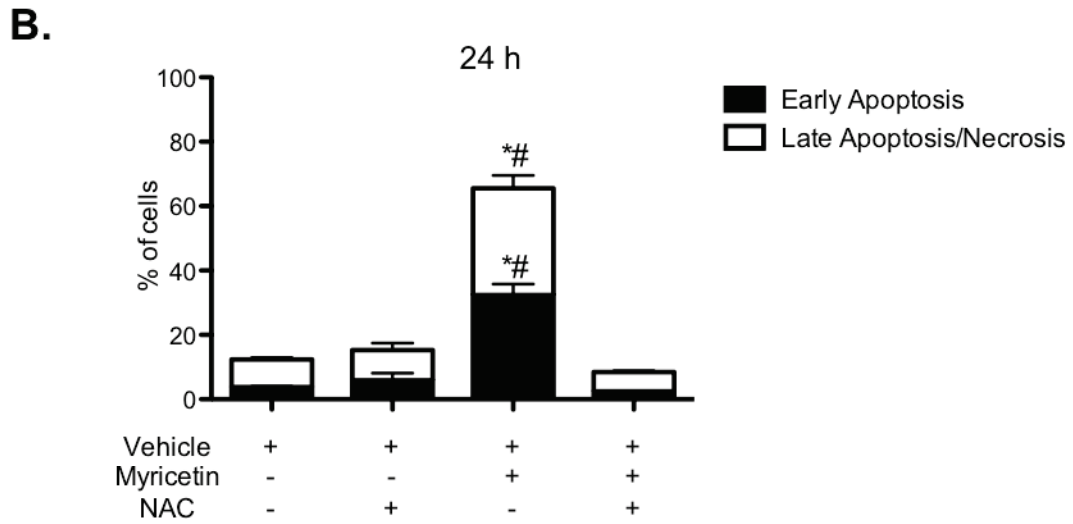
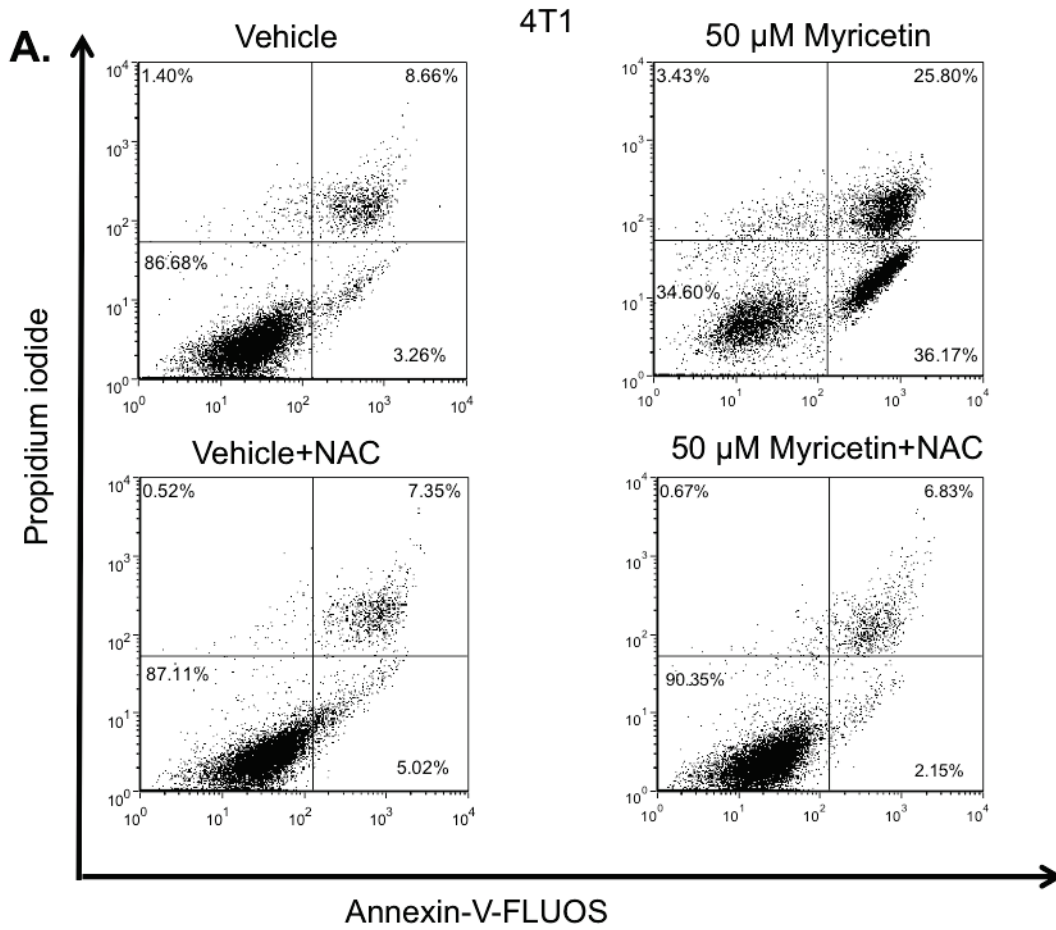


Figure 3.13

Figure 3.14. Changes in mitochondrial membrane stability caused by myricetin are inhibited by NAC. (A) MDA-MB-231 and **(B)** MDA-MB-468 cells were incubated with NAC for 30 min and then incubated with the indicated concentrations of myricetin for 4 or 24 h. The cells were stained with DiOC₆ and fluorescence was measured by flow cytometry. The percent mitochondrial membrane decrease is indicated by decreased fluorescence. Data shown are the mean percent mitochondrial membrane stability decrease for **(A)** MDA-MB-231 and **(B)** MDA-MB-468 cells treated for 4 h (left) and 24 h (right) from 3 independent experiments \pm SEM; * denotes $p < 0.05$ and ns denotes not significant compared to DMSO vehicle.

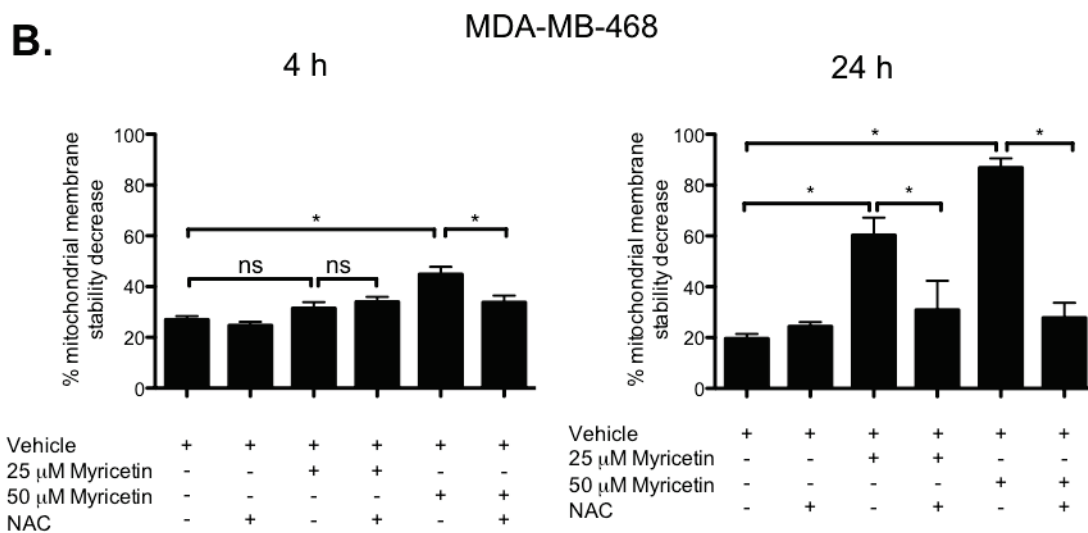
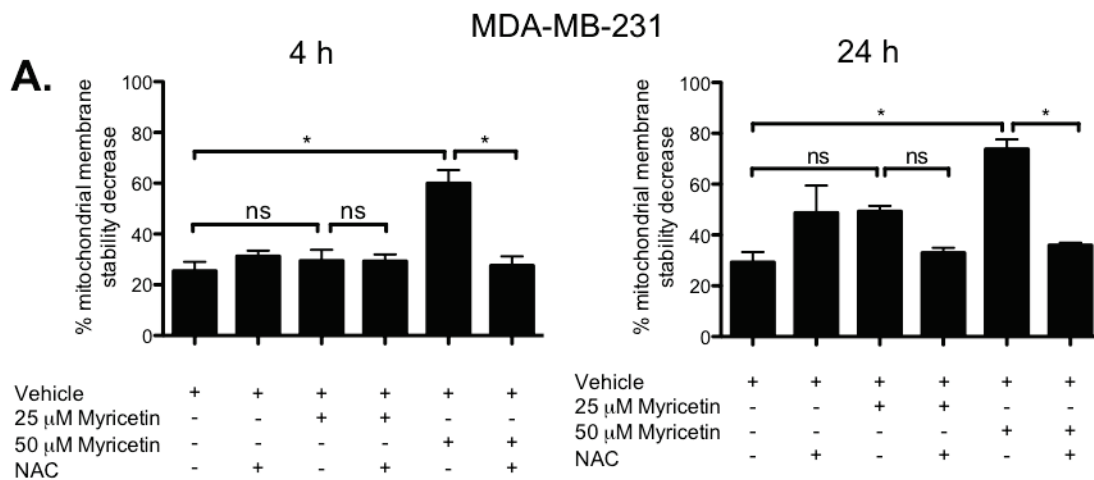
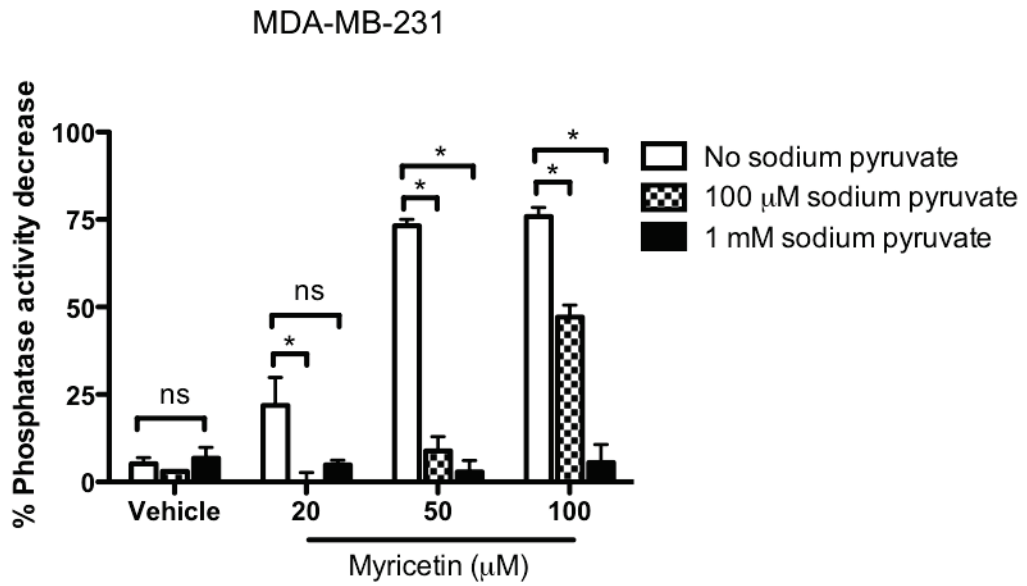


Figure 3.14

Figure 3.15. Sodium pyruvate added to cell culture medium prevents myricetin-induced decreases in mammary carcinoma cell growth. (A) MDA-MB-231 and **(B)** MDA-MB-468 cells were incubated with the indicated concentrations of myricetin diluted in cell culture medium containing the indicated concentrations of sodium pyruvate for 24 h. The acid phosphatase colorimetric assay was used to measure cell number, and at 24 h the cells were lysed and acid phosphatase substrate was incubated with the lysate for 2 h. The percent phosphatase activity decrease is relative to the medium control. The data shown are the mean of 3 or 4 independent experiments \pm SEM; * denotes $p < 0.05$ and ns denotes not significant compared to myricetin as determined by ANOVA with the Tukey-Kramer multiple comparisons post-test.

A.



B.

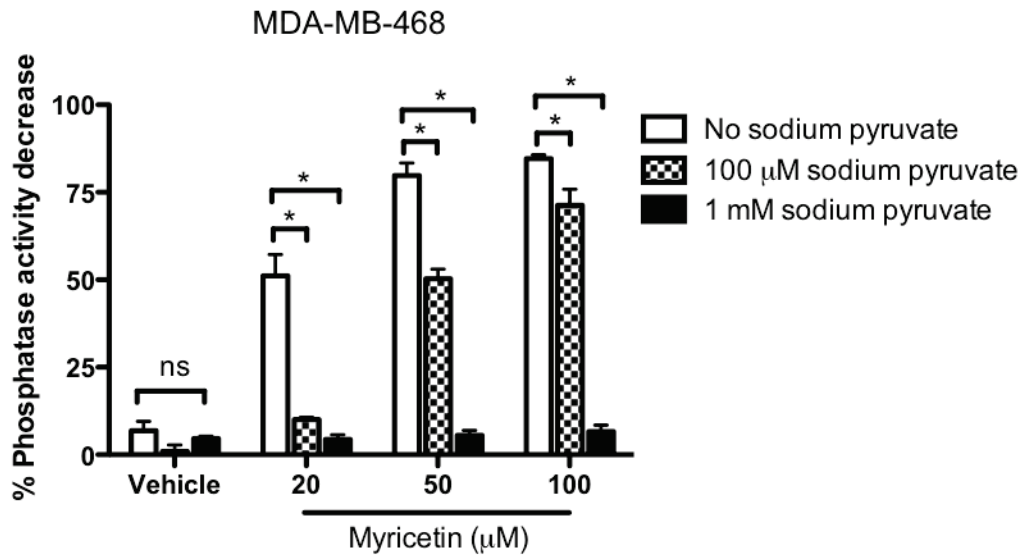


Figure 3.15

Figure 3.16. The levels of a double-stranded DNA damage marker, γ -H2AX, are increased in mammary carcinoma cells treated with myricetin, and the increase in γ -H2AX is prevented by NAC. (A), (B) MDA-MB-231 and (C), (D) MDA-MB-468 cells were incubated with NAC for 30 min and then incubated with myricetin for 4 h. The cells were stained with eFluor 660-anti-human γ -H2AX or isotype control antibodies. The fluorescent intensity (γ -H2AX expression) was measured by flow cytometry. Data shown are (A), (C) representative flow cytometry histograms from one experiment for (A) MDA-MB-231 and (C) MDA-MB-468 cells, and (B), (D) the mean percent of cells positive for increased γ -H2AX for (B) MDA-MB-231 and (D) MDA-MB-468 cells treated from 3 independent experiments \pm SEM; * denotes $p < 0.05$, as determined by ANOVA with the Tukey-Kramer multiple comparisons post-test, compared to DMSO vehicle or myricetin + NAC treatment as indicated.

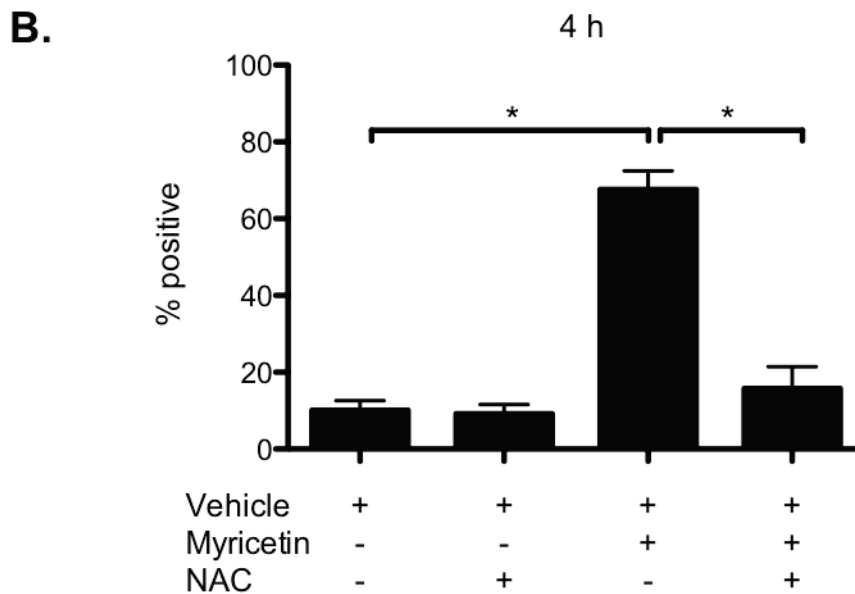
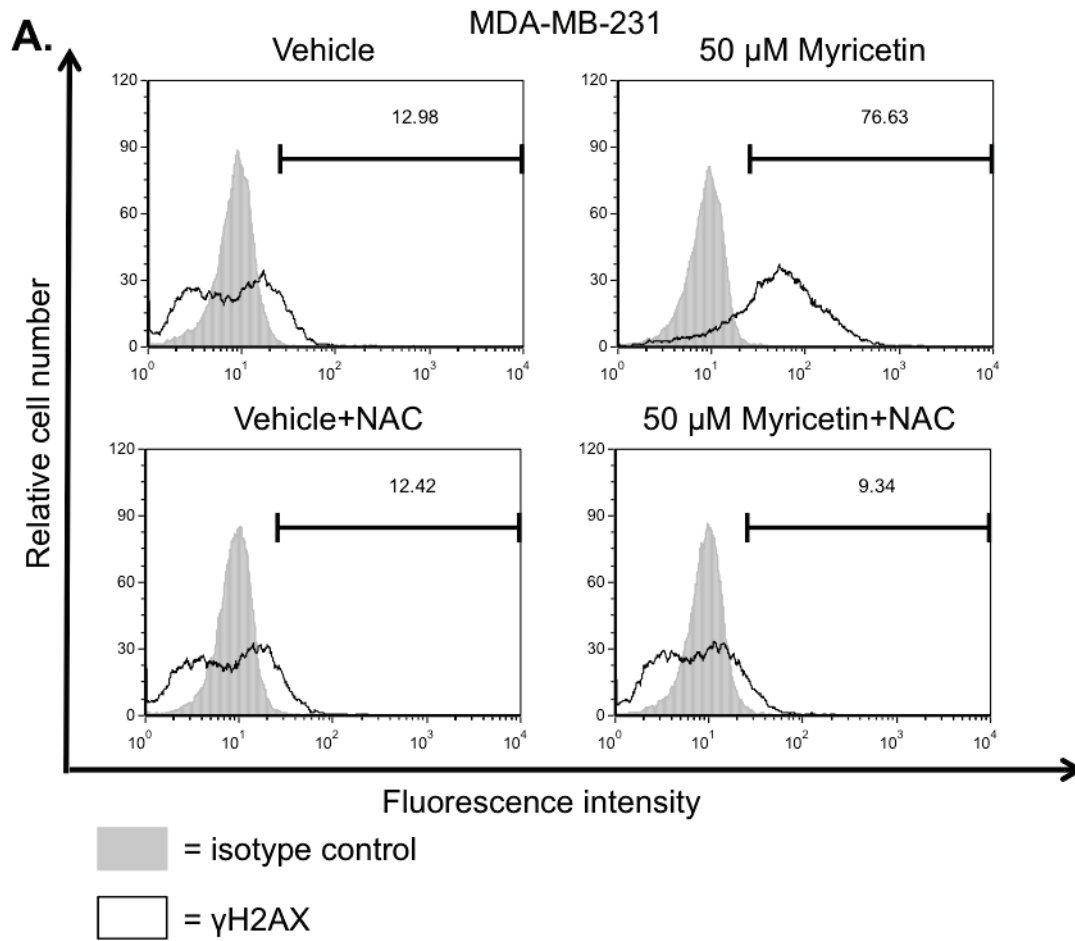


Figure 3.16

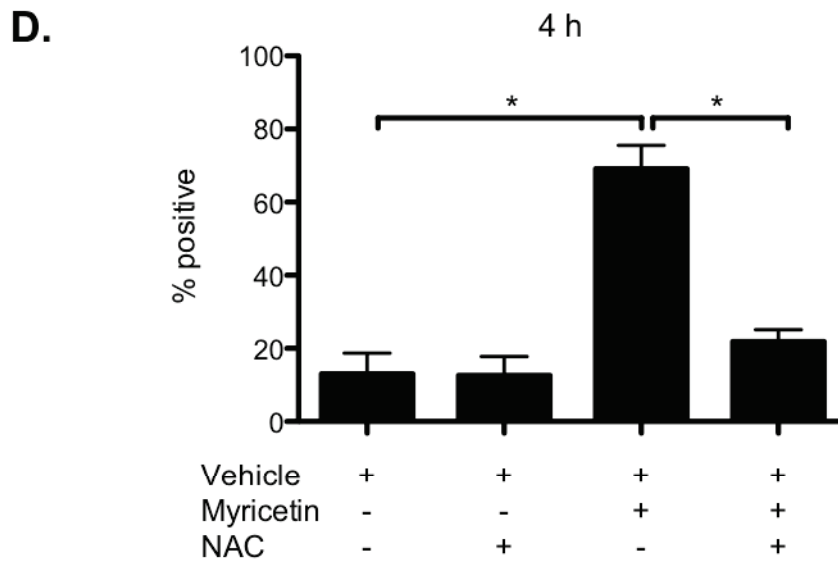
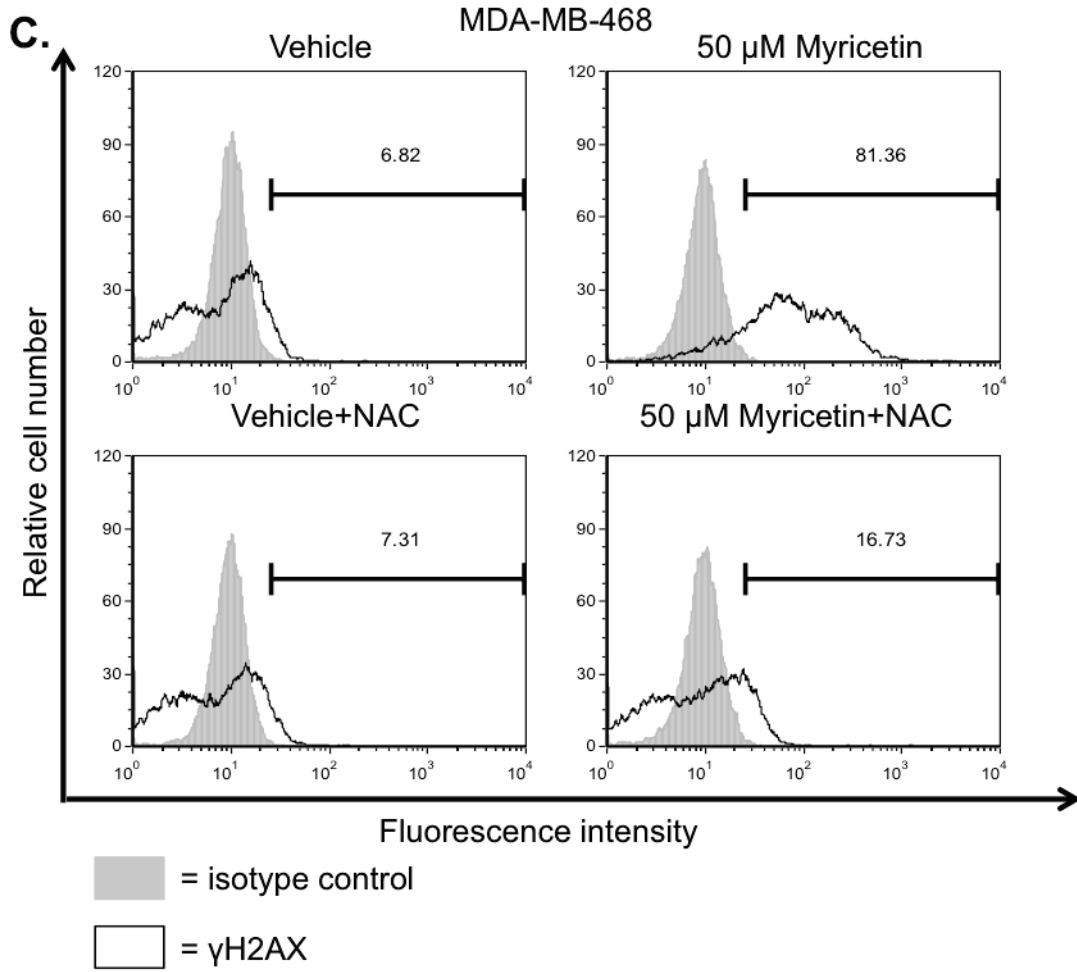


Figure 3.16 (continued)

Figure 3.17. Extracellular H₂O₂ is formed in cell culture medium in the presence of myricetin. The indicated concentrations of myricetin were added to cell culture medium without cells **(A)** and **(B)** in the presence of MDA-MB-468 cells; 100 μ M H₂O₂ was used as a positive control. Amplex red and HRP were added to the cell culture medium and incubated for 4 and 24 h. After 4 and 24 h the absorbance at 570 nm was measured. The data shown are the mean of 3 independent experiments \pm SEM; * denotes $p < 0.05$ and ns denotes not significant compared to DMSO vehicle control as determined by ANOVA with the Tukey-Kramer multiple comparisons post-test.

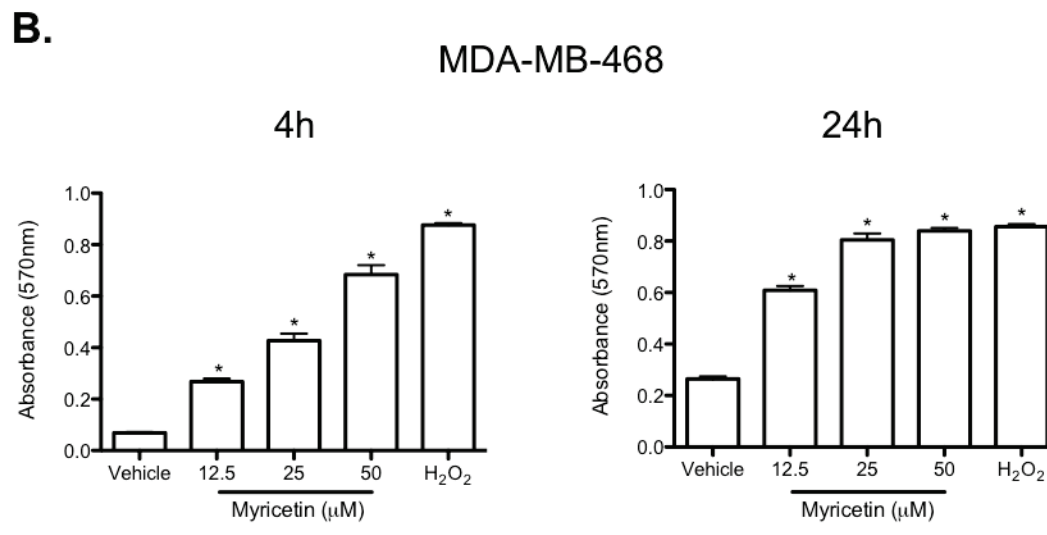
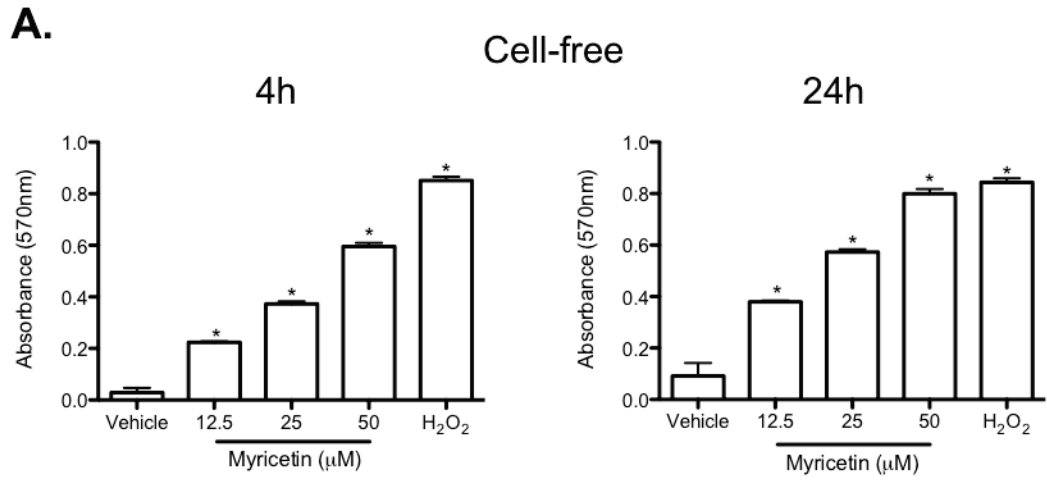
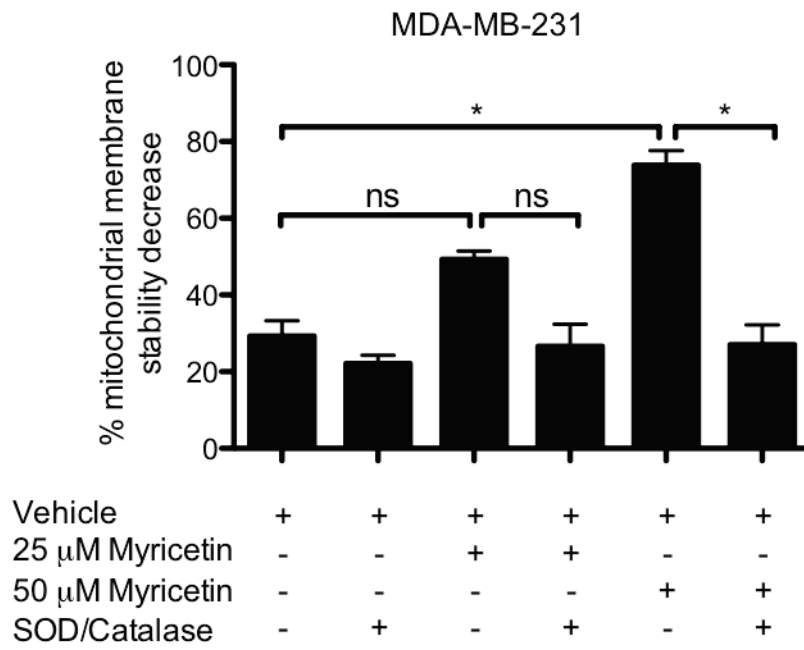


Figure 3.17

Figure 3.18. SOD and catalase prevent myricetin-induced decreases in mitochondrial membrane stability. (A) MDA-MB-231 and (B) MDA-MB-468 cells were incubated with SOD and catalase and the indicated concentrations of myricetin for 24 h. The cells were stained with DiOC₆ and fluorescence was measured by flow cytometry. The percent mitochondrial membrane decrease is indicated by decreased fluorescence (leftward shift in DiOC₆ staining intensity). Data shown are the mean percent mitochondrial membrane stability decrease for **(A) MDA-MB-231** and **(B) MDA-MB-468** cells treated for 24 h from 3 independent experiments \pm SEM; * denotes $p < 0.05$ and ns denotes not significant compared to DMSO vehicle and cells treated with both myricetin and SOD/catalase as indicated and determined by ANOVA with the Tukey-Kramer multiple comparisons post-test.

A.



B.

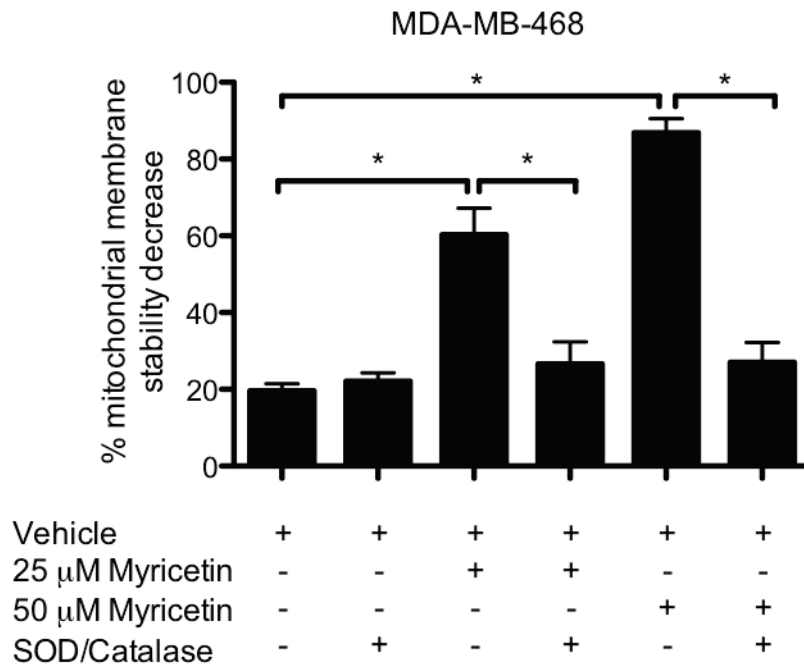
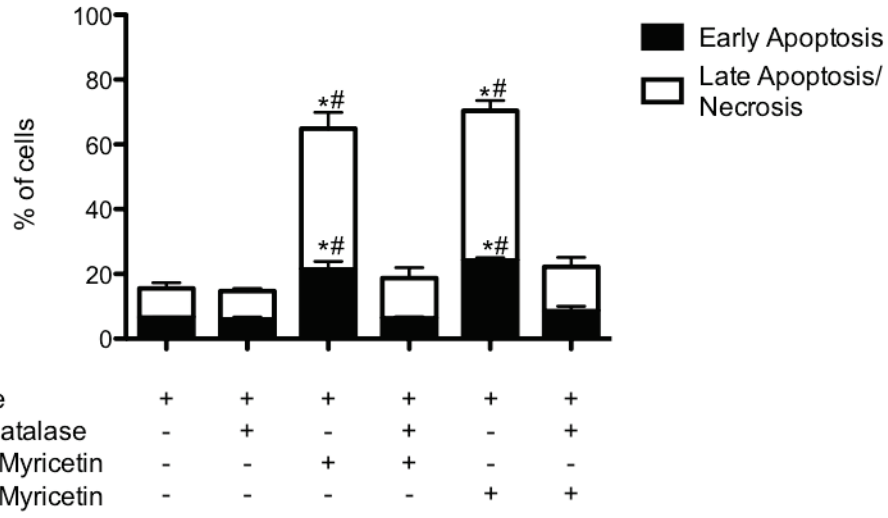


Figure 3.18

Figure 3.19. SOD and catalase prevent myricetin-induced mammary carcinoma cell death. (A) MDA-MB-231 cells and (B) MDA-MB-468 cells were incubated with SOD/catalase and the indicated concentration of myricetin for 24 h. The cells were stained with Annexin-V-FLUOS/PI and fluorescence was measured by flow cytometry. The percent of cells undergoing early apoptosis and late apoptosis were based on the percent of cells that were Annexin-V only positive (early apoptosis) and the cells that were both Annexin-V and PI positive (late apoptosis/necrosis). Data shown are the mean early and late apoptosis/necrosis of cells for (A) MDA-MB-231 and (B) MDA-MB-468 from 3 independent experiments \pm SEM; * denotes $p < 0.05$ compared to DMSO vehicle and # denotes $p < 0.05$ compared to myricetin + SOD/catalase treated cells as determined by ANOVA with the Tukey-Kramer multiple comparisons post-test. For the statistical analysis the percent of cells undergoing early apoptosis for each treatment condition was compared separately from the percent of cells undergoing late apoptosis/necrosis for each condition.

A.

MDA-MB-231



B.

MDA-MB-468

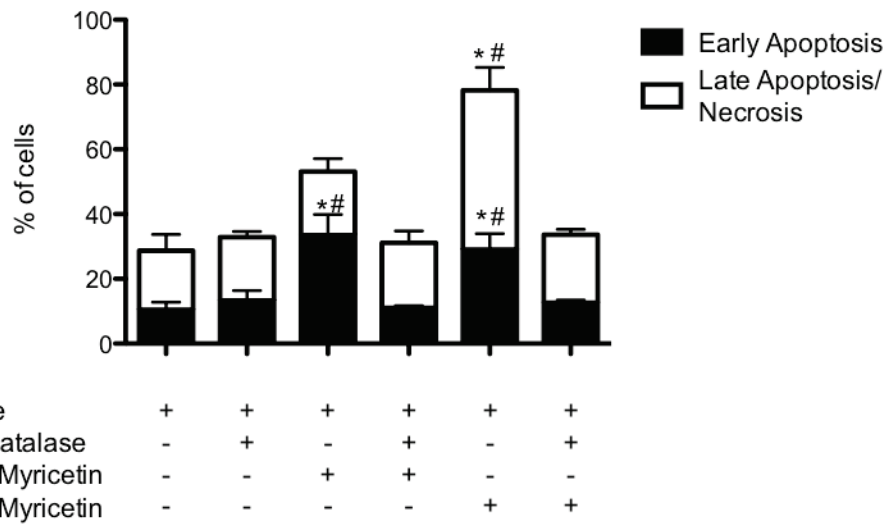


Figure 3.19

Figure 3.20. Myricetin promotes p38 MAPK phosphorylation in mammary carcinoma cells. (A), (B) MDA-MB-231 and (C), (D) MDA-MB-468 cells were incubated for 30 min with NAC and were then incubated with the indicated concentration of myricetin for 30 min or 3 h. The cells were lysed, protein was isolated and separated by western blotting. Nitrocellulose membranes were probed with the indicated antibodies and appropriate secondary antibodies. Data shown are (A), (C) one representative western blot and (B), (D) the mean density of phosphorylated p38 MAPK normalized to the medium and total p38 MAPK early and late apoptosis/necrosis of cells from 5 (MDA-MB-231) or 3 (MDA-MB-468) independent experiments \pm SEM; * denotes $p < 0.05$ and ns denotes not significant compared to DMSO vehicle and myricetin + NAC treatments as indicated, and as determined by ANOVA with the Tukey-Kramer multiple comparisons post-test.

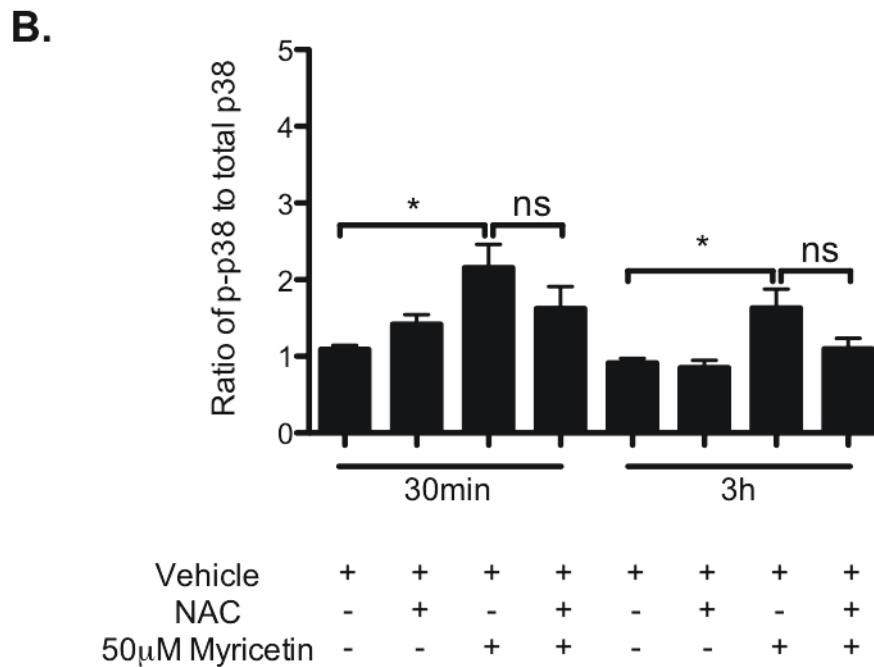
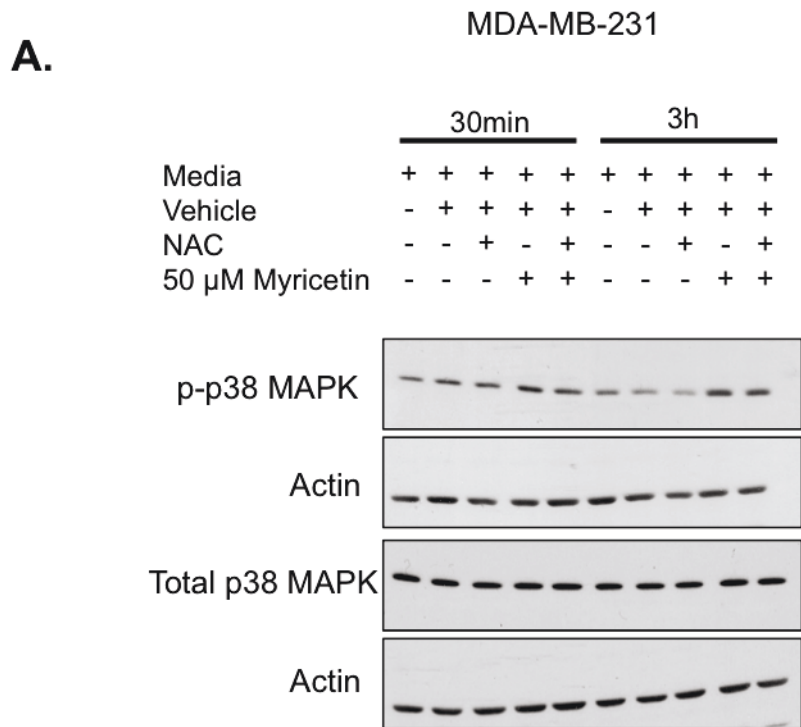
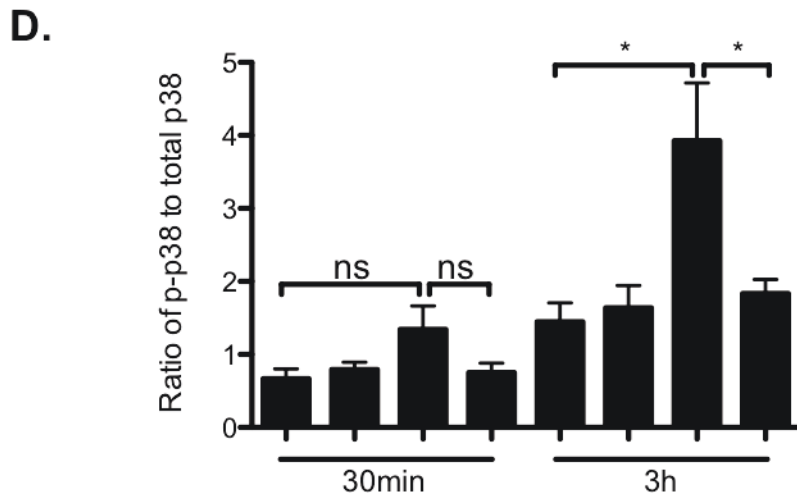
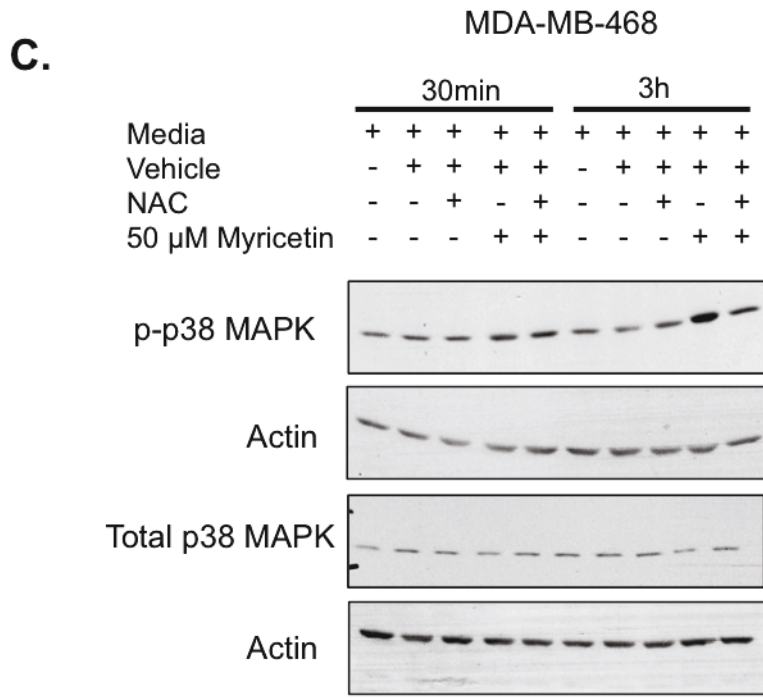


Figure 3.20



| | | | | | | | | |
|----------------------|---|---|---|---|---|---|---|---|
| Vehicle | + | + | + | + | + | + | + | + |
| NAC | - | + | - | + | - | + | - | + |
| 50 μ M Myricetin | - | - | + | + | - | - | + | + |

Figure 3.20 (continued)

Figure 3.21. Inhibition of p38 MAPK does not prevent myricetin-induced mammary carcinoma cell death. (A) MDA-MB-231 cells and (B) MDA-MB-468 cells were incubated p38 MAPK inhibitor III (10 μ M) for 30 min and then incubated with the in 50 μ M myricetin for 24 h. The cells were stained with Annexin-V-FLUOS/PI and fluorescence was measured by flow cytometry. The percent of cells undergoing early apoptosis and late apoptosis were based on the percent of cells that were Annexin-V only positive (early apoptosis) and the cells that were both Annexin-V and PI positive (late apoptosis/necrosis). Data shown are the mean early and late apoptosis/necrosis of cells for (A) MDA-MB-231 and (B) MDA-MB-468 from 3 independent experiments \pm SEM; * denotes $p < 0.05$ compared to DMSO vehicle as determined by ANOVA with the Tukey-Kramer multiple comparisons post-test. For the statistical analysis the percent of cells undergoing early apoptosis for each treatment condition was compared separately from the percent of cells undergoing late apoptosis/necrosis for each condition.

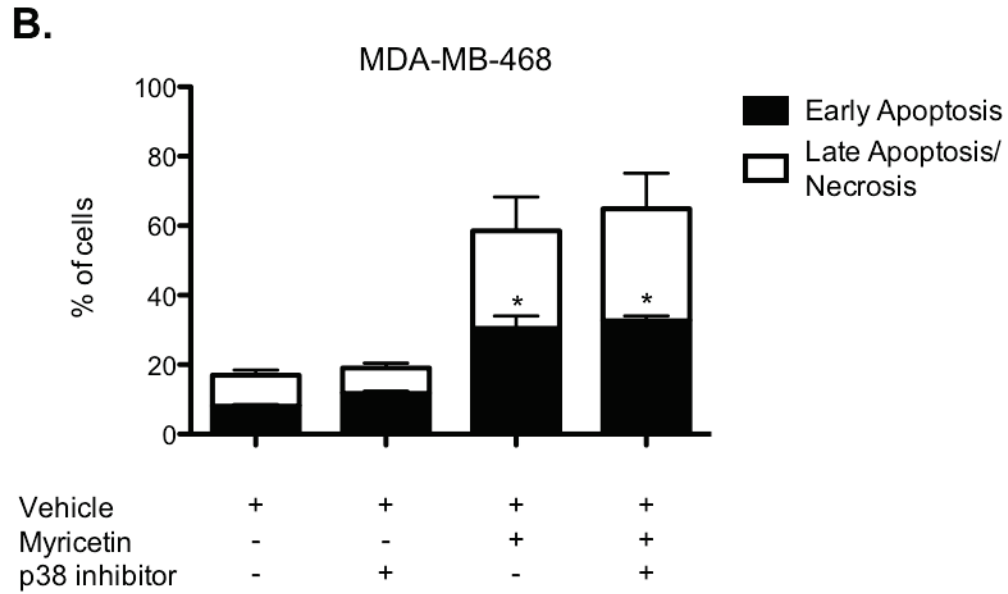
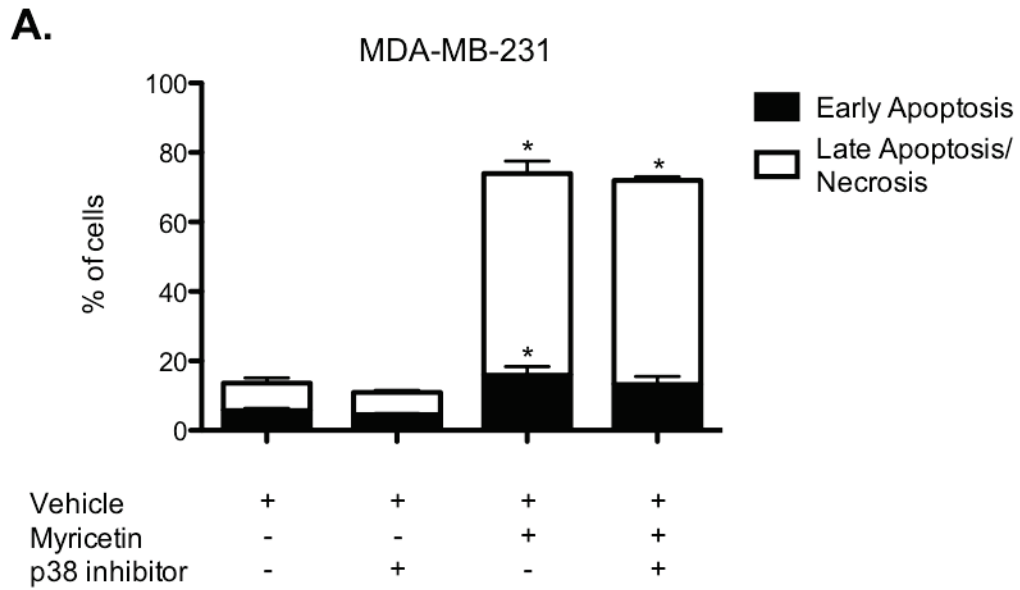


Figure 3.21

CHAPTER 4

DISCUSSION

Phytochemicals are compounds found in plant-based foods that have anti-cancer properties. In particular, the phenolic class of phytochemicals is currently being studied for use in cancer prevention and treatment. Myricetin is a phenolic phytochemical that has been shown to have anti-cancer properties for a variety of different types of cancer. However, there is very little research examining the effect of myricetin on breast cancer cells. This is the first study to examine the effects of myricetin on triple-negative breast cancer cells and to show that myricetin-induced cancer cell death is dependent on ROS formation in the extracellular environment.

4.1. Myricetin is cytotoxic for breast cancer cells

Previous studies have shown that myricetin is cytotoxic and growth inhibitory for cancer cells; however, there are conflicting reports regarding the growth inhibitory effect of myricetin for breast cancer cells (276, 298). This study examined the cytotoxic effect of myricetin on breast cancer cells by first determining if myricetin altered the viability of a variety of mammary carcinoma cell lines, including human triple-negative and other mammary carcinoma cell lines, as well as mouse mammary carcinoma cell lines. Myricetin caused a decrease in cell viability (as indicated by decreased acid phosphatase activity) of all types of mammary carcinoma cell lines tested, including the triple-negative cell lines MDA-MB-231 and MDA-MB-468 in a dose-dependent manner (Figure 3.1). This result is similar to a study by Kuntz *et al.* that showed myricetin to have an inhibitory effect on MCF-7 cell viability (298). The effect of myricetin on viable cell number was also compared to the effects of two other well-studied phytochemicals: EGCG and resveratrol, which are found in green tea and red wine, respectively. This is the first study to directly compare the effects of myricetin, EGCG, and resveratrol on breast cancer cells. Myricetin and EGCG

caused similar decreases in the total number of viable human triple-negative (MDA-MB-231 and MBA-MB-468) and mouse (4T1) mammary carcinoma cells. The decreases in viable cell number caused by resveratrol were significantly lower than the decreases caused by myricetin or EGCG (Figure 3.3). EGCG and resveratrol are often considered to be largely responsible for the chemopreventative properties of green tea and red wine observed in epidemiological studies (231, 299). However, this study indicates that myricetin, which is found in both green tea and red wine, is as effective as EGCG and more effective than resveratrol at decreasing viable mammary carcinoma cell number. EGCG, the most abundant phenolic in green tea, has a relative level that is about four times higher than the level of myricetin in green tea (300). The relative levels of myricetin and resveratrol in red wine are variable depending on the type of wine; some types have higher levels of resveratrol than myricetin while other varieties have higher levels of myricetin than resveratrol (301–303). Myricetin may therefore be an important component of the anticancer properties of green tea and red wine. This study also showed that myricetin could decrease viable mammary carcinoma cell number to a similar extent as two conventional chemotherapeutic drugs, doxorubicin and docetaxel, used in breast cancer treatment (Figure 3.4).

In addition to investigating the effects of myricetin on mammary carcinoma cells, this study also examined whether myricetin altered the viability of normal cells. Myricetin did not affect the total number of viable human dermal fibroblasts but did decrease the number of viable human mammary epithelial cells (Figure 3.2). The decrease in human mammary epithelial cell viability induced by myricetin may be due to increased cell death and/or decreased cell proliferation since the assay used to measure total cell viability (acid phosphatase assay) does not discriminate between the two possible mechanisms. Previous studies have shown that myricetin is not toxic to normal cells such as primary human polymorphonuclear cells and mouse peritoneal macrophages (269). Taken together with the results of this study, this suggests that for some tissue types, myricetin may alter normal cell viability while not

affecting other tissue types. However, in the previous studies of the effects of myricetin on normal cell viability an antioxidant could have been present in cell culture medium affecting the results, though the previous studies do not specify that an antioxidant was added (269). Although this study showed *in vitro* that myricetin may affect normal cell viability, *in vivo* studies have demonstrated that myricetin is safe with no toxicity observed (263, 268, 278). However, longer-term studies of the safety of myricetin treatment have not yet been conducted *in vivo*.

The decrease in total viable mammary carcinoma cells with myricetin treatment was attributable to increased cell death due to apoptosis and necrosis induced by myricetin, as measured by Annexin-V-FLUOS/PI staining (Figure 3.6 and 3.7). This was in contrast to findings by Kuntz *et al.* that demonstrated that myricetin inhibited growth and proliferation of MCF-7 breast cancer cells but did not induce cell death; however, the experimental design and assays used by Kuntz *et al.* were different from my study and were not designed to examine cell death in great detail. (298). Firstly, they used caspase-3 activity as the only indicator of apoptosis and cell death (298). In the present study myricetin caused cell death in a manner that could be caspase-independent, so by using caspase-3 activity as the only indicator of cell death Kuntz *et al.* ignored caspase-independent cell death induced by myricetin. Secondly, in the study by Kuntz *et al.* the MCF-7 cell culture medium contained 1 mM sodium pyruvate (298), which, as shown in this study, can decrease the effect of myricetin on breast cancer cell viability by inhibiting ROS-dependent cell death.

Myricetin also caused increased mitochondrial membrane permeability in mammary carcinoma cells (Figure 3.8 and 3.9), indicating that myricetin-induced cell death may be mediated through changes in the mitochondria that activate cell death pathways, such as the intrinsic apoptotic pathway or necroptosis. These results were similar to reported effects of myricetin in other types of cancers that showed changes to the mitochondria that promote the intrinsic apoptotic pathway or cause AIF release from the mitochondria to promote cancer cell death by necroptosis (262, 268–270). In HL-60 leukemia cells myricetin caused activation of caspase-3 and caspase-9, and similarly to this study,

increased mitochondrial permeability to promote apoptosis (269). Myricetin also promoted increased expression of the pro-apoptotic proteins Bax and Bad in HL-60 cells (269). Likewise, myricetin caused increased expression of Bax in HCT-15 colon cancer cells (262). However, myricetin did not cause activation of caspase-3 or caspase-9, but did cause AIF release from the mitochondria to promote cell death independent of caspases in HCT-15 cells (262); caspase-independent cell death also appears to be important for myricetin-induced mammary carcinoma cell death as demonstrated in this study. The differing results of these studies indicate that myricetin can act through different mechanisms to promote cell death depending on the cell type. Though, in the study involving HL-60 cells the authors did not specify that their culture medium contained sodium pyruvate, whereas the study with HCT-15 cells contained 1 mM sodium pyruvate (262, 269). If sodium pyruvate was present in one study and not the other, then this difference may be a contributing factor to the varying effects of myricetin on each cell line.

To further delineate which cell death pathways were important for myricetin-induced mammary carcinoma cell death, the pan-caspase inhibitor Z-VAD-fmk and the RIPK1 inhibitor necrostatin-1 were used in combination with myricetin treatment. Neither Z-VAD-fmk or necrostatin-1 treatment prevented myricetin-induced cell death and did not alter the proportion of cells undergoing early apoptosis versus late apoptosis/necrosis (Figure 3.10). This indicates that myricetin-induced cell death is caspase-independent and RIPK1-independent. However, even though cell death is often considered caspase-dependent if it is inhibited by Z-VAD-fmk, this assumption may not be correct. There are several issues with Z-VAD-fmk treatment. First, all caspases are not inhibited with equal efficiency by Z-VAD-fmk, and Z-VAD-fmk may have off-target effects and inhibit other proteins that are important for apoptosis (35, 304). Additionally, inhibition of caspases may prevent cell death by the apoptotic pathway but cause a shift to other cell death pathways such as necroptosis or necrosis (35, 56, 58, 285, 304, 305). Further study is therefore needed to confirm if myricetin-induced cell death involves caspases. Co-treatment with Z-VAD-fmk and necrostatin-1 may provide

more information about the cell death pathways that are triggered by myricetin because both the necroptotic and apoptotic cell death pathways would be inhibited at the same time, thereby excluding possible compensation by the uninhibited pathway. Also, investigating caspase cleavage and subsequent activation by western blot or by using assays that involve monitoring cleavage of caspase-substrates could be used in combination with caspase inhibitors to reveal more about the role of caspases in myricetin-induced cell death. Myricetin also induced double-stranded DNA breaks to form in mammary carcinoma cells 4 h after treatment, before significant cell death was observed (Figure 3.16). This finding indicates that the myricetin-induced DNA damage happens before, and promotes, mammary carcinoma cell death.

4.2 Myricetin-induced mammary carcinoma cell death is ROS-dependent.

Several phytochemicals promote cancer cell death by inducing formation of ROS that cause cell death (199, 231, 291, 296, 297). Myricetin caused significant accumulation of ROS in mammary carcinoma cells 4 h after myricetin treatment (Figure 3.11). N-acetylcysteine (NAC) is a molecule that is a component of the antioxidant glutathione pathway but also has intrinsic antioxidant activity (306). In this study, NAC was used as an antioxidant to protect cells from myricetin-induced ROS. When mammary carcinoma cells were pretreated with NAC and then also treated with myricetin, myricetin-induced apoptosis and necrosis were completely abolished (Figure 3.12). Also, NAC prevented decreased mammary carcinoma mitochondrial membrane stability induced by myricetin (Figure 3.14). Myricetin-induced DNA damage in mammary carcinoma cells was also prevented by NAC (Figure 3.16). Taken together, this data indicates that myricetin-induced mammary carcinoma cell death is ROS-dependent. Furthermore, the antioxidant enzymes catalase and SOD prevented myricetin-induced death (Figure 3.18 and 3.19), supporting the hypothesis that myricetin induces mammary carcinoma cell death in a ROS-dependent manner. These findings are in direct contrast to a previous study by

Ko *et al.* (269) that examined the effects of myricetin on human leukemia HL-60 cells. In this study myricetin did not induce intracellular accumulation of ROS, as measured by DCFDA assay, and antioxidants such as NAC, SOD, and catalase did not protect HL-60 cells from myricetin-induced cell death (269). Also, in a study by Morales and Haza, ROS was not increased in HepG2 hepatocellular carcinoma cells following myricetin treatment, and the ROS levels actually decreased over time with myricetin treatment (270). Cancer cell lines from different tissues may have different sensitivities to myricetin-induced ROS because of differences in total antioxidant capacity. Further studies are therefore needed to determine if this difference exists between mammary carcinoma and leukemia cell lines. Differences in antioxidant capacity may also explain the differential effect of myricetin on the growth of human mammary epithelial cells and dermal fibroblasts, although there are no studies directly comparing the antioxidant capacity of the two cell types. The discrepancies between this study and the studies by Ko *et al.* and Morales and Haza may also be explained by differences in cell culture conditions since addition of the antioxidant sodium pyruvate (a common supplement in cell culture medium) could have a significant impact on ROS levels and therefore diminish the growth inhibitory effects of myricetin on cancer cells (as observed in Figure 3.15). In this regard, neither Ko *et al.* or Morales and Haza specify whether sodium pyruvate is present in their cell culture medium.

4.3 Myricetin forms ROS in the extracellular environment.

Several phytochemicals, including many phenolics such as EGCG and quercetin, undergo autoxidation in cell culture medium *in vitro*, i.e., they are oxidized by dioxygen (O_2), forming ROS such as H_2O_2 and super oxide (295, 297, 307). Myricetin caused formation of H_2O_2 in cell culture medium both in the absence and presence of mammary carcinoma cells (Figure 3.17), which was in contrast to other studies that have demonstrated that H_2O_2 formed by phytochemical autoxidation is decreased in the presence of cells (296, 297). It is

interesting that when cells were present the level of H₂O₂ was slightly increased at the lower concentrations of myricetin, indicating that the cells may be contributing additional ROS along with the ROS produced by myricetin autoxidation (Figure 3.17). The assay used in this study to measure H₂O₂ was the Amplex® Red assay. Some phytochemicals interfere with this assay by reacting with HRP to make HRP more active (308). The reaction of phytochemicals with HRP in the Amplex® Red Assay can therefore cause the amount of H₂O₂ being produced to be overestimated (308), which could potentially explain the difference between this study and studies with other phytochemicals that show a decrease in H₂O₂ produced by autoxidation in the presence of cells using a method other than the Amplex® Red Assay (296). Nevertheless, myricetin has previously been shown to produce significant H₂O₂ in the absence of cells (309, 310), which is consistent with the findings of my study. ROS formed as a result of autoxidation of phytochemicals can have significant effects on cancer cells *in vitro* (231, 294, 296). For example, H₂O₂ produced by autoxidation of the phenolic phytochemicals oleuropein and hydroxytyrosol causes oxidative DNA damage and a decrease in viability of MDA-MB-231 cells (294). To examine whether the extracellular ROS produced by myricetin was responsible for myricetin-induced cell death, SOD and catalase were incubated with mammary carcinoma cells. Because of their molecular sizes, SOD and catalase will not cross cell membranes, unlike NAC that can cross cell membranes. SOD and catalase completely inhibited myricetin-induced cell death (Figure 3.19) and decreases in mammary carcinoma mitochondrial membrane stability (Figure 3.18). This finding indicates that extracellular ROS formed by myricetin is largely responsible for the growth inhibitory effects of myricetin on breast cancer cell cultures. Given that SOD plus catalase (which can quench extracellular ROS) and NAC (which can quench intracellular and extracellular ROS) inhibit myricetin-induced apoptosis to the same extent, myricetin-induced accumulation of intracellular ROS most likely results from the extracellular ROS formed by myricetin, indicating that myricetin-induced mammary carcinoma cell death is completely dependent on extracellular ROS formation. Similar

observations have been made with other phytochemicals that undergo autoxidation to produce ROS, including hydroxytyrosol and EGCG (231, 296). In the case of EGCG, SOD plus catalase partially inhibited intracellular ROS accumulation and mitochondrial membrane decrease in lung carcinoma cells, whereas NAC fully inhibited it, indicating that EGCG can induce some intracellular ROS separately from ROS formed by its autoxidation (231).

The composition of cell culture medium can have a large impact on the autoxidation reaction. A more basic pH promotes autoxidation, and sodium bicarbonate has been shown to be important for autoxidation in culture medium as it stabilizes the pH of the medium in the presence of CO₂ by producing hydroxide ions; without sodium bicarbonate, H⁺ is produced, causing the pH to lower and preventing autoxidation (294, 297, 307). Supplementation of culture medium with FBS lowers the amount of H₂O₂ produced in culture medium by autoxidation of phytochemicals due to antioxidants present in FBS; although the amount of H₂O₂ is decreased, it remains significant (294). In addition, the presence of sodium pyruvate in culture medium can impact on the ROS produced from autoxidation of phytochemicals (294, 311). Sodium pyruvate is an antioxidant that is commonly added to cell culture media and is a component of DMEM/F12 medium. When the phytochemical oleuropein was added to DMEM/F12 medium very little H₂O₂ was detected compared to the amount of H₂O₂ produced when oleuropein was added to DMEM, i.e., there was five-fold more H₂O₂ produced in DMEM versus DMEM/F12 (294). The fact that sodium pyruvate can inhibit ROS formed by autoxidation of phytochemicals explains the inhibition of myricetin-induced decrease in viable cell number when sodium pyruvate was added to the culture medium (Figure 3.17). Since sodium pyruvate is a common supplement in normal cell culture medium, but not cancer cell culture medium, it is important to conduct all experiments in the same medium (as was done in this study) when comparing the effects of ROS-inducing drugs on normal versus cancer cells.

Autoxidation of several phytochemicals has been observed *in vitro*, but whether or not this phenomenon occurs *in vivo* and its implications remain

unclear. In mouse xenograft models of human lung carcinoma, Li et al. found there was evidence of EGCG-induced oxidative stress and damage in tumors *in vivo*, resulting in reduced tumor growth (231). Whether or not the oxidative damage was the result of extracellular ROS or due to intracellular induction of ROS from EGCG treatment was unclear; however, the authors speculate that it was likely due to intracellular induction of ROS by EGCG (231). More research is needed to determine the *in vivo* implications of phytochemical autoxidation.

4.4 Summary of the effects of myricetin on mammary carcinoma cells.

Myricetin caused decreases in total cell viability for several different mammary carcinoma cell lines, including both triple-negative and estrogen receptor positive human mammary carcinoma cells. Myricetin promotes mammary carcinoma cell death by inducing apoptosis and/or necrosis. The proposed model of myricetin-induced mammary carcinoma cell death *in vitro* is summarized in Figure 4.1. Myricetin is subjected to auto-oxidation in cell culture medium, which causes formation of ROS, including H₂O₂. The ROS formed as a result of autoxidation of myricetin can cross the cell membrane, resulting in increased intracellular ROS levels. Intracellular ROS promote mitochondrial outer membrane permeabilization, which can induce apoptosis or caspase-independent necroptosis. Intracellular ROS also causes DNA damage that can lead to cell death. Furthermore, myricetin causes activation of p38 MAPK, potentially in a ROS-dependent manner depending on the cell line being used, which could contribute to cell death (109). It is likely that the ROS induced by myricetin promotes several cell death pathways simultaneously as both apoptotic and necrotic populations of cells are observed when triple-negative human mammary carcinoma cells are treated with myricetin.

4.5. Limitations of this study

This study, like all studies, has limitations that must be considered when interpreting results and applying them to future studies. This study was conducted using human and mouse mammary carcinoma cell lines instead of using cancer cells isolated from primary tumors. Use of clinical samples from breast tumors of patients, as well as normal tissue samples, could reveal more about the clinical relevance and toxicity of myricetin. Whether myricetin could affect viability and growth of cancer cells from patients will be important for future studies of myricetin as there are no previous studies that have examined the effects of myricetin on primary clinical tumor samples for any type of cancer. Also, this study was conducted using 2D monolayer culture models of mammary carcinoma cells, which are commonly used in studying the effects of phytochemicals on cancer cells. However, more relevant data is obtained from using *in vitro* models that are more representative of *in vivo* tumors (312, 313). For example, there are 3D tissue culture models of tumors, such as tumor spheroids, that better re-create *in vivo* tumor growth *in vitro* compared to 2D models; for example, the gene expression profiles of 2D and 3D tissue culture models are different, with the 3D models being more similar to *in vivo* gene expression (312). Several phytochemicals have been shown to inhibit tumor spheroid growth and viability *in vitro* (279, 314). Thus, testing myricetin in 3D tissue culture models could reveal more about the anticancer properties of myricetin, and how autoxidation of myricetin could affect multicellular tumors.

The tumor microenvironment is predicted to have a large impact on autoxidation of myricetin, but my study does not examine the impact of the tumor microenvironment on myricetin-induced cell death. *In vivo* studies are therefore needed to capture the complexity of the tumor microenvironment. Because this study only assessed the toxicity of myricetin on two normal cell lines, it is difficult to make generalizations about the effects of myricetin on normal cells. The effects of myricetin on a wider variety of normal cells from different tissue types

must therefore be determined. This study does not compare the effects of myricetin with myricetin metabolites, which may have different effects than myricetin on mammary cancer cells; this would be important information when considering the effects of myricetin on breast tumors following oral ingestion of myricetin. In addition, the bioavailability of myricetin *in vivo* must be determined before one can conclude whether the concentrations of myricetin used in this study represent clinically achievable doses. Previous studies of quercetin, a flavonol with a structure very similar to myricetin, suggests that the bioavailability is good and that the half-life is relatively long (approximately 24 h) (140, 157, 168). Nevertheless, it is unlikely that the levels of myricetin used in this study can be achieved through dietary sources. Hence, the route of administration is important to consider when determining strategies to reach maximum levels of myricetin in different tissues.

The only specific ROS produced by myricetin that this study measured was H₂O₂; however, myricetin may interfere with the Amplex® Red assay that was used to measure H₂O₂ (308). Measurement of a variety of types of ROS using assays other than the Amplex® Red assay, such as the ferrous ion oxidation-xylenol orange assay, are needed to fully understand the autoxidation of myricetin. Although SOD and catalase were used in combination to inhibit ROS in this study, examining their effects separately could reveal more about the type of ROS produced by myricetin autoxidation, and the type of ROS important for myricetin-induced cell death.

4.6 Future Directions

This study revealed that ROS, such as H₂O₂, formed by myricetin autoxidation in cell culture medium inhibits the growth and viability of mammary carcinoma cells by promoting cell death. The full mechanism of myricetin autoxidation, the types and amounts of ROS produced, and the conditions affecting myricetin autoxidation were beyond the scope of this study. Further

investigations of the autoxidation mechanisms for myricetin are needed to better understand the implications of myricetin autoxidation in cell culture. In addition, most previous studies of the anti-cancer properties of myricetin have not determined whether myricetin-induced ROS is involved. It is therefore necessary to show that myricetin-induced ROS is an underlying cause of the effects seen in previous studies of myricetin and other types of cancer. Also, comparing the effects of myricetin and H₂O₂ on both cancer and normal cell viability will indicate whether myricetin and H₂O₂ have similar effects on cells to further reveal the mechanisms involved in myricetin-induced cell death.

The effects of the glycoside form of myricetin, myricitrin, on breast cancer cells have not been studied, and it is not known if myricitrin is subject to autoxidation. Since myricetin is commonly found in its glycoside form in plant-based foods it will be important to compare the effects of myricetin and myricitrin on breast cancer cells in order to determine if one has better anti-cancer activity, or if they could work synergistically when used simultaneously. A previous study has shown that myricitrin induces less apoptosis in a prostate cancer cell line than myricetin; however, myricetin and myricitrin together have a synergistic inhibitory effect on prostate cancer cell growth (315).

The preliminary *in vitro* effects of myricetin on breast cancer were investigated in this study; however, future studies should focus on *in vivo* studies, using both human xenograft and mouse mammary carcinoma cell models. Determining if myricetin can affect breast tumor growth and metastasis in animal models is important for determining whether myricetin will be effective in humans, as it is not known if autoxidation occurs *in vivo* and what its impact might be. If myricetin does impact tumor growth *in vivo*, then determining whether or not this effect is ROS-independent or ROS-dependent will be important for further developing myricetin as a therapeutic agent. Understanding the mode of action of myricetin *in vivo* is important for determining the best route of administration and potential interactions with other cancer therapeutics. Also, if myricetin is known to act in a ROS-dependent manner *in vivo* then monitoring for ROS-specific toxicities and side effects can occur. Understanding the long-term effects of

myricetin treatment *in vivo* will be necessary for revealing more about the therapeutic potential of myricetin.

This study did not address the potential of myricetin to inhibit invasion and metastasis of breast cancer cells, although previous studies with other types cancer have shown that myricetin can inhibit cancer cell migration and invasion (250, 263, 264, 267). Since most cancer-related deaths for patients with solid tumors are due to metastasis, it will be important to investigate the effects of myricetin on metastasis of breast cancer cells and determine if the effects are ROS-dependent or independent. Also, the effects myricetin on immune-mediated cancer cell death need to be addressed. Some phytochemicals, including EGCG, can enhance antitumor immunity (316). In addition, H₂O₂ can enhance T cell proliferation, suggesting that myricetin could enhance immune cell activity against cancer cells (317). Finally, studies are needed to assess if myricetin may be able to act as an adjuvant to conventional breast cancer therapies, enhancing the effects of radiation therapy or chemotherapeutic drugs.

4.7 Concluding remarks

Triple-negative breast cancer is a subset of breast cancer that generally has a worse prognosis and limited treatment options; therefore, new therapies are needed. This study demonstrated that myricetin decreased the viability of human triple-negative breast cancer cells. Myricetin caused ROS production that promoted breast cancer cell death. While ROS production is often associated with cancer promotion, ROS also have anti-cancer properties and several current cancer therapies act on cancer cells, at least in part, by inducing ROS (84, 85, 117). Moreover, some studies have demonstrated that some antioxidant therapies targeting ROS can actually enhance tumor growth and progression by inhibiting the expression of the tumor suppressor p53 (318). The role of ROS in the anti-breast cancer properties of myricetin *in vitro* are apparent in this study but it is not known whether ROS is important for the *in vivo* activities of myricetin. The use of myricetin in a rat model of breast cancer and in other mouse cancer

models suggests that myricetin prevents and inhibits tumor growth and is safe to use *in vivo* as there were no signs of toxicity, even up to 200 mg/kg given orally every day for 16 weeks in the rat model of breast cancer (263, 268, 278). If myricetin is metabolized *in vivo* similarly to the structurally related phytochemical quercetin then it may have a relatively long half-life and good bioavailability indicating that it would be a good candidate for therapeutic development. Given that myricetin caused significant triple-negative breast cancer cell death *in vitro*, and was as or more effective at inhibiting breast cancer cell growth than several other well-studied phytochemicals, the further investigation of myricetin as a potential breast cancer therapeutic is warranted.

Figure 4.1. Proposed model of myricetin-induced mammary carcinoma cell death. Myricetin undergoes autoxidation in the extracellular environment to produce H_2O_2 . The H_2O_2 can cross the cell membrane to enter the cell, where it causes an increase in intracellular ROS that activates signaling pathways such as p38 MAPK. Mitochondrial permeabilization, and DNA damage are triggered by ROS and culminate in causing mammary carcinoma cell death. Additionally, and the p38 MAPK signaling pathway is activated by ROS and may contribute to cell death. Addition of the antioxidant NAC or the antioxidant enzymes SOD and catalase can quench H_2O_2 thereby preventing cell death.

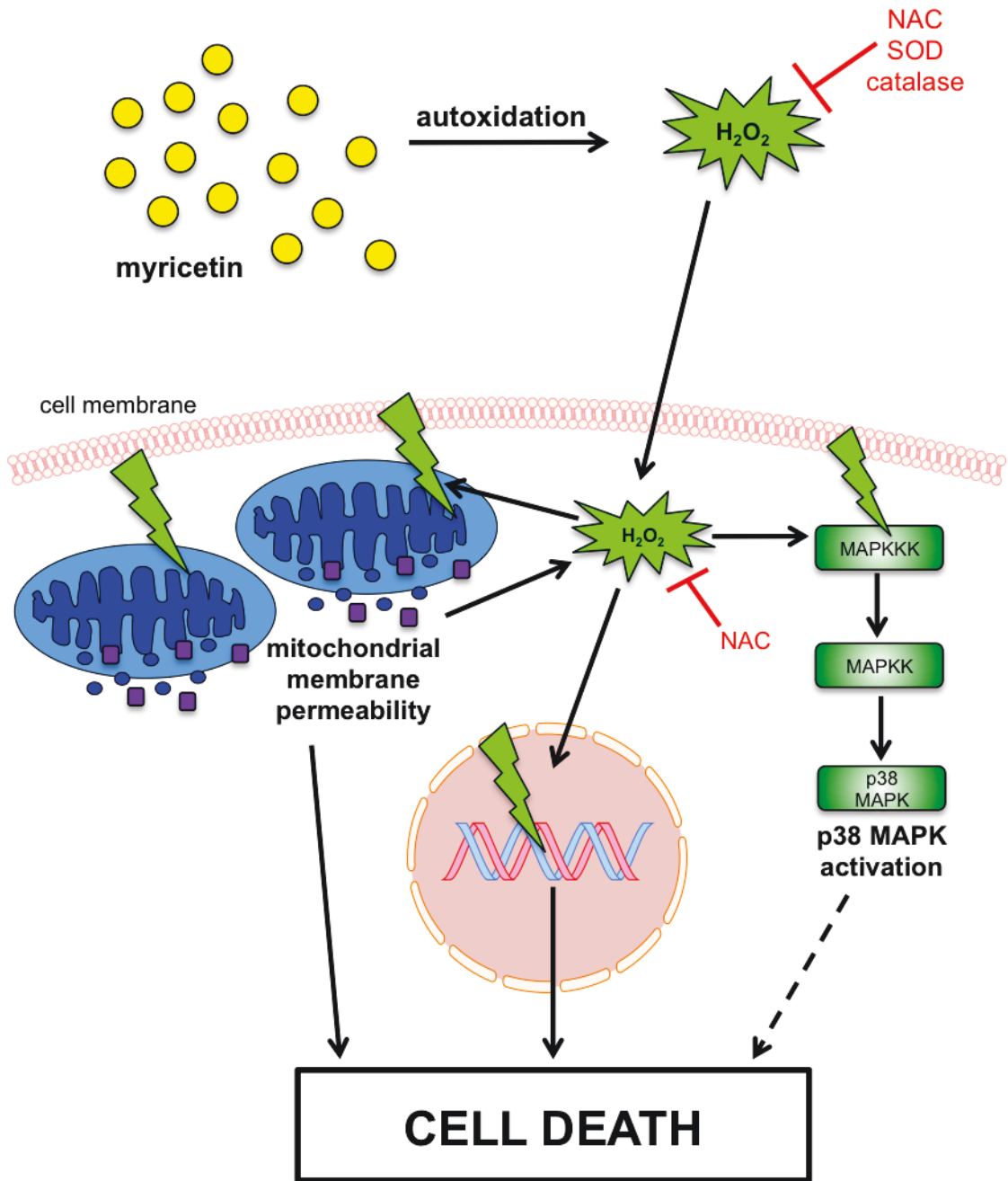
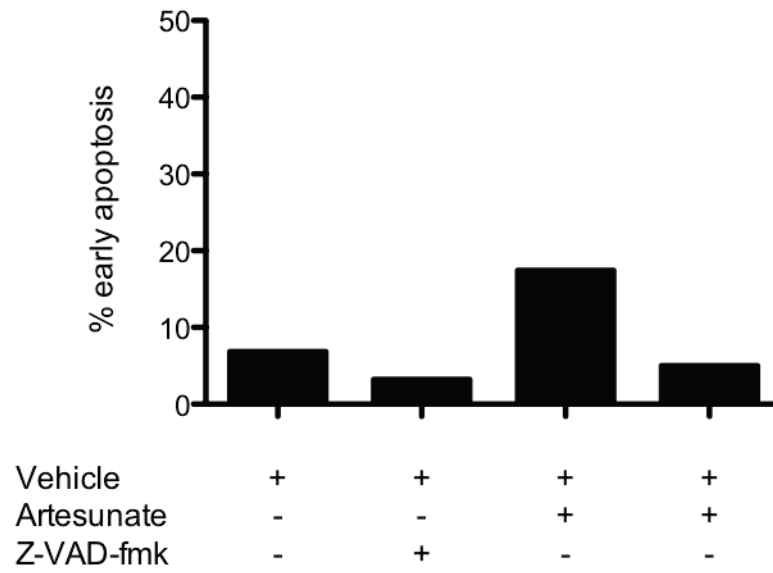


Figure 4.1

APPENDIX

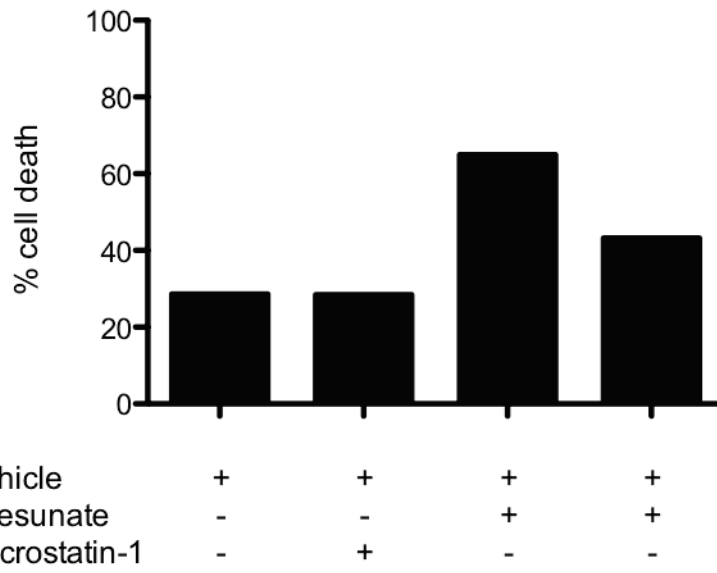
Appendix Figure 1. Z-VAD-fmk inhibits early apoptosis induced by artesunate. MDA-MB-468 cells were incubated with 50 μ M Z-VAD-fmk for 1 h and then treated with 50 μ M artesunate, or DMSO (vehicle) for 24 h. At 24 h the cells were stained with Annexin V-FLUOS and early apoptosis was measured by flow cytometry.



Appendix Figure 1

Appendix Figure 2. Necrostatin-1 inhibits cell death induced by artesunate.

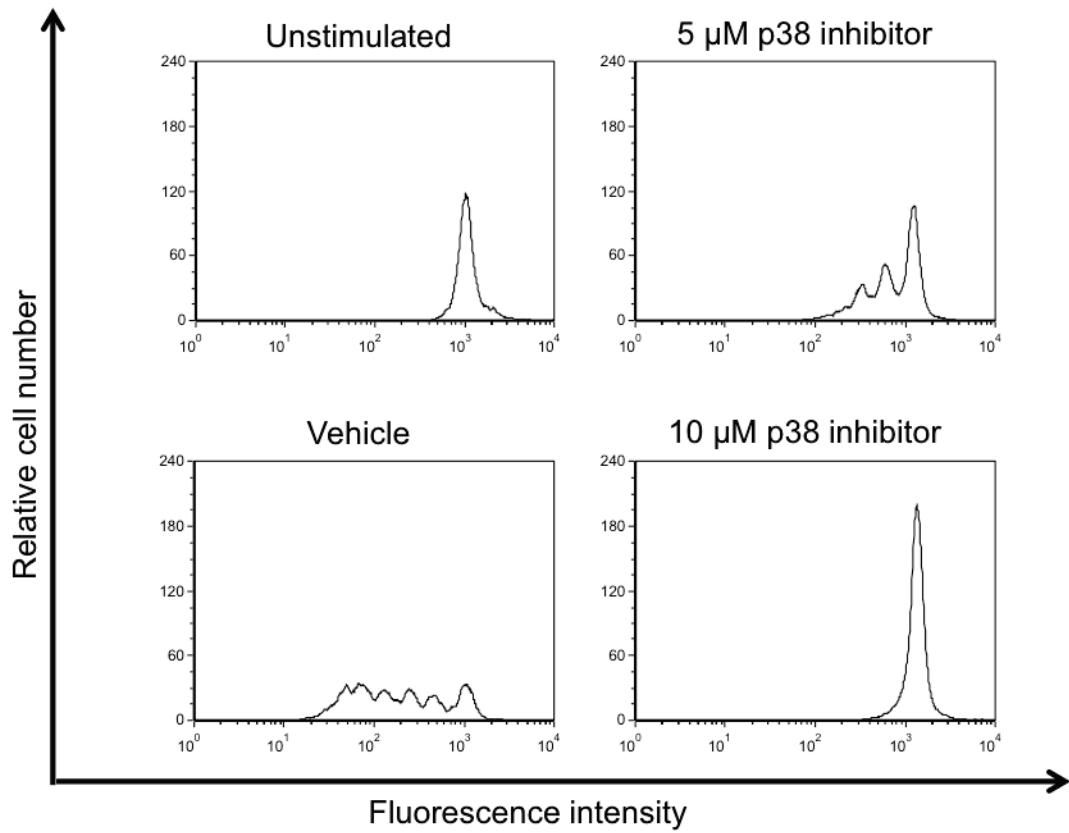
HEY-1 ovarian carcinoma cells were incubated with 40 μ M necrostatin-1 for 1 h and then treated with 50 μ M artesunate, or DMSO (vehicle) for 24 hr. At 48 h the cells were stained with Annexin V-FLUOS and PI, and total cell death was measured by flow cytometry.



Appendix Figure 2

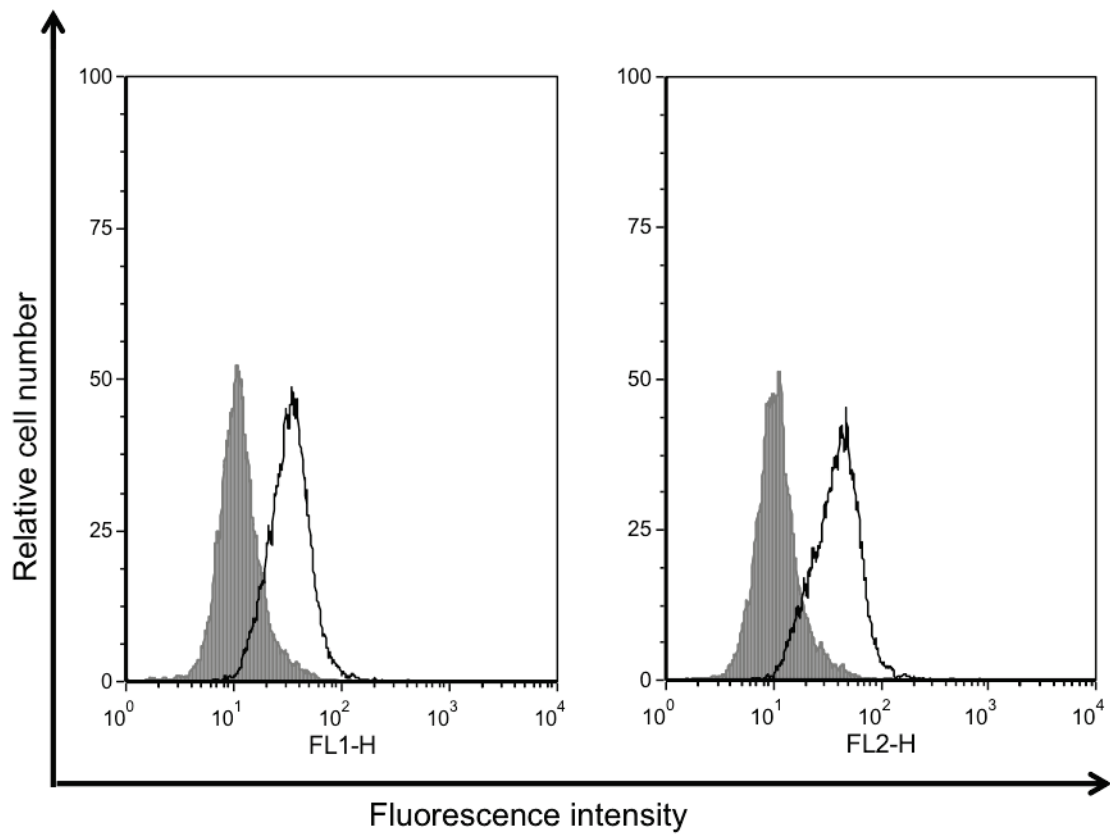
Appendix Figure 3. T-cell proliferation is inhibited by p38 MAPK inhibitor III.


A female C57/BL6 mouse (purchased from Charles River Canada, Lasalle, QC) was used as a source of primary T cells. The mouse was housed in the Carleton Animal Care Facility at Dalhousie University. The animal protocol was approved by the Dalhousie University Committee on Laboratory Animals. The mouse was euthanized by cervical dislocation and the spleen excised and homogenized. Magnetic bead isolation columns (Miltenyi Biotech, Auburn, CA) were used to isolate CD3⁺ T cells by negative selection and red blood cells lysed by osmotic shock. Cell number was determined by a trypan blue exclusion assay. The T cells were labeled with 2 μ M Oregon Green 488 dye (Invitrogen) for 15 min, then 2.5×10^5 cells/well were cultured (at 37°C and 5% CO₂) in 96-well plates in RPMI-1640 culture medium (supplemented with 5% FBS, 5 mM HEPES, 100 U/ml penicillin, 100 μ g/ml streptomycin, and 2 mM L-glutamine) without (unstimulated) or with 1.25×10^5 anti-CD3/anti-CD28 antibody-coated T cell expander beads (Invitrogen) per well, and treated with p38 inhibitor III or vehicle (DMSO) for 72 h. At 72 h the cell fluorescence was analyzed by flow cytometry, which was gated on live cells. Decreased fluorescence indicates more proliferation, with each fluorescent peak corresponding to a round of cell division.




Appendix Figure 3

Appendix Figure 4. Myricetin has a slight inherent fluorescence. MDA-MB-468 cells were treated with or without myricetin for 24 h, then the cells were harvested and fluorescence of the cells was determined by flow cytometry for both the FL-1 and FL-2 flow cytometry channels. Since myricetin only caused a slight shift in fluorescence compared to the large shifts seen in the experiments involving flow cytometry in this study, this shift was considered negligible.



 = medium only

 = 50 μ M Myricetin

Appendix Figure 4

REFERENCES

1. Nowell, P. C. 1976. The clonal evolution of tumor cell populations. *Science* 194: 23–28.
2. Foulds, L. 1954. The Experimental Study of Tumor Progression : A Review
The Experimental Study of Tumor Progression : A Review. *Cancer Res.* 14: 327–339.
3. Hanahan, D., and R. A. Weinberg. 2011. Hallmarks of cancer: the next generation. *Cell* 144: 646–74.
4. Hanahan, D., and R. A. Weinberg. 2000. The Hallmarks of Cancer. *Cell* 100: 57–70.
5. International Agency for Research on Cancer. 2014. GLOBOCAN 2012: Estimated Cancer Incidence, Mortality and Prevalence Worldwide in 2012. .
6. Canadian Cancer Society's Advisory Committee on Cancer Statistics. 2014. *Canadian Cancer Statistics 2014*,. Toronto, ON.
7. Public Health Agency of Canada. 2014. *Economic burden of illness in Canada, 2005-2008*. Ottawa, ON, Canada.
8. Weigelt, B., and J. S. Reis-Filho. 2009. Histological and molecular types of breast cancer: is there a unifying taxonomy? *Nat. Rev. Clin. Oncol.* 6: 718–30.
9. Vollenweider-Zerargui, L., L. Barrelet, Y. Wong, T. Lemarchand-Béraud, and F. Gómez. 1986. The predictive value of estrogen and progesterone receptors' concentrations on the clinical behavior of breast cancer in women °clinical correlation on 547 patients. *Cancer* 57: 1171–1180.

10. Perou, C. M., T. Sørlie, M. B. Eisen, M. van de Rijn, S. S. Jeffrey, C. A. Rees, J. R. Pollack, D. T. Ross, H. Johnsen, L. A. Akslen, O. Fluge, A. Pergamenschikov, C. Williams, S. X. Zhu, P. E. Lønning, A. L. Børresen-Dale, P. O. Brown, and D. Botstein. 2000. Molecular portraits of human breast tumours. *Nature* 406: 747–52.
11. Slamon, D., G. Clark, S. Wong, W. Levin, A. Ullrich, and W. McGuire. 1987. Human breast cancer: correlation of relapse and survival with amplification of the HER-2/neu oncogene. *Science* (80-.). 235: 177–182.
12. Slamon, D. J., B. Leyland-Jones, S. Shak, H. Fuchs, V. Paton, A. Bajamonde, T. Fleming, W. Eiermann, J. Wolter, M. Pegram, J. Baselga, and L. Norton. 2001. *Use of chemotherapy plus a monoclonal antibody against HER2 for metastatic breast cancer that overexpresses HER2*. ; :783–792.
13. Sørlie, T., C. M. Perou, R. Tibshirani, T. Aas, S. Geisler, H. Johnsen, T. Hastie, M. B. Eisen, M. van de Rijn, S. S. Jeffrey, T. Thorsen, H. Quist, J. C. Matese, P. O. Brown, D. Botstein, P. E. Lønning, and A. L. Børresen-Dale. 2001. Gene expression patterns of breast carcinomas distinguish tumor subclasses with clinical implications. *Proc. Natl. Acad. Sci. U. S. A.* 98: 10869–74.
14. Sorlie, T., R. Tibshirani, J. Parker, T. Hastie, J. S. Marron, A. Nobel, S. Deng, H. Johnsen, R. Pesich, S. Geisler, J. Demeter, C. M. Perou, P. E. Lønning, P. O. Brown, A.-L. Børresen-Dale, and D. Botstein. 2003. Repeated observation of breast tumor subtypes in independent gene expression data sets. *Proc. Natl. Acad. Sci. U. S. A.* 100: 8418–23.
15. Kittaneh, M., and A. J. Montero. 2013. Biomarkers in Cancer Molecular Profiling for Breast Cancer : A Comprehensive Review. *Biomark. Cancer* 5: 61–70.
16. Schmidt, M. 2014. Chemotherapy in early breast cancer: when, how and which one? *Breast Care (Basel)*. 9: 154–60.

17. Maughan, K. L., M. A. Lutterbie, and P. S. Ham. 2010. Treatment of breast cancer. *Am. Fam. Physician* 81: 1339–1346.
18. Tessari, A., D. Palmieri, and S. Di Cosimo. 2013. Overview of diagnostic/targeted treatment combinations in personalized medicine for breast cancer patients. *Pharmgenomics. Pers. Med.* 7: 1–19.
19. Slamon, D. J., B. Leyland-Jones, S. Shak, H. Fuchs, V. Paton, A. Bajamonde, T. Fleming, W. Eiermann, J. Wolter, M. Pegram, J. Baselga, and L. Norton. 2001. Use of chemotherapy plus a monoclonal antibody against HER2 for metastatic breast cancer that overexpresses HER2. *N. Engl. J. Med.* 344: 783–92.
20. Lara-Medina, F., V. Pérez-Sánchez, D. Saavedra-Pérez, M. Blake-Cerda, C. Arce, D. Motola-Kuba, C. Villarreal-Garza, A. M. González-Angulo, E. Bargalló, J. L. Aguilar, A. Mohar, and Ó. Arrieta. 2011. Triple-negative breast cancer in Hispanic patients: high prevalence, poor prognosis, and association with menopausal status, body mass index, and parity. *Cancer* 117: 3658–69.
21. Carey, L. A., C. M. Perou, C. A. Livasy, L. G. Dressler, D. Cowan, K. Conway, G. Karaca, M. A. Troester, C. K. Tse, S. Edmiston, S. L. Deming, J. Geradts, M. C. U. Cheang, T. O. Nielsen, P. G. Moorman, H. S. Earp, and R. C. Millikan. 2006. Race, breast cancer subtypes, and survival in the Carolina Breast Cancer Study. *JAMA* 295: 2492–502.
22. Bertucci, F., P. Finetti, N. Cervera, B. Esterni, F. Hermitte, P. Viens, and D. Birnbaum. 2008. How basal are triple-negative breast cancers? *Int. J. Cancer* 123: 236–40.
23. Kaplan, H. G., and J. A. Malmgren. Impact of triple negative phenotype on breast cancer prognosis. *Breast J.* 14: 456–63.

24. Dent, R., M. Trudeau, K. I. Pritchard, W. M. Hanna, H. K. Kahn, C. A. Sawka, L. A. Lickley, E. Rawlinson, P. Sun, and S. A. Narod. 2007. Triple-negative breast cancer: clinical features and patterns of recurrence. *Clin. Cancer Res.* 13: 4429–34.
25. Rhee, J., S.-W. Han, D.-Y. Oh, J. H. Kim, S.-A. Im, W. Han, I. A. Park, D.-Y. Noh, Y.-J. Bang, and T.-Y. Kim. 2008. The clinicopathologic characteristics and prognostic significance of triple-negativity in node-negative breast cancer. *BMC Cancer* 8: 307.
26. Parikh, R. R., D. Housman, Q. Yang, D. Toppmeyer, L. D. Wilson, and B. G. Haffty. 2008. Prognostic value of triple-negative phenotype at the time of locally recurrent, conservatively treated breast cancer. *Int. J. Radiat. Oncol. Biol. Phys.* 72: 1056–63.
27. Carey, L. A., E. C. Dees, L. Sawyer, L. Gatti, D. T. Moore, F. Collichio, D. W. Ollila, C. I. Sartor, M. L. Graham, and C. M. Perou. 2007. The triple negative paradox: primary tumor chemosensitivity of breast cancer subtypes. *Clin. Cancer Res.* 13: 2329–34.
28. De Ruijter, T. C., J. Veeck, J. P. J. de Hoon, M. van Engeland, and V. C. Tjan-Heijnen. 2011. Characteristics of triple-negative breast cancer. *J. Cancer Res. Clin. Oncol.* 137: 183–92.
29. Norum, J. H., K. Andersen, and T. Sørli. 2014. Lessons learned from the intrinsic subtypes of breast cancer in the quest for precision therapy. *Br. J. Surg.* 101: 925–38.
30. Neve, R. M., K. Chin, J. Fridlyand, J. Yeh, F. L. Baehner, T. Fevr, L. Clark, N. Bayani, J.-P. Coppe, F. Tong, T. Speed, P. T. Spellman, S. DeVries, A. Lapuk, N. J. Wang, W.-L. Kuo, J. L. Stilwell, D. Pinkel, D. G. Albertson, F. M. Waldman, F. McCormick, R. B. Dickson, M. D. Johnson, M. Lippman, S. Ethier, A. Gazdar,

and J. W. Gray. 2006. A collection of breast cancer cell lines for the study of functionally distinct cancer subtypes. *Cancer Cell* 10: 515–27.

31. Soule, H. D., J. Vazquez, A. Long, S. Albert, and M. Brennan. 1973. A Human Cell Line From a Pleural Effusion Derived From a Breast Carcinoma. *J Natl Cancer Inst* 51: 1409–1416.

32. Cailleau, R., R. Young, M. Olivé, and W. J. Reeves. 1974. Breast tumor cell lines from pleural effusions. *J. Natl. Cancer Inst.* 53: 661–674.

33. Zhang, R. D., I. J. Fidler, and J. E. Price. 1991. Relative malignant potential of human breast carcinoma cell lines established from pleural effusions and a brain metastasis. *Invasion Metastasis* 11: 204–215.

34. Burdall, S. E., A. M. Hanby, M. R. J. Lansdown, and V. Speirs. 2003. Breast cancer cell lines: friend or foe? *Breast Cancer Res.* 5: 89–95.

35. Kroemer, G., L. Galluzzi, P. Vandenabeele, J. Abrams, E. S. Alnemri, E. H. Baehrecke, M. V Blagosklonny, W. S. El-Deiry, P. Golstein, D. R. Green, M. Hengartner, R. A. Knight, S. Kumar, S. A. Lipton, W. Malorni, G. Nuñez, M. E. Peter, J. Tschopp, J. Yuan, M. Piacentini, B. Zhivotovsky, and G. Melino. 2009. Classification of cell death: recommendations of the Nomenclature Committee on Cell Death 2009. *Cell Death Differ.* 16: 3–11.

36. Galluzzi, L., I. Vitale, J. M. Abrams, E. S. Alnemri, E. H. Baehrecke, M. V Blagosklonny, T. M. Dawson, V. L. Dawson, W. S. El-Deiry, S. Fulda, E. Gottlieb, D. R. Green, M. O. Hengartner, O. Kepp, R. A. Knight, S. Kumar, S. A. Lipton, X. Lu, F. Madeo, W. Malorni, P. Mehlen, G. Nuñez, M. E. Peter, M. Piacentini, D. C. Rubinsztein, Y. Shi, H.-U. Simon, P. Vandenabeele, E. White, J. Yuan, B. Zhivotovsky, G. Melino, and G. Kroemer. 2012. Molecular definitions of cell death subroutines: recommendations of the Nomenclature Committee on Cell Death 2012. *Cell Death Differ.* 19: 107–20.

37. Galluzzi, L., J. M. Bravo-San Pedro, I. Vitale, S. A. Aaronson, J. M. Abrams, D. Adam, E. S. Alnemri, L. Altucci, D. Andrews, M. Annicchiarico-Petruzzelli, E. H. Baehrecke, N. G. Bazan, M. J. Bertrand, K. Bianchi, M. V Blagosklonny, K. Blomgren, C. Borner, D. E. Bredesen, C. Brenner, M. Campanella, E. Candi, F. Cecconi, F. K. Chan, N. S. Chandel, E. H. Cheng, J. E. Chipuk, J. A. Cidlowski, A. Ciechanover, T. M. Dawson, V. L. Dawson, V. De Laurenzi, R. De Maria, K.-M. Debatin, N. Di Daniele, V. M. Dixit, B. D. Dynlacht, W. S. El-Deiry, G. M. Fimia, R. A. Flavell, S. Fulda, C. Garrido, M.-L. Gougeon, D. R. Green, H. Gronemeyer, G. Hajnoczky, J. M. Hardwick, M. O. Hengartner, H. Ichijo, B. Joseph, P. J. Jost, T. Kaufmann, O. Kepp, D. J. Klionsky, R. A. Knight, S. Kumar, J. J. Lemasters, B. Levine, A. Linkermann, S. A. Lipton, R. A. Lockshin, C. López-Otín, E. Lugli, F. Madeo, W. Malorni, J.-C. Marine, S. J. Martin, J.-C. Martinou, J. P. Medema, P. Meier, S. Melino, N. Mizushima, U. Moll, C. Muñoz-Pinedo, G. Nuñez, A. Oberst, T. Panaretakis, J. M. Penninger, M. E. Peter, M. Piacentini, P. Pinton, J. H. Prehn, H. Puthalakath, G. A. Rabinovich, K. S. Ravichandran, R. Rizzuto, C. M. Rodrigues, D. C. Rubinsztein, T. Rudel, Y. Shi, H.-U. Simon, B. R. Stockwell, G. Szabadkai, S. W. Tait, H. L. Tang, N. Tavernarakis, Y. Tsujimoto, T. Vanden Berghe, P. Vandenabeele, A. Villunger, E. F. Wagner, H. Walczak, E. White, W. G. Wood, J. Yuan, Z. Zakeri, B. Zhivotovsky, G. Melino, and G. Kroemer. 2014. Essential versus accessory aspects of cell death: recommendations of the NCCD 2015. *Cell Death Differ.* .
38. Kerr, J. F. R., A. H. Wyllie, and A. R. Currie. 1972. Apoptosis: A Basic Biological Phenomenon with Wideranging Implications in Tissue Kinetics. *Br. J. Cancer* 26: 239–257.
39. Long, J. S., and K. M. Ryan. 2012. New frontiers in promoting tumour cell death: targeting apoptosis, necroptosis and autophagy. *Oncogene* .
40. Ellis, H. M., and H. R. Horvitz. 1986. Genetic control of programmed cell death in the nematode *C. elegans*. *Cell* 44: 817–29.

41. Enari, M., H. Hug, and S. Nagata. 1995. Involvement of an ICE-like protease in Fas-mediated apoptosis. *Nature* 375: 78–81.
42. Kumar, S., and N. L. Harvey. 1995. Role of multiple cellular proteases in the execution of programmed cell death. *FEBS Lett.* 375: 169–173.
43. Li, J., and J. Yuan. 2008. Caspases in apoptosis and beyond. *Oncogene* 27: 6194–206.
44. Srinivasula, S. M., M. Ahmad, T. Fernandes-Alnemri, G. Litwack, and E. S. Alnemri. 1996. Molecular ordering of the Fas-apoptotic pathway: the Fas/APO-1 protease Mch5 is a CrmA-inhibitable protease that activates multiple Ced-3/ICE-like cysteine proteases. *Proc. Natl. Acad. Sci. U. S. A.* 93: 14486–91.
45. Matthews, G. M., A. Newbold, and R. W. Johnstone. 2012. Intrinsic and extrinsic apoptotic pathway signaling as determinants of histone deacetylase inhibitor antitumor activity. *Adv. Cancer Res.* 116: 165–97.
46. Ashkenazi, A., and V. M. Dixit. 1998. Death receptors: signaling and modulation. *Science* 281: 1305–8.
47. Lavrik, I., A. Golks, and P. H. Krammer. 2005. Death receptor signaling. *J. Cell Sci.* 118: 265–7.
48. Walczak, H., and P. H. Krammer. 2000. The CD95 (APO-1/Fas) and the TRAIL (APO-2L) apoptosis systems. *Exp. Cell Res.* 256: 58–66.
49. Billen, L. P., A. Shamas-Din, and D. W. Andrews. 2008. Bid: a Bax-like BH3 protein. *Oncogene* 27 Suppl 1: S93–104.
50. Kantari, C., and H. Walczak. 2011. Caspase-8 and bid: caught in the act between death receptors and mitochondria. *Biochim. Biophys. Acta* 1813: 558–63.

51. Mayer, B., and R. Oberbauer. 2003. Mitochondrial Regulation of Apoptosis. *News Physiol Sci* 18: 89–94.
52. Elmore, S. 2007. Apoptosis: a review of programmed cell death. *Toxicol. Pathol.* 35: 495–516.
53. Cory, S., and J. M. Adams. 2002. The Bcl2 family: regulators of the cellular life-or-death switch. *Nat. Rev. Cancer* 2: 647–56.
54. Yoshida, H., Y. Y. Kong, R. Yoshida, A. J. Elia, A. Hakem, R. Hakem, J. M. Penninger, and T. W. Mak. 1998. Apaf1 is required for mitochondrial pathways of apoptosis and brain development. *Cell* 94: 739–50.
55. Ferraro, E., M. Corvaro, and F. Cecconi. Physiological and pathological roles of Apaf1 and the apoptosome. *J. Cell. Mol. Med.* 7: 21–34.
56. Vandenabeele, P., L. Galluzzi, T. Vanden Berghe, and G. Kroemer. 2010. Molecular mechanisms of necroptosis: an ordered cellular explosion. *Nat. Rev. Mol. Cell Biol.* 11: 700–14.
57. Vercammen, D., G. Brouckaert, G. Denecker, M. Van de Craen, W. Declercq, W. Fiers, and P. Vandenabeele. 1998. Dual signaling of the Fas receptor: initiation of both apoptotic and necrotic cell death pathways. *J. Exp. Med.* 188: 919–30.
58. Vercammen, D., R. Beyaert, G. Denecker, V. Goossens, G. Van Loo, W. Declercq, J. Grooten, W. Fiers, and P. Vandenabeele. 1998. Inhibition of caspases increases the sensitivity of L929 cells to necrosis mediated by tumor necrosis factor. *J. Exp. Med.* 187: 1477–85.
59. Laster, S. M., J. G. Wood, and L. R. Gooding. 1988. Tumor necrosis factor can induce both apoptic and necrotic forms of cell lysis. *J. Immunol.* 141: 2629–34.

60. Degterev, A., Z. Huang, M. Boyce, Y. Li, P. Jagtap, N. Mizushima, G. D. Cuny, T. J. Mitchison, M. A. Moskowitz, and J. Yuan. 2005. Chemical inhibitor of nonapoptotic cell death with therapeutic potential for ischemic brain injury. *Nat. Chem. Biol.* 1: 112–9.
61. Wu, W., P. Liu, and J. Li. 2012. Necroptosis: an emerging form of programmed cell death. *Crit. Rev. Oncol. Hematol.* 82: 249–58.
62. Declercq, W., T. Vanden Berghe, and P. Vandenabeele. 2009. RIP kinases at the crossroads of cell death and survival. *Cell* 138: 229–32.
63. Wright, A., W. W. Reiley, M. Chang, W. Jin, A. J. Lee, M. Zhang, and S. C. Sun. 2007. Regulation of Early Wave of Germ Cell Apoptosis and Spermatogenesis by Deubiquitinating Enzyme CYLD. *Dev. Cell* 13: 705–716.
64. Lin, Y., A. Devin, Y. Rodriguez, and Z. G. Liu. 1999. Cleavage of the death domain kinase RIP by Caspase-8 prompts TNF-induced apoptosis. *Genes Dev.* 13: 2514–2526.
65. Holler, N., R. Zaru, O. Micheau, M. Thome, A. Attinger, S. Valitutti, J. L. Bodmer, P. Schneider, B. Seed, and J. Tschopp. 2000. Fas triggers an alternative, caspase-8-independent cell death pathway using the kinase RIP as effector molecule. *Nat. Immunol.* 1: 489–495.
66. Marshall, K. D., and C. P. Baines. 2014. Necroptosis: is there a role for mitochondria? *Front. Physiol.* 5: 323.
67. Lin, Y., S. Choksi, H. M. Shen, Q. F. Yang, G. M. Hur, Y. S. Kim, J. H. Tran, S. A. Nedospasov, and Z. G. Liu. 2004. Tumor Necrosis Factor-induced Nonapoptotic Cell Death Requires Receptor-interacting Protein-mediated Cellular Reactive Oxygen Species Accumulation. *J. Biol. Chem.* 279: 10822–10828.

68. Delavallée, L., L. Cabon, P. Galán-Malo, H. K. Lorenzo, and S. A. Susin. 2011. AIF-mediated caspase-independent necroptosis: A new chance for targeted therapeutics. *IUBMB Life* 63: 221–232.
69. Artus, C., H. Boujrad, A. Bouharrou, M.-N. Brunelle, S. Hoos, V. J. Yuste, P. Lenormand, J.-C. Rousselle, A. Namane, P. England, H. K. Lorenzo, and S. A. Susin. 2010. AIF promotes chromatinolysis and caspase-independent programmed necrosis by interacting with histone H2AX. *EMBO J.* 29: 1585–1599.
70. Vanden Berghe, T., A. Linkermann, S. Jouan-Lanhouet, H. Walczak, and P. Vandenabeele. 2014. Regulated necrosis: the expanding network of non-apoptotic cell death pathways. *Nat. Rev. Mol. Cell Biol.* 15: 135–47.
71. Broker, L. E., F. A. E. Kruyt, and G. Giaccone. 2005. Cell death independent of caspases: A review. *Clin. Cancer Res.* 11: 3155–3162.
72. Tait, S. W. G., and D. R. Green. 2010. Mitochondria and cell death: outer membrane permeabilization and beyond. *Nat. Rev. Mol. Cell Biol.* 11: 621–32.
73. Verhagen, A. M., J. Silke, P. G. Ekert, M. Pakusch, H. Kaufmann, L. M. Connolly, C. L. Day, A. Tikoo, R. Burke, C. Wrobel, R. L. Moritz, R. J. Simpson, and D. L. Vaux. 2002. HtrA2 promotes cell death through its serine protease activity and its ability to antagonize inhibitor of apoptosis proteins. *J. Biol. Chem.* 277: 445–454.
74. Hegde, R., S. M. Srinivasula, Z. Zhang, R. Wassell, R. Mukattash, L. Cilenti, G. DuBois, Y. Lazebnik, A. S. Zervos, T. Fernandes-Alnemri, and E. S. Alnemri. 2002. Identification of Omi/HtrA2 as a mitochondrial apoptotic serine protease that disrupts inhibitor of apoptosis protein-caspase interaction. *J. Biol. Chem.* 277: 432–8.

75. Li, L. Y., X. Luo, and X. Wang. 2001. Endonuclease G is an apoptotic DNase when released from mitochondria. *Nature* 412: 95–9.
76. Baritaud, M., H. Boujrad, H. K. Lorenzo, S. Krantic, and S. A. Susin. 2010. Histone H2AX: The missing link in AIF-mediated caspase-independent programmed necrosis. *Cell Cycle* 9: 3166–73.
77. Polster, B. M., G. Basañez, A. Etxebarria, J. M. Hardwick, and D. G. Nicholls. 2005. Calpain I induces cleavage and release of apoptosis-inducing factor from isolated mitochondria. *J. Biol. Chem.* 280: 6447–54.
78. Bidère, N., H. K. Lorenzo, S. Carmona, M. Laforge, F. Harper, C. Dumont, and A. Senik. 2003. Cathepsin D triggers Bax activation, resulting in selective apoptosis-inducing factor (AIF) relocation in T lymphocytes entering the early commitment phase to apoptosis. *J. Biol. Chem.* 278: 31401–31411.
79. Oberg, K. A. R., and U. N. O. J. Ohansson. 1999. Lysosomal release of Cathepsin D precedes relocation of potential during apoptosis induced by oxidative stress. *Free Radic. Biol. Med.* 27: 1228–1237.
80. Fatokun, A. A., V. L. Dawson, and T. M. Dawson. 2014. Parthanatos: mitochondrial-linked mechanisms and therapeutic opportunities. *Br. J. Pharmacol.* 171: 2000–16.
81. Dickinson, B. C., and C. J. Chang. 2011. Chemistry and biology of reactive oxygen species in signaling or stress responses. *Nat. Chem. Biol.* 7: 504–11.
82. Panieri, E., V. Gogvadze, E. Norberg, R. Venkatesh, S. Orrenius, and B. Zhivotovsky. 2013. Reactive oxygen species generated in different compartments induce cell death, survival, or senescence. *Free Radic. Biol. Med.* 57: 176–87.
83. Son, Y., S. Kim, H.-T. Chung, and H.-O. Pae. 2013. Reactive oxygen species in the activation of MAP kinases. *Methods Enzymol.* 528: 27–48.

84. Nogueira, V., and N. Hay. 2013. Molecular pathways: reactive oxygen species homeostasis in cancer cells and implications for cancer therapy. *Clin. Cancer Res.* 19: 4309–14.
85. Gupta, S. C., D. Hevia, S. Patchva, B. Park, W. Koh, and B. B. Aggarwal. 2012. Upsides and downsides of reactive oxygen species for cancer: the roles of reactive oxygen species in tumorigenesis, prevention, and therapy. *Antioxid. Redox Signal.* 16: 1295–322.
86. Inoue, M., E. F. Sato, M. Nishikawa, A.-M. Park, Y. Kira, I. Imada, and K. Utsumi. 2003. Mitochondrial generation of reactive oxygen species and its role in aerobic life. *Curr. Med. Chem.* 10: 2495–505.
87. Murphy, M. P. 2009. How mitochondria produce reactive oxygen species. *Biochem. J.* 417: 1–13.
88. Reczek, C. R., and N. S. Chandel. 2014. ROS-dependent signal transduction. *Curr. Opin. Cell Biol.* 33C: 8–13.
89. Rhee, S. G. 2006. Cell signaling. H₂O₂, a necessary evil for cell signaling. *Science* 312: 1882–3.
90. Rhee, S. G., S. W. Kang, W. Jeong, T.-S. Chang, K.-S. Yang, and H. A. Woo. 2005. Intracellular messenger function of hydrogen peroxide and its regulation by peroxiredoxins. *Curr. Opin. Cell Biol.* 17: 183–9.
91. Rhee, S. G., Y. S. Bae, S. R. Lee, and J. Kwon. 2000. Hydrogen peroxide: a key messenger that modulates protein phosphorylation through cysteine oxidation. *Sci. STKE* 2000: pe1.
92. Finkel, T. 2001. Reactive oxygen species and signal transduction. *IUBMB Life* 52: 3–6.

93. Thannickal, V. J., and B. L. Fanburg. 2000. Reactive oxygen species in cell signaling. *Am. J. Physiol. Lung Cell. Mol. Physiol.* 279: L1005–28.
94. Lee, S. R., K. S. Kwon, S. R. Kim, and S. G. Rhee. 1998. Reversible inactivation of protein-tyrosine phosphatase 1B in A431 cells stimulated with epidermal growth factor. *J. Biol. Chem.* 273: 15366–72.
95. Mahadev, K., A. Zilbering, L. Zhu, and B. J. Goldstein. 2001. Insulin-stimulated hydrogen peroxide reversibly inhibits protein-tyrosine phosphatase 1b in vivo and enhances the early insulin action cascade. *J. Biol. Chem.* 276: 21938–42.
96. Leslie, N. R., D. Bennett, Y. E. Lindsay, H. Stewart, A. Gray, and C. P. Downes. 2003. Redox regulation of PI 3-kinase signalling via inactivation of PTEN. *EMBO J.* 22: 5501–10.
97. Kwon, J., S.-R. Lee, K.-S. Yang, Y. Ahn, Y. J. Kim, E. R. Stadtman, and S. G. Rhee. 2004. Reversible oxidation and inactivation of the tumor suppressor PTEN in cells stimulated with peptide growth factors. *Proc. Natl. Acad. Sci. U. S. A.* 101: 16419–24.
98. Giannoni, E., F. Buricchi, G. Raugei, G. Ramponi, and P. Chiarugi. 2005. Intracellular reactive oxygen species activate Src tyrosine kinase during cell adhesion and anchorage-dependent cell growth. *Mol. Cell. Biol.* 25: 6391–403.
99. Nathan, C., and A. Cunningham-Bussel. 2013. Beyond oxidative stress: an immunologist's guide to reactive oxygen species. *Nat. Rev. Immunol.* 13: 349–61.
100. Ruchko, M. V, O. M. Gorodnya, V. M. Pastukh, B. M. Swiger, N. S. Middleton, G. L. Wilson, and M. N. Gillespie. 2009. Hypoxia-induced oxidative base modifications in the VEGF hypoxia-response element are associated with transcriptionally active nucleosomes. *Free Radic. Biol. Med.* 46: 352–9.

101. Ju, B.-G., V. V Lunnyak, V. Perissi, I. Garcia-Bassets, D. W. Rose, C. K. Glass, and M. G. Rosenfeld. 2006. A topoisomerase IIbeta-mediated dsDNA break required for regulated transcription. *Science* 312: 1798–802.
102. Koul, H. K., M. Pal, and S. Koul. 2013. Role of p38 MAP Kinase Signal Transduction in Solid Tumors. *Genes Cancer* 4: 342–59.
103. Friday, B. B., and A. A. Adjei. 2008. Advances in targeting the Ras/Raf/MEK/Erk mitogen-activated protein kinase cascade with MEK inhibitors for cancer therapy. *Clin. Cancer Res.* 14: 342–6.
104. Yong, H.-Y., M.-S. Koh, and A. Moon. 2009. The p38 MAPK inhibitors for the treatment of inflammatory diseases and cancer. *Expert Opin. Investig. Drugs* 18: 1893–905.
105. Johnson, G. L., and R. Lapadat. 2002. Mitogen-activated protein kinase pathways mediated by ERK, JNK, and p38 protein kinases. *Science* 298: 1911–1912.
106. Tsai, P.-W., S.-G. Shiah, M.-T. Lin, C.-W. Wu, and M.-L. Kuo. 2003. Up-regulation of vascular endothelial growth factor C in breast cancer cells by heregulin-beta 1. A critical role of p38/nuclear factor-kappa B signaling pathway. *J. Biol. Chem.* 278: 5750–5759.
107. Suarez-Cuervo, C., M. A. Merrell, L. Watson, K. W. Harris, E. L. Rosenthal, H. K. Väänänen, and K. S. Selander. 2004. Breast cancer cells with inhibition of p38 α have decreased MMP-9 activity and exhibit decreased bone metastasis in mice. *Clin. Exp. Metastasis* 21: 525–533.
108. Iyoda, K., Y. Sasaki, M. Horimoto, T. Toyama, T. Yakushijin, M. Sakakibara, T. Takehara, J. Fujimoto, M. Hori, J. R. Wands, and N. Hayashi. 2003. Involvement of the p38 mitogen-activated protein kinase cascade in hepatocellular carcinoma. *Cancer* 97: 3017–3026.

109. Olson, J. M., and A. R. Hallahan. 2004. p38 MAP kinase: a convergence point in cancer therapy. *Trends Mol. Med.* 10: 125–9.
110. Wada, T., and J. M. Penninger. 2004. Mitogen-activated protein kinases in apoptosis regulation. *Oncogene* 23: 2838–2849.
111. Han, Y.-C., X.-X. Zeng, R. Wang, Y. Zhao, B.-L. Li, and M. Song. 2007. Correlation of p38 mitogen-activated protein kinase signal transduction pathway to uPA expression in breast cancer. *Ai Zheng* 26: 48–53.
112. Galliher, A. J., and W. P. Schiemann. 2007. Src phosphorylates Tyr284 in TGF-beta type II receptor and regulates TGF-beta stimulation of p38 MAPK during breast cancer cell proliferation and invasion. *Cancer Res.* 67: 3752–3758.
113. Haagenson, K. K., and G. S. Wu. 2010. The role of MAP kinases and MAP kinase phosphatase-1 in resistance to breast cancer treatment. *Cancer Metastasis Rev* 29: 143–149.
114. Zhou, J. Y., Y. Liu, and S. W. Gen. 2006. The role of mitogen-activated protein kinase phosphatase-1 in oxidative damage-induced cell death. *Cancer Res.* 66: 4888–4894.
115. Schraufstatter, I., P. A. Hyslop, J. H. Jackson, and C. G. Cochrane. 1988. Oxidant-induced DNA damage of target cells. *J. Clin. Invest.* 82: 1040–1050.
116. Fang, J., T. Seki, and H. Maeda. 2009. Therapeutic strategies by modulating oxygen stress in cancer and inflammation. *Adv. Drug Deliv. Rev.* 61: 290–302.
117. Waris, G., and H. Ahsan. 2006. Reactive oxygen species: role in the development of cancer and various chronic conditions. *J. Carcinog.* 5: 14.

118. Yu, D., J. A. Berlin, T. M. Penning, and J. Field. 2002. Reactive oxygen species generated by PAH o-quinones cause change-in-function mutations in p53. *Chem. Res. Toxicol.* 15: 832–42.
119. Reuter, S., S. C. Gupta, M. M. Chaturvedi, and B. B. Aggarwal. 2010. Oxidative stress, inflammation, and cancer: how are they linked? *Free Radic. Biol. Med.* 49: 1603–1616.
120. Yan, B., Y. Peng, and C. Y. Li. 2009. Molecular analysis of genetic instability caused by chronic inflammation. *Methods Mol Biol* 512: 15–28.
121. Na, A. R., Y. M. Chung, S. B. Lee, S. H. Park, M. S. Lee, and Y. Do Yoo. 2008. A critical role for Romo1-derived ROS in cell proliferation. *Biochem. Biophys. Res. Commun.* 369: 672–678.
122. Hu, Y., D. G. Rosen, Y. Zhou, L. Feng, G. Yang, J. Liu, and P. Huang. 2005. Mitochondrial manganese-superoxide dismutase expression in ovarian cancer: role in cell proliferation and response to oxidative stress. *J. Biol. Chem.* 280: 39485–39492.
123. Liu, S.-L., X. Lin, D.-Y. Shi, J. Cheng, C.-Q. Wu, and Y.-D. Zhang. 2002. Reactive oxygen species stimulated human hepatoma cell proliferation via cross-talk between PI3-K/PKB and JNK signaling pathways. *Arch. Biochem. Biophys.* 406: 173–182.
124. Ruiz-Ramos, R., L. Lopez-Carrillo, A. D. Rios-Perez, A. De Vizcaya-Ruiz, and M. E. Cebrian. 2009. Sodium arsenite induces ROS generation, DNA oxidative damage, HO-1 and c-Myc proteins, NF-kappaB activation and cell proliferation in human breast cancer MCF-7 cells. *Mutat. Res.* 674: 109–115.

125. Denning, T. L., H. Takaishi, S. E. Crowe, I. Boldogh, A. Jevnikar, and P. B. Ernst. 2002. Oxidative stress induces the expression of Fas and Fas ligand and apoptosis in murine intestinal epithelial cells. *Free Radic. Biol. Med.* 33: 1641–1650.
126. Nakata, W., Y. Hayakawa, H. Nakagawa, K. Sakamoto, H. Kinoshita, R. Takahashi, Y. Hirata, S. Maeda, and K. Koike. 2011. Anti-tumor activity of the proteasome inhibitor bortezomib in gastric cancer. *Int. J. Oncol.* 39: 1529–1536.
127. Bejarano, I., J. Espino, A. M. Marchena, C. Barriga, S. D. Paredes, A. B. Rodríguez, and J. A. Pariente. 2011. Melatonin enhances hydrogen peroxide-induced apoptosis in human promyelocytic leukaemia HL-60 cells. *Mol. Cell. Biochem.* 353: 167–176.
128. Valdameri, G., M. Trombetta-Lima, P. R. Worfel, A. R. A. Pires, G. R. Martinez, G. R. Noleto, S. M. S. C. Cadena, M. C. Sogayar, S. M. B. Winnischofer, and M. E. M. Rocha. 2011. Involvement of catalase in the apoptotic mechanism induced by apigenin in HepG2 human hepatoma cells. *Chem. Biol. Interact.* 193: 180–189.
129. Moon, D.-O., M.-O. Kim, Y. H. Choi, J. W. Hyun, W. Y. Chang, and G.-Y. Kim. 2010. Butein induces G(2)/M phase arrest and apoptosis in human hepatoma cancer cells through ROS generation. *Cancer Lett.* 288: 204–13.
130. Qu, Y., J. Wang, P. S. Ray, H. Guo, J. Huang, M. Shin-Sim, B. A. Bukoye, B. Liu, A. V Lee, X. Lin, P. Huang, J. W. Martens, A. E. Giuliano, N. Zhang, N.-H. Cheng, and X. Cui. 2011. Thioredoxin-like 2 regulates human cancer cell growth and metastasis via redox homeostasis and NF- κ B signaling. *J. Clin. Invest.* 121: 212–25.
131. Szatrowski, T. P., and C. F. Nathan. 1991. Production of large amounts of hydrogen peroxide by human tumor cells. *Cancer Res.* 51: 794–798.

132. Toyokuni, S., K. Okamoto, J. Yodoi, and H. Hiai. 1995. Persistent oxidative stress in cancer. *FEBS Lett.* 358: 1–3.
133. Behrend, L., G. Henderson, and R. Zwacka. 2003. Reactive oxygen species in oncogenic transformation. *Biochem. Soc.* 31: 1441–4.
134. Farber, E., and H. Rubin. 1991. Cellular adaptation in the origin and development of cancer. *Cancer Res.* 51: 2751–61.
135. Pollycove, M. 2007. Radiobiological basis of low-dose irradiation in prevention and therapy of cancer. *Dose. Response.* 5: 26–38.
136. Liu, R. H. 2004. Potential synergy of phytochemicals in cancer prevention: mechanism of action. *J. Nutr.* 134: 3479S–3485S.
137. Del Rio, D., A. Rodriguez-Mateos, J. P. E. Spencer, M. Tognolini, G. Borges, and A. Crozier. 2013. Dietary (poly)phenolics in human health: structures, bioavailability, and evidence of protective effects against chronic diseases. *Antioxid. Redox Signal.* 18: 1818–92.
138. 2006. *Plant Secondary Metabolites*, (A. Crozier, M. N. Clifford, and H. Ashihara, eds). Blackwell Publishing Ltd, Oxford, UK.
139. Bravo, L. 1998. Polyphenols: chemistry, dietary sources, metabolism, and nutritional significance. *Nutr. Rev.* 56: 317–333.
140. Tapiero, H., K. D. Tew, G. N. Ba, and G. Mathé. 2002. Polyphenols: do they play a role in the prevention of human pathologies? *Biomed. Pharmacother.* 56: 200–7.
141. Knekt, P., J. Kumpulainen, R. Järvinen, H. Rissanen, M. Heliövaara, A. Reunanen, T. Hakulinen, and A. Aromaa. 2002. Flavonoid intake and risk of chronic diseases. *Am. J. Clin. Nutr.* 76: 560–568.

142. Hertog, M. G., E. J. Feskens, P. C. Hollman, M. B. Katan, and D. Kromhout. 1993. Dietary antioxidant flavonoids and risk of coronary heart disease: the Zutphen Elderly Study. *Lancet* 342: 1007–11.
143. Hollman, P. C. H., and M. B. Katan. 1999. Dietary flavonoids: Intake, health effects and bioavailability. *Food Chem. Toxicol.* 37: 937–942.
144. Yao, L. H., Y. M. Jiang, J. Shi, F. A. Tomás-Barberán, N. Datta, R. Singanusong, and S. S. Chen. 2004. Flavonoids in food and their health benefits. *Plant Foods Hum. Nutr.* 59: 113–122.
145. Sargeant, L. A., K. T. Khaw, S. Bingham, N. E. Day, R. N. Luben, S. Oakes, A. Welch, and N. J. Wareham. 2001. Fruit and vegetable intake and population glycosylated haemoglobin levels: the EPIC-Norfolk Study. *Eur. J. Clin. Nutr.* 55: 342–8.
146. He, F. J., C. A. Nowson, and G. A. MacGregor. 2006. Fruit and vegetable consumption and stroke: meta-analysis of cohort studies. *Lancet* 367: 320–6.
147. Croft, K. D. 1998. The chemistry and biological effects of flavonoids and phenolic acids. In *Annals of the New York Academy of Sciences* vol. 854. 435–442.
148. Kühnau, J. 1976. The flavonoids. A class of semi-essential food components: their role in human nutrition. *World Rev. Nutr. Diet.* 24: 117–191.
149. Hertog, M. G., P. C. Hollman, M. B. Katan, and D. Kromhout. 1993. Intake of potentially anticarcinogenic flavonoids and their determinants in adults in The Netherlands. *Nutr. Cancer* 20: 21–29.
150. Grosso, G., U. Stepaniak, R. Topor-Mądry, K. Szafraniec, and A. Pająk. Estimated dietary intake and major food sources of polyphenols in the Polish arm of the HAPIEE study. *Nutrition* 30: 1398–403.

151. Chun, O. K., S. J. Chung, and W. O. Song. 2007. Estimated dietary flavonoid intake and major food sources of U.S. adults. *J. Nutr.* 137: 1244–52.
152. Zamora-Ros, R., C. Andres-Lacueva, R. M. Lamuela-Raventós, T. Berenguer, P. Jakszyn, A. Barricarte, E. Ardanaz, P. Amiano, M. Dorronsoro, N. Larrañaga, C. Martínez, M. J. Sánchez, C. Navarro, M. D. Chirlaque, M. J. Tormo, J. R. Quirós, and C. A. González. 2010. Estimation of dietary sources and flavonoid intake in a Spanish adult population (EPIC-Spain). *J. Am. Diet. Assoc.* 110: 390–8.
153. Ross, J. A., and C. M. Kasum. 2002. Dietary flavonoids: bioavailability, metabolic effects, and safety. *Annu. Rev. Nutr.* 22: 19–34.
154. Bohn, T. 2014. Dietary factors affecting polyphenol bioavailability. *Nutr. Rev.* 72: 429–52.
155. Hollman, P. C., M. N. Bijlsman, Y. van Gameren, E. P. Cnossen, J. H. de Vries, and M. B. Katan. 1999. *The sugar moiety is a major determinant of the absorption of dietary flavonoid glycosides in man., ;* :569–573.
156. Day, A. J., F. J. Cañada, J. C. Díaz, P. A. Kroon, R. McLauchlan, C. B. Faulds, G. W. Plumb, M. R. A. Morgan, and G. Williamson. 2000. Dietary flavonoid and isoflavone glycosides are hydrolysed by the lactase site of lactase phlorizin hydrolase. *FEBS Lett.* 468: 166–170.
157. Hollman, P. C. H., J. H. M. De Vries, S. D. Van Leeuwen, M. J. B. Mengelers, and M. B. Katan. 1995. Absorption of dietary quercetin glycosides and quercetin in healthy ileostomy volunteers. *Am. J. Clin. Nutr.* 62: 1276–1282.
158. Németh, K., G. W. Plumb, J.-G. Berrin, N. Juge, R. Jacob, H. Y. Naim, G. Williamson, D. M. Swallow, and P. A. Kroon. 2003. Deglycosylation by small intestinal epithelial cell beta-glucosidases is a critical step in the absorption and metabolism of dietary flavonoid glycosides in humans. *Eur. J. Nutr.* 42: 29–42.

159. Day, A. J., M. S. Dupont, S. Ridley, M. Rhodes, M. J. c Rhodes, M. R. a Morgan, and G. Williamson. 1998. Deglycosylation of flavonoid and isoflavonoid glycosides by human small intestine and liver β -glucosidase activity. *FEBS Lett.* 436: 71–75.
160. Jaganath, I. B., W. Mullen, C. A. Edwards, and A. Crozier. 2006. The relative contribution of the small and large intestine to the absorption and metabolism of rutin in man. *Free Radic. Res.* 40: 1035–1046.
161. Bokkenheuser, V. D., C. H. Shackleton, and J. Winter. 1987. Hydrolysis of dietary flavonoid glycosides by strains of intestinal Bacteroides from humans. *Biochem. J.* 248: 953–956.
162. Schneider, H., A. Schwiertz, M. D. Collins, and M. Blaut. 1999. Anaerobic transformation of quercetin-3-glucoside by bacteria from the human intestinal tract. *Arch. Microbiol.* 171: 81–91.
163. Adlercreutz, H., H. Markkanen, and S. Watanabe. 1993. Plasma concentrations of phyto-oestrogens in Japanese men. *Lancet* 342: 1209–1210.
164. Xu, X., H. J. Wang, P. A. Murphy, L. Cook, and S. Hendrich. 1994. Daidzein is a more bioavailable soymilk isoflavone than is genistein in adult women. *J. Nutr.* 124: 825–832.
165. Scalbert, A., and G. Williamson. 2000. Dietary intake and bioavailability of polyphenols. *J. Nutr.* 130: 2073S–85S.
166. Kanellos, P. T., A. C. Kaliora, A. Gioxari, G. O. Christopoulou, N. Kalogeropoulos, and V. T. Karathanos. 2013. Absorption and Bioavailability of Antioxidant Phytochemicals and Increase of Serum Oxidation Resistance in Healthy Subjects Following Supplementation with Raisins. *Plant Foods Hum. Nutr.* 68: 411–415.

167. De Vries, J. H., P. C. Hollman, I. van Amersfoort, M. R. Olthof, and M. B. Katan. 2001. *Red wine is a poor source of bioavailable flavonols in men...*; :745–748.
168. Hollman, P. C. H., J. M. P. Van Trijp, M. N. C. P. Buysman, M. S. V.d. Gaag, M. J. B. Mengelers, J. H. M. De Vries, and M. B. Katan. 1997. Relative bioavailability of the antioxidant flavonoid quercetin from various foods in man. *FEBS Lett.* 418: 152–156.
169. De Vries, J. H. M., P. C. H. Hollman, S. Meyboom, M. N. C. P. Buysman, P. L. Zock, W. A. Van Staveren, and M. B. Katan. 1998. Plasma concentrations and urinary excretion of the antioxidant flavonols quercetin and kaempferol as biomarkers for dietary intake. *Am. J. Clin. Nutr.* 68: 60–65.
170. Dangles, O., C. Dufour, C. Manach, C. Morand, and C. Remesy. 2001. Binding of flavonoids to plasma proteins. *Methods Enzymol.* 335: 319–333.
171. Wang, S., R. Su, S. Nie, M. Sun, J. Zhang, D. Wu, and N. Moustaid-Moussa. 2014. Application of nanotechnology in improving bioavailability and bioactivity of diet-derived phytochemicals. *J. Nutr. Biochem.* 25: 363–376.
172. Block, G., B. Patterson, and A. Subar. 1992. Fruit, vegetables, and cancer prevention: a review of the epidemiological evidence. *Nutr. Cancer* 18: 1–29.
173. Riboli, E., and T. Norat. 2003. Epidemiologic evidence of the protective effect of fruit and vegetables on cancer risk. *Am. J. Clin. Nutr.* 78: 559S–569S.
174. Sak, K. 2014. Cytotoxicity of dietary flavonoids on different human cancer types. *Pharmacogn. Rev.* 8: 122–46.
175. Grosso, G., S. Buscemi, F. Galvano, A. Mistretta, S. Marventano, V. La Vela, F. Drago, S. Gangi, F. Basile, and A. Biondi. 2013. Mediterranean diet and cancer: epidemiological evidence and mechanism of selected aspects. *BMC Surg.* 13 Suppl 2: S14.

176. Pantavos, A., R. Ruiter, E. Feskens, C. E deKeyser, A. Hofman, B. H Stricker, O. H Franco, and J. C Kieffe-deJong. 2014. Total dietary antioxidant capacity, individual antioxidant intake and breast cancer risk: The rotterdam study. *Int. J. Cancer* .
177. Albuquerque, R. C. R., V. T. Baltar, and D. M. L. Marchioni. 2014. Breast cancer and dietary patterns: A systematic review. *Nutr. Rev.* 72: 1–17.
178. Sun, J., Y. F. Chu, X. Z. Wu, and R. H. Liu. 2002. Antioxidant and anti proliferative activities of common fruits. *J. Agric. Food Chem.* 50: 7449–7454.
179. Chu, Y. F., J. Sun, X. Wu, and R. H. Liu. 2002. Antioxidant and antiproliferative activities of common vegetables. *J. Agric. Food Chem.* 50: 6910–6916.
180. Samarghandian, S., J. T. Afshari, and S. Davoodi. 2011. Chrysin reduces proliferation and induces apoptosis in the human prostate cancer cell line pc-3. *Clin. (Sao Paulo)* 66: 1073–1079.
181. Li-Weber, M. 2009. New therapeutic aspects of flavones: The anticancer properties of Scutellaria and its main active constituents Wogonin, Baicalein and Baicalin. *Cancer Treat. Rev.* 35: 57–68.
182. Tokalov, S. V, A. M. Abramyuk, and N. D. Abolmaali. 2010. Protection of p53 wild type cells from taxol by genistein in the combined treatment of lung cancer. *Nutr. Cancer* 62: 795–801.
183. Gupta, S., F. Afaq, and H. Mukhtar. 2001. Selective growth-inhibitory, cell-cycle deregulatory and apoptotic response of apigenin in normal versus human prostate carcinoma cells. *Biochem. Biophys. Res. Commun.* 287: 914–920.
184. Hirano, T., K. Abe, M. Gotoh, and K. Oka. 1995. Citrus flavone tangeretin inhibits leukaemic HL-60 cell growth partially through induction of apoptosis with less cytotoxicity on normal lymphocytes. *Br. J. Cancer* 72: 1380–1388.

185. Rodriguez, J., J. Yáñez, V. Vicente, M. Alcaraz, O. Benavente-García, J. Castillo, J. Lorente, and J. A. Lozano. 2002. Effects of several flavonoids on the growth of B16F10 and SK-MEL-1 melanoma cell lines: relationship between structure and activity. *Melanoma Res.* 12: 99–107.
186. Ying, T.-H., S.-F. Yang, S.-J. Tsai, S.-C. Hsieh, Y.-C. Huang, D.-T. Bau, and Y.-H. Hsieh. 2012. Fisetin induces apoptosis in human cervical cancer HeLa cells through ERK1/2-mediated activation of caspase-8-/caspase-3-dependent pathway. *Arch. Toxicol.* 86: 263–73.
187. Jeong, J. C., M. S. Kim, T. H. Kim, and Y. K. Kim. 2009. Kaempferol induces cell death through ERK and Akt-dependent down-regulation of XIAP and survivin in human glioma cells. *Neurochem. Res.* 34: 991–1001.
188. Torkin, R., J.-F. Lavoie, D. R. Kaplan, and H. Yeger. 2005. Induction of caspase-dependent, p53-mediated apoptosis by apigenin in human neuroblastoma. *Mol. Cancer Ther.* 4: 1–11.
189. Zhao, X., G. Shu, L. Chen, X. Mi, Z. Mei, and X. Deng. 2012. A flavonoid component from *Docynia delavayi* (Franch.) Schneid represses transplanted H22 hepatoma growth and exhibits low toxic effect on tumor-bearing mice. *Food Chem. Toxicol.* 50: 3166–73.
190. Lee, E.-J., S.-Y. Oh, and M.-K. Sung. 2012. Luteolin exerts anti-tumor activity through the suppression of epidermal growth factor receptor-mediated pathway in MDA-MB-231 ER-negative breast cancer cells. *Food Chem. Toxicol.* 50: 4136–43.
191. Tsai, C.-F., W.-L. Yeh, S. M. Huang, T.-W. Tan, and D.-Y. Lu. 2012. Wogonin induces reactive oxygen species production and cell apoptosis in human glioma cancer cells. *Int. J. Mol. Sci.* 13: 9877–92.

192. Matsuo, M., N. Sasaki, K. Saga, and T. Kaneko. 2005. Cytotoxicity of flavonoids toward cultured normal human cells. *Biol. Pharm. Bull.* 28: 253–9.
193. Lee, K. W., H. J. Hur, H. J. Lee, and C. Y. Lee. 2005. Antiproliferative effects of dietary phenolic substances and hydrogen peroxide. *J. Agric. Food Chem.* 53: 1990–5.
194. Yuan, L., J. Wang, H. Xiao, C. Xiao, Y. Wang, and X. Liu. 2012. Isoorientin induces apoptosis through mitochondrial dysfunction and inhibition of PI3K/Akt signaling pathway in HepG2 cancer cells. *Toxicol. Appl. Pharmacol.* 265: 83–92.
195. Jeong, J.-H., J. Y. An, Y. T. Kwon, J. G. Rhee, and Y. J. Lee. 2009. Effects of low dose quercetin: cancer cell-specific inhibition of cell cycle progression. *J. Cell. Biochem.* 106: 73–82.
196. Yin, F., A. E. Giuliano, R. E. Law, and A. J. Van Herle. Apigenin inhibits growth and induces G2/M arrest by modulating cyclin-CDK regulators and ERK MAP kinase activation in breast carcinoma cells. *Anticancer Res.* 21: 413–20.
197. Choi, E. J. 2007. Hesperetin induced G1-phase cell cycle arrest in human breast cancer MCF-7 cells: involvement of CDK4 and p21. *Nutr. Cancer* 59: 115–9.
198. Lu, X., J. in Jung, H. J. Cho, D. Y. Lim, H. S. Lee, H. S. Chun, D. Y. Kwon, and J. H. Y. Park. 2005. Fisetin inhibits the activities of cyclin-dependent kinases leading to cell cycle arrest in HT-29 human colon cancer cells. *J. Nutr.* 135: 2884–90.
199. Kim, T. H., J. S. Woo, Y. K. Kim, and K. H. Kim. 2014. Silibinin induces cell death through reactive oxygen species-dependent downregulation of notch-1/ERK/Akt signaling in human breast cancer cells. *J. Pharmacol. Exp. Ther.* 349: 268–78.

200. Chen, H., Q. Miao, M. Geng, J. Liu, Y. Hu, L. Tian, J. Pan, and Y. Yang. 2013. Anti-tumor effect of rutin on human neuroblastoma cell lines through inducing G2/M cell cycle arrest and promoting apoptosis. *Scientific World Journal*. 2013: 269165.
201. Bao, C., H. Namgung, J. Lee, H.-C. Park, J. Ko, H. Moon, H. W. Ko, and H. J. Lee. 2014. Daidzein suppresses tumor necrosis factor- α induced migration and invasion by inhibiting hedgehog/Gli1 signaling in human breast cancer cells. *J. Agric. Food Chem.* 62: 3759–67.
202. Cai, J., X.-L. Zhao, A.-W. Liu, H. Nian, and S.-H. Zhang. 2011. Apigenin inhibits hepatoma cell growth through alteration of gene expression patterns. *Phytomedicine* 18: 366–73.
203. Xie, F., M. Su, W. Qiu, M. Zhang, Z. Guo, B. Su, J. Liu, X. Li, and L. Zhou. 2013. Kaempferol promotes apoptosis in human bladder cancer cells by inducing the tumor suppressor, PTEN. *Int. J. Mol. Sci.* 14: 21215–26.
204. Wu, S., B. Liu, Q. Zhang, J. Liu, W. Zhou, C. Wang, M. Li, S. Bao, and R. Zhu. 2013. Dihydromyricetin reduced Bcl-2 expression via p53 in human hepatoma HepG2 cells. *PLoS One* 8: e76886.
205. Fotsis, T., M. S. Pepper, R. Montesano, E. Aktas, S. Breit, L. Schweigerer, S. Rasku, K. Wähälä, and H. Adlercreutz. 1998. Phytoestrogens and inhibition of angiogenesis. *Baillieres. Clin. Endocrinol. Metab.* 12: 649–66.
206. Fotsis, T., M. S. Pepper, E. Aktas, S. Breit, S. Rasku, H. Adlercreutz, K. Wähälä, R. Montesano, and L. Schweigerer. 1997. Flavonoids, dietary-derived inhibitors of cell proliferation and in vitro angiogenesis. *Cancer Res.* 57: 2916–21.
207. Weng, C. J., and G. C. Yen. 2012. Flavonoids, a ubiquitous dietary phenolic subclass, exert extensive in vitro anti-invasive and in vivo anti-metastatic activities. *Cancer Metastasis Rev.* 31: 323–351.

208. Deep, G., S. C. Gangar, C. Agarwal, and R. Agarwal. 2011. Role of E-cadherin in antimigratory and antiinvasive efficacy of silibinin in prostate cancer cells. *Cancer Prev. Res. (Phila)*. 4: 1222–32.
209. Vazquez-Martin, A., S. Fernández-Arroyo, S. Cufí, C. Oliveras-Ferraro, J. Lozano-Sánchez, L. Vellón, V. Micol, J. Joven, A. Segura-Carretero, and J. A. Menendez. 2012. Phenolic secoiridoids in extra virgin olive oil impede fibrogenic and oncogenic epithelial-to-mesenchymal transition: extra virgin olive oil as a source of novel antiaging phytochemicals. *Rejuvenation Res*. 15: 3–21.
210. Li, R., Y. Zhao, J. Chen, S. Shao, and X. Zhang. 2014. Fisetin inhibits migration, invasion and epithelial-mesenchymal transition of LMP1-positive nasopharyngeal carcinoma cells. *Mol. Med. Rep*. 9: 413–8.
211. Takahashi, A., T. Watanabe, A. Mondal, K. Suzuki, M. Kurusu-Kanno, Z. Li, T. Yamazaki, H. Fujiki, and M. Suganuma. 2014. Mechanism-based inhibition of cancer metastasis with (-)-epigallocatechin gallate. *Biochem. Biophys. Res. Commun*. 443: 1–6.
212. Kin, R., S. Kato, N. Kaneto, H. Sakurai, Y. Hayakawa, F. Li, K. Tanaka, I. Saiki, and S. Yokoyama. 2013. Procyanidin C1 from Cinnamomi Cortex inhibits TGF- β -induced epithelial-to-mesenchymal transition in the A549 lung cancer cell line. *Int. J. Oncol*. 43: 1901–6.
213. Chen, K.-C., C.-Y. Chen, C.-R. Lin, C.-J. Lin, T.-Y. Yang, T.-H. Chen, L.-C. Wu, and C.-C. Wu. 2013. Luteolin attenuates TGF- β 1-induced epithelial-mesenchymal transition of lung cancer cells by interfering in the PI3K/Akt-NF- κ B-Snail pathway. *Life Sci*. 93: 924–33.
214. Chien, C.-S., K.-H. Shen, J.-S. Huang, S.-C. Ko, and Y.-W. Shih. 2010. Antimetastatic potential of fisetin involves inactivation of the PI3K/Akt and JNK signaling pathways with downregulation of MMP-2/9 expressions in prostate cancer PC-3 cells. *Mol. Cell. Biochem*. 333: 169–80.

215. Park, S.-H., J.-H. Kim, D.-H. Lee, J.-W. Kang, H.-H. Song, S.-R. Oh, and D.-Y. Yoon. 2013. Luteolin 8-C- β -fucopyranoside inhibits invasion and suppresses TPA-induced MMP-9 and IL-8 via ERK/AP-1 and ERK/NF- κ B signaling in MCF-7 breast cancer cells. *Biochimie* 95: 2082–90.
216. Adams, L. S., S. Phung, N. Yee, N. P. Seeram, L. Li, and S. Chen. 2010. Blueberry phytochemicals inhibit growth and metastatic potential of MDA-MB-231 breast cancer cells through modulation of the phosphatidylinositol 3-kinase pathway. *Cancer Res.* 70: 3594–605.
217. Lee, S.-J., S. Hong, S.-H. Yoo, and G.-W. Kim. 2013. Cyanidin-3-O-sambubioside from *Acanthopanax sessiliflorus* fruit inhibits metastasis by downregulating MMP-9 in breast cancer cells MDA-MB-231. *Planta Med.* 79: 1636–40.
218. Singh, B. N., S. Shankar, and R. K. Srivastava. 2011. Green tea catechin, epigallocatechin-3-gallate (EGCG): mechanisms, perspectives and clinical applications. *Biochem. Pharmacol.* 82: 1807–21.
219. Lecumberri, E., Y. M. Dupertuis, R. Miralbell, and C. Pichard. 2013. Green tea polyphenol epigallocatechin-3-gallate (EGCG) as adjuvant in cancer therapy. *Clin. Nutr.* 32: 894–903.
220. Baur, J. A., and D. A. Sinclair. 2006. Therapeutic potential of resveratrol: the in vivo evidence. *Nat. Rev. Drug Discov.* 5: 493–506.
221. Shukla, Y., and R. Singh. 2011. Resveratrol and cellular mechanisms of cancer prevention. *Ann. N. Y. Acad. Sci.* 1215: 1–8.
222. Mukhtar, H., and N. Ahmad. 2000. Tea polyphenols: prevention of cancer and optimizing health. *Am. J. Clin. Nutr.* 71: 1698S–702S; discussion 1703S–4S.
223. Aggarwal, B. B., and S. Shishodia. 2006. Molecular targets of dietary agents for prevention and therapy of cancer. *Biochem. Pharmacol.* 71: 1397–421.

224. Khan, N., F. Afaq, M. Saleem, N. Ahmad, and H. Mukhtar. 2006. Targeting multiple signaling pathways by green tea polyphenol (-)-epigallocatechin-3-gallate. *Cancer Res.* 66: 2500–5.
225. Hastak, K., S. Gupta, N. Ahmad, M. K. Agarwal, M. L. Agarwal, and H. Mukhtar. 2003. Role of p53 and NF-kappaB in epigallocatechin-3-gallate-induced apoptosis of LNCaP cells. *Oncogene* 22: 4851–9.
226. Shankar, S., G. Suthakar, and R. K. Srivastava. 2007. Epigallocatechin-3-gallate inhibits cell cycle and induces apoptosis in pancreatic cancer. *Front. Biosci.* 12: 5039–51.
227. Masuda, M., M. Suzui, and I. B. Weinstein. 2001. Effects of epigallocatechin-3-gallate on growth, epidermal growth factor receptor signaling pathways, gene expression, and chemosensitivity in human head and neck squamous cell carcinoma cell lines. *Clin. Cancer Res.* 7: 4220–9.
228. Gupta, S., T. Hussain, and H. Mukhtar. 2003. Molecular pathway for (-)-epigallocatechin-3-gallate-induced cell cycle arrest and apoptosis of human prostate carcinoma cells. *Arch. Biochem. Biophys.* 410: 177–85.
229. Khan, N., and H. Mukhtar. 2013. Modulation of signaling pathways in prostate cancer by green tea polyphenols. *Biochem. Pharmacol.* 85: 667–72.
230. Tao, L., J.-Y. Park, and J. D. Lambert. 2014. The differential pro-oxidative effects of the green tea polyphenol, (-)-epigallocatechin-3-gallate, in normal and oral cancer cells are related to differences in sirtuin 3 signaling. *Mol. Nutr. Food Res.* .

231. Li, G.-X., Y.-K. Chen, Z. Hou, H. Xiao, H. Jin, G. Lu, M.-J. Lee, B. Liu, F. Guan, Z. Yang, A. Yu, and C. S. Yang. 2010. Pro-oxidative activities and dose-response relationship of (-)-epigallocatechin-3-gallate in the inhibition of lung cancer cell growth: a comparative study in vivo and in vitro. *Carcinogenesis* 31: 902–10.
232. Liu, L.-C., T. C.-Y. Tsao, S.-R. Hsu, H.-C. Wang, T.-C. Tsai, J.-Y. Kao, and T.-D. Way. 2012. EGCG inhibits transforming growth factor- β -mediated epithelial-to-mesenchymal transition via the inhibition of Smad2 and Erk1/2 signaling pathways in nonsmall cell lung cancer cells. *J. Agric. Food Chem.* 60: 9863–73.
233. Whitlock, N. C., and S. J. Baek. 2012. The anticancer effects of resveratrol: modulation of transcription factors. *Nutr. Cancer* 64: 493–502.
234. Pervaiz, S. 2001. Resveratrol--from the bottle to the bedside? *Leuk. Lymphoma* 40: 491–8.
235. Roy, P., E. Madan, N. Kalra, N. Nigam, J. George, R. S. Ray, R. K. Hans, S. Prasad, and Y. Shukla. 2009. Resveratrol enhances ultraviolet B-induced cell death through nuclear factor-kappaB pathway in human epidermoid carcinoma A431 cells. *Biochem. Biophys. Res. Commun.* 384: 215–20.
236. Csaki, C., A. Mobasheri, and M. Shakibaei. 2009. Synergistic chondroprotective effects of curcumin and resveratrol in human articular chondrocytes: inhibition of IL-1 β -induced NF-kappaB-mediated inflammation and apoptosis. *Arthritis Res. Ther.* 11: R165.
237. Liu, Y.-Z., K. Wu, J. Huang, Y. Liu, X. Wang, Z.-J. Meng, S.-X. Yuan, D.-X. Wang, J.-Y. Luo, G.-W. Zuo, L.-J. Yin, L. Chen, Z.-L. Deng, J.-Q. Yang, W.-J. Sun, and B.-C. He. 2014. The PTEN/PI3K/Akt and Wnt/ β -catenin signaling pathways are involved in the inhibitory effect of resveratrol on human colon cancer cell proliferation. *Int. J. Oncol.* 45: 104–12.

238. Fu, Y., H. Chang, X. Peng, Q. Bai, L. Yi, Y. Zhou, J. Zhu, and M. Mi. 2014. Resveratrol inhibits breast cancer stem-like cells and induces autophagy via suppressing Wnt/ β -catenin signaling pathway. *PLoS One* 9: e102535.
239. Zhao, W., P. Bao, H. Qi, and H. You. 2010. Resveratrol down-regulates survivin and induces apoptosis in human multidrug-resistant SPC-A-1/CDDP cells. *Oncol. Rep.* 23: 279–86.
240. Bai, Y., Q.-Q. Mao, J. Qin, X.-Y. Zheng, Y.-B. Wang, K. Yang, H.-F. Shen, and L.-P. Xie. 2010. Resveratrol induces apoptosis and cell cycle arrest of human T24 bladder cancer cells in vitro and inhibits tumor growth in vivo. *Cancer Sci.* 101: 488–93.
241. Parekh, P., L. Motiwale, N. Naik, and K. V. K. Rao. 2011. Downregulation of cyclin D1 is associated with decreased levels of p38 MAP kinases, Akt/PKB and Pak1 during chemopreventive effects of resveratrol in liver cancer cells. *Exp. Toxicol. Pathol.* 63: 167–73.
242. Lee, S.-J., and M.-M. Kim. 2011. Resveratrol with antioxidant activity inhibits matrix metalloproteinase via modulation of SIRT1 in human fibrosarcoma cells. *Life Sci.* 88: 465–72.
243. Li, W., J. Ma, Q. Ma, B. Li, L. Han, J. Liu, Q. Xu, W. Duan, S. Yu, F. Wang, and E. Wu. 2013. Resveratrol inhibits the epithelial-mesenchymal transition of pancreatic cancer cells via suppression of the PI-3K/Akt/NF- κ B pathway. *Curr. Med. Chem.* 20: 4185–94.
244. Walle, T., F. Hsieh, M. H. DeLegge, J. E. Oatis, and U. K. Walle. 2004. High absorption but very low bioavailability of oral resveratrol in humans. *Drug Metab. Dispos.* 32: 1377–82.

245. Athar, M., J. H. Back, X. Tang, K. H. Kim, L. Kopelovich, D. R. Bickers, and A. L. Kim. 2007. Resveratrol: a review of preclinical studies for human cancer prevention. *Toxicol. Appl. Pharmacol.* 224: 274–83.
246. Mian, K. H., and S. Mohamed. 2001. Flavonoid (myricetin, quercetin, kaempferol, luteolin, and apigenin) content of edible tropical plants. *J. Agric. Food Chem.* 49: 3106–12.
247. Hertog, M. G. L., P. C. H. Hollman, and B. van de Putte. 1993. Content of potentially anticarcinogenic flavonoids of tea infusions, wines, and fruit juices. *J. Agric. Food Chem.* 41: 1242–1246.
248. Moniruzzaman, M., C. Yung An, P. V. Rao, M. N. I. Hawlader, S. A. B. M. Azlan, S. A. Sulaiman, and S. H. Gan. 2014. Identification of phenolic acids and flavonoids in monofloral honey from Bangladesh by high performance liquid chromatography: determination of antioxidant capacity. *Biomed Res. Int.* 2014: 737490.
249. Ruiz, A., L. Bustamante, C. Vergara, D. von Baer, I. Hermosín-Gutiérrez, L. Obando, and C. Mardones. 2015. Hydroxycinnamic acids and flavonols in native edible berries of South Patagonia. *Food Chem.* 167: 84–90.
250. Zang, W., T. Wang, Y. Wang, M. Li, X. Xuan, Y. Ma, Y. Du, K. Liu, Z. Dong, and G. Zhao. 2014. Myricetin exerts anti-proliferative, anti-invasive, and pro-apoptotic effects on esophageal carcinoma EC9706 and KYSE30 cells via RSK2. *Tumour Biol.* .
251. Aquila, S., M. Santoro, F. De Amicis, C. Guido, D. Bonofiglio, M. Lanzino, M. G. Cesario, I. Perrotta, D. Sisci, and C. Morelli. 2013. Red wine consumption may affect sperm biology: the effects of different concentrations of the phytoestrogen myricetin on human male gamete function. *Mol. Reprod. Dev.* 80: 155–65.

252. Kandasamy, N., and N. Ashokkumar. 2014. Protective effect of bioflavonoid myricetin enhances carbohydrate metabolic enzymes and insulin signaling molecules in streptozotocin-cadmium induced diabetic nephrotoxic rats. *Toxicol. Appl. Pharmacol.* 279: 173–85.
253. Pandey, K. B., N. Mishra, and S. I. Rizvi. Myricetin may provide protection against oxidative stress in type 2 diabetic erythrocytes. *Z. Naturforsch. C.* 64: 626–30.
254. Ying, X., X. Chen, Y. Feng, H. Z. Xu, H. Chen, K. Yu, S. Cheng, and L. Peng. 2014. Myricetin enhances osteogenic differentiation through the activation of canonical Wnt/ β -catenin signaling in human bone marrow stromal cells. *Eur. J. Pharmacol.* 738: 22–30.
255. Pandey, K. B., N. Mishra, and S. I. Rizvi. 2009. Protective role of myricetin on markers of oxidative stress in human erythrocytes subjected to oxidative stress. *Nat. Prod. Commun.* 4: 221–6.
256. Tiwari, R., M. Mohan, S. Kasture, A. Maxia, and M. Ballero. 2009. Cardioprotective potential of myricetin in isoproterenol-induced myocardial infarction in Wistar rats. *Phytother. Res.* 23: 1361–6.
257. Kuo, P.-L. 2005. Myricetin inhibits the induction of anti-Fas IgM-, tumor necrosis factor-alpha- and interleukin-1beta-mediated apoptosis by Fas pathway inhibition in human osteoblastic cell line MG-63. *Life Sci.* 77: 2964–76.
258. Ong, K. C., and H. E. Khoo. 2000. Effects of myricetin on glycemia and glycogen metabolism in diabetic rats. *Life Sci.* 67: 1695–705.
259. Hui, C., X. Qi, Z. Qianyong, P. Xiaoli, Z. Jundong, and M. Mantian. 2013. Flavonoids, flavonoid subclasses and breast cancer risk: a meta-analysis of epidemiologic studies. *PLoS One* 8: e54318.

260. Griffiths, L. A., and G. E. Smith. 1972. Metabolism of myricetin and related compounds in the rat. Metabolite formation in vivo and by the intestinal microflora in vitro. *Biochem. J.* 130: 141–51.
261. Iswaldi, I., D. Arráez-Román, A. M. Gómez-Caravaca, M. D. M. Contreras, J. Uberos, A. Segura-Carretero, and A. Fernández-Gutiérrez. 2013. Identification of polyphenols and their metabolites in human urine after cranberry-syrup consumption. *Food Chem. Toxicol.* 55: 484–92.
262. Kim, M. E., T. K. Ha, J. H. Yoon, and J. S. Lee. 2014. Myricetin induces cell death of human colon cancer cells via BAX/BCL2-dependent pathway. *Anticancer Res.* 34: 701–6.
263. Sun, F., X. Y. Zheng, J. Ye, T. T. Wu, J. li Wang, and W. Chen. 2012. Potential anticancer activity of myricetin in human T24 bladder cancer cells both in vitro and in vivo. *Nutr. Cancer* 64: 599–606.
264. Shih, Y.-W., P.-F. Wu, Y.-C. Lee, M.-D. Shi, and T.-A. Chiang. 2009. Myricetin suppresses invasion and migration of human lung adenocarcinoma A549 cells: possible mediation by blocking the ERK signaling pathway. *J. Agric. Food Chem.* 57: 3490–9.
265. Maggioni, D., G. Nicolini, R. Rigolio, L. Biffi, L. Pignataro, R. Gaini, and W. Garavello. 2014. Myricetin and naringenin inhibit human squamous cell carcinoma proliferation and migration in vitro. *Nutr. Cancer* 66: 1257–67.
266. Kim, W., H. J. Yang, H. Youn, Y. J. Yun, K. M. Seong, and B. Youn. 2010. Myricetin inhibits Akt survival signaling and induces Bad-mediated apoptosis in a low dose ultraviolet (UV)-B-irradiated HaCaT human immortalized keratinocytes. *J. Radiat. Res.* 51: 285–96.

267. Labbé, D., M. Provençal, S. Lamy, D. Boivin, D. Gingras, and R. Béliveau. 2009. The flavonols quercetin, kaempferol, and myricetin inhibit hepatocyte growth factor-induced medulloblastoma cell migration. *J. Nutr.* 139: 646–52.
268. Phillips, P. A., V. Sangwan, D. Borja-Cacho, V. Dudeja, S. M. Vickers, and A. K. Saluja. 2011. Myricetin induces pancreatic cancer cell death via the induction of apoptosis and inhibition of the phosphatidylinositol 3-kinase (PI3K) signaling pathway. *Cancer Lett.* 308: 181–8.
269. Ko, C. H., S.-C. Shen, C.-S. Hsu, and Y.-C. Chen. 2005. Mitochondrial-dependent, reactive oxygen species-independent apoptosis by myricetin: roles of protein kinase C, cytochrome c, and caspase cascade. *Biochem. Pharmacol.* 69: 913–27.
270. Morales, P., and A. I. Haza. 2012. Selective apoptotic effects of piceatannol and myricetin in human cancer cells. *J. Appl. Toxicol.* 32: 986–93.
271. Wang, I. K., S. Y. Lin-Shiau, and J. K. Lin. 1999. Induction of apoptosis by apigenin and related flavonoids through cytochrome c release and activation of caspase-9 and caspase-3 in leukaemia HL-60 cells. *Eur. J. Cancer* 35: 1517–25.
272. Lu, J., L. V Papp, J. Fang, S. Rodriguez-Nieto, B. Zhivotovsky, and A. Holmgren. 2006. Inhibition of Mammalian thioredoxin reductase by some flavonoids: implications for myricetin and quercetin anticancer activity. *Cancer Res.* 66: 4410–8.
273. Zhang, S., L. Wang, H. Liu, G. Zhao, and L. Ming. 2014. Enhancement of recombinant myricetin on the radiosensitivity of lung cancer A549 and H1299 cells. *Diagn. Pathol.* 9: 68.

274. Choi, S.-J., S.-C. Shin, and J.-S. Choi. 2011. Effects of myricetin on the bioavailability of doxorubicin for oral drug delivery in rats: possible role of CYP3A4 and P-glycoprotein inhibition by myricetin. *Arch. Pharm. Res.* 34: 309–15.
275. Li, C., S.-C. Lim, J. Kim, and J.-S. Choi. 2011. Effects of myricetin, an anticancer compound, on the bioavailability and pharmacokinetics of tamoxifen and its main metabolite, 4-hydroxytamoxifen, in rats. *Eur. J. Drug Metab. Pharmacokinet.* 36: 175–82.
276. Rodgers, E. H., and M. H. Grant. 1998. The effect of the flavonoids, quercetin, myricetin and epicatechin on the growth and enzyme activities of MCF7 human breast cancer cells. *Chem. Biol. Interact.* 116: 213–28.
277. Kuntz, S., U. Wenzel, and H. Daniel. 1999. Comparative analysis of the effects of flavonoids on proliferation, cytotoxicity, and apoptosis in human colon cancer cell lines. *Eur. J. Nutr.* 38: 133–42.
278. Jayakumar, J. K., P. Nirmala, B. A. Praveen Kumar, and A. P. Kumar. 2014. Evaluation of protective effect of myricetin, a bioflavonoid in dimethyl benzanthracene-induced breast cancer in female Wistar rats. *South Asian J. cancer* 3: 107–11.
279. Yaffe, P. B., M. R. Power Coombs, C. D. Doucette, M. Walsh, and D. W. Hoskin. 2014. Piperine, an alkaloid from black pepper, inhibits growth of human colon cancer cells via G1 arrest and apoptosis triggered by endoplasmic reticulum stress. *Mol. Carcinog.* doi: 10.1002/mc.22176
280. Yang, T. T., P. Sinai, and S. R. Kain. 1996. An acid phosphatase assay for quantifying the growth of adherent and nonadherent cells. *Anal. Biochem.* 241: 103–8.

281. Zhou, M., Z. Diwu, N. Panchuk-Voloshina, and R. P. Haugland. 1997. A stable nonfluorescent derivative of resorufin for the fluorometric determination of trace hydrogen peroxide: applications in detecting the activity of phagocyte NADPH oxidase and other oxidases. *Anal. Biochem.* 253: 162–8.
282. Fadok, V. A., D. R. Voelker, P. A. Campbell, J. J. Cohen, D. L. Bratton, and P. M. Henson. 1992. Exposure of phosphatidylserine on the surface of apoptotic lymphocytes triggers specific recognition and removal by macrophages. *J. Immunol.* 148 : 2207–2216.
283. Raynal, P., and H. B. Pollard. 1994. Annexins: the problem of assessing the biological role for a gene family of multifunctional calcium- and phospholipid-binding proteins. *Biochim. Biophys. Acta - Rev. Biomembr.* 1197: 63–93.
284. Vermes, I., C. Haanen, H. Steffens-Nakken, and C. Reutellingsperger. 1995. A novel assay for apoptosis Flow cytometric detection of phosphatidylserine expression on early apoptotic cells using fluorescein labelled Annexin V. *J. Immunol. Methods* 184: 39–51.
285. Marchetti, P., T. Hirsch, N. Zamzami, M. Castedo, D. Decaudin, S. A. Susin, B. Marse, and G. Kroemer. 1996. Mitochondrial permeability transition triggers lymphocyte apoptosis. *J. Immunol.* 157 : 4830–4836.
286. Eruslanov, E., and S. Kusmartsev. 2010. Identification of ROS using oxidized DCFDA and flow-cytometry. *Methods Mol. Biol.* 594: 57–72.
287. Mah, L.-J., A. El-Osta, and T. C. Karagiannis. 2010. gammaH2AX: a sensitive molecular marker of DNA damage and repair. *Leukemia* 24: 679–86.
288. Kruger, N., J. 2002. *The Protein Protocols Handbook*, Second. (J. M. Walker, ed). Humana Press, Totowa: 15–21.

289. Lv, Z.-D., X.-P. Liu, W.-J. Zhao, Q. Dong, F.-N. Li, H.-B. Wang, and B. Kong. 2014. Curcumin induces apoptosis in breast cancer cells and inhibits tumor growth in vitro and in vivo. *Int. J. Clin. Exp. Pathol.* 7: 2818–24.
290. Chen, D., K. R. Landis-Piowar, M. S. Chen, and Q. P. Dou. 2007. Inhibition of proteasome activity by the dietary flavonoid apigenin is associated with growth inhibition in cultured breast cancer cells and xenografts. *Breast Cancer Res.* 9: R80.
291. Jin, H.-O., Y.-H. Lee, J.-A. Park, H.-N. Lee, J.-H. Kim, J.-Y. Kim, B. Kim, S.-E. Hong, H.-A. Kim, E.-K. Kim, W. C. Noh, J.-I. Kim, Y. H. Chang, S.-I. Hong, Y.-J. Hong, I.-C. Park, and J. K. Lee. 2014. Piperlongumine induces cell death through ROS-mediated CHOP activation and potentiates TRAIL-induced cell death in breast cancer cells. *J. Cancer Res. Clin. Oncol.* 140: 2039–46.
292. Braicu, C., C. D. Gherman, A. Irimie, and I. Berindan-Neagoe. 2013. Epigallocatechin-3-Gallate (EGCG) inhibits cell proliferation and migratory behaviour of triple negative breast cancer cells. *J. Nanosci. Nanotechnol.* 13: 632–7.
293. Lee, H. S., A. W. Ha, and W. K. Kim. 2012. Effect of resveratrol on the metastasis of 4T1 mouse breast cancer cells in vitro and in vivo. *Nutr. Res. Pract.* 6: 294–300.
294. Odiatou, E. M., A. L. Skaltsounis, and A. I. Constantinou. 2013. Identification of the factors responsible for the in vitro pro-oxidant and cytotoxic activities of the olive polyphenols oleuropein and hydroxytyrosol. *Cancer Lett.* 330: 113–21.
295. Long, L. H., M. V. Clement, and B. Halliwell. 2000. Artifacts in cell culture: rapid generation of hydrogen peroxide on addition of (-)-epigallocatechin, (-)-epigallocatechin gallate, (+)-catechin, and quercetin to commonly used cell culture media. *Biochem. Biophys. Res. Commun.* 273: 50–3.

296. Fabiani, R., R. Fuccelli, F. Pieravanti, A. De Bartolomeo, and G. Morozzi. 2009. Production of hydrogen peroxide is responsible for the induction of apoptosis by hydroxytyrosol on HL60 cells. *Mol. Nutr. Food Res.* 53: 887–96.
297. Bellion, P., M. Oik, F. Will, H. Dietrich, M. Baum, G. Eisenbrand, and C. Janzowski. 2009. Formation of hydrogen peroxide in cell culture media by apple polyphenols and its effect on antioxidant biomarkers in the colon cell line HT-29. *Mol. Nutr. Food Res.* 53: 1226–36.
298. Kuntz, S., U. Wenzel, and H. Daniel. 1999. Comparative analysis of the effects of flavonoids on proliferation, cytotoxicity, and apoptosis in human colon cancer cell lines. *Eur. J. Nutr.* 38: 133–142.
299. Yang, X., X. Li, and J. Ren. 2014. From French Paradox to cancer treatment: anti-cancer activities and mechanisms of resveratrol. *Anticancer. Agents Med. Chem.* 14: 806–25.
300. Pękal, A., P. Drózdź, M. Biesaga, and K. Pyrzyńska. 2012. Screening of the antioxidant properties and polyphenol composition of aromatised green tea infusions. *J. Sci. Food Agric.* 92: 2244–9.
301. Csomós, E., K. Héberger, and L. Simon-Sarkadi. 2002. Principal Component Analysis of Biogenic Amines and Polyphenols in Hungarian Wines. *J. Agric. Food Chem.* 50: 3768–3774.
302. Fang, F., J.-M. Li, Q.-H. Pan, and W.-D. Huang. 2007. Determination of red wine flavonoids by HPLC and effect of aging. *Food Chem.* 101: 428–433.
303. Serrano-Lourido, D., J. Saurina, S. Hernández-Cassou, and A. Checa. 2012. Classification and characterisation of Spanish red wines according to their appellation of origin based on chromatographic profiles and chemometric data analysis. *Food Chem.* 135: 1425–31.

304. Vandenabeele, P., T. Vanden Berghe, and N. Festjens. 2006. Caspase inhibitors promote alternative cell death pathways. *Sci. STKE* 2006: pe44.
305. Golstein, P., and G. Kroemer. 2005. Redundant cell death mechanisms as relics and backups. *Cell Death Differ.* 12 Suppl 2: 1490–6.
306. Dekhuijzen, P. N. R. 2004. Antioxidant properties of N-acetylcysteine: their relevance in relation to chronic obstructive pulmonary disease. *Eur. Respir. J.* 23: 629–36.
307. Mochizuki, M., S. Yamazaki, K. Kano, and T. Ikeda. 2002. Kinetic analysis and mechanistic aspects of autoxidation of catechins. *Biochim. Biophys. Acta* 1569: 35–44.
308. Serrano, J., M. Jové, J. Boada, M. J. Bellmunt, R. Pamplona, and M. Portero-Otín. 2009. Dietary antioxidants interfere with Amplex Red-coupled-fluorescence assays. *Biochem. Biophys. Res. Commun.* 388: 443–9.
309. Lea, M. A., C. Ibeh, J. K. Deutsch, I. Hamid, and C. desBordes. 2010. Inhibition of growth and induction of alkaline phosphatase in colon cancer cells by flavonols and flavonol glycosides. *Anticancer Res.* 30: 3629–35.
310. Agullo, G., L. Gamet-Payraastre, Y. Fernandez, N. Anciaux, C. Demigné, and C. Rémésy. 1996. Comparative effects of flavonoids on the growth, viability and metabolism of a colonic adenocarcinoma cell line (HT29 cells). *Cancer Lett.* 105: 61–70.
311. Long, L. H., and B. Halliwell. 2009. Artefacts in cell culture: pyruvate as a scavenger of hydrogen peroxide generated by ascorbate or epigallocatechin gallate in cell culture media. *Biochem. Biophys. Res. Commun.* 388: 700–4.
312. Kunz-Schughart, L. A., J. P. Freyer, F. Hofstaedter, and R. Ebner. 2004. The use of 3-D cultures for high-throughput screening: the multicellular spheroid model. *J. Biomol. Screen.* 9: 273–85.

313. LaBarbera, D. V., B. G. Reid, and B. H. Yoo. 2012. The multicellular tumor spheroid model for high-throughput cancer drug discovery. *Expert Opin. Drug Discov.* 7: 819–30.
314. McLoughlin, P., M. Roengvoraphoj, C. Gissel, J. Hescheler, U. Certa, and A. Sachinidis. 2004. Transcriptional responses to epigallocatechin-3 gallate in HT 29 colon carcinoma spheroids. *Genes Cells* 9: 661–9.
315. Xu, R., Y. Zhang, X. Ye, S. Xue, J. Shi, J. Pan, and Q. Chen. 2013. Inhibition effects and induction of apoptosis of flavonoids on the prostate cancer cell line PC-3 in vitro. *Food Chem.* 138: 48–53.
316. Butt, M. S., and M. T. Sultan. 2009. Green tea: nature's defense against malignancies. *Crit. Rev. Food Sci. Nutr.* 49: 463–73.
317. Los, M., W. Dröge, K. Stricker, P. A. Baeuerle, and K. Schulze-Osthoff. 1995. Hydrogen peroxide as a potent activator of T lymphocyte functions. *Eur. J. Immunol.* 25: 159–65.
318. Sayin, V. I., M. X. Ibrahim, E. Larsson, J. A. Nilsson, P. Lindahl, and M. O. Bergo. 2014. Antioxidants accelerate lung cancer progression in mice. *Sci. Transl. Med.* 6: 221ra15.